# APPLICATIONS AND INTERPRETATION OF KRYPTON 81M VENTILATION/ TECHNETIUM 99M MACROAGGREGATE PERFUSION LUNG SCANNING IN CHILDHOOD.

M.D. THESIS

SUBMITTED BY

HUGH DAVIES BA, MB BS, MRCP

THE HOSPITAL FOR SICK CHILDREN

GREAT ORMOND STREET

LONDON WC1N 3JH

1990

INDEX OF CONTENTS

## CHAPTER 1: HISTORICAL REVIEW



## CHAPTER 2: APPARATUS AND METHODS

## CHAPTER 3: THEORETICAL ANALYSIS OF KR81M VENTILATION AND TC99M PERFUSION IMAGES

PAGE



## CHAPTER 4: DYNAMIC STEADY STATE VENTILATION IMAGING

PAGE

## CHAPTER 5: CLINICAL STUDIES

PAGE

## CHAPTER 6: EFFECT OF POSTURE ON REGIONAL VENTILATION IN CHILDREN AND ADULTS



## CHAPTER 7 EFFECT OF POSTURE ON THE DISTRIBUTION OF PULMONARY PERFUSION IN CHILDREN

## CHAPTER 8 APPLICATIONS OF DYNAMIC KR81M VENTILATION IMAGING

PAGE

# INTRODUCTION

Radionuclide ventilation perfusion lung scans now play an important part in the investigation of paediatric lung disease, providing a safe, noninvasive assessment of regional lung function in children with suspected pulmonary disease (Treves et al 1974, Godfrey et al 1977, Ciofetta et al 1980, Gordon et al 1981, Gordon and Helms 1982).

In paediatric practice the most suitable radionuclides are Krypton 81m (Kr81m) and Technetium 99m (Tc99m), which are jointly used in the Kr81m ventilation/Tc99m macroaggregate perfusion lung scan (V/Q lung scan). The Kr81m ventilation scan involves a low radiation dose (Myers 1981), requires little or no subject cooperation and because of the very short half life of Kr81m (13 seconds) the steady state image acquired during continuous inhalation of the radionuclide is considered to reflect regional distribution of ventilation (Fazio and Jones 1975). It is now the most important noninvasive method available for the investigation of the regional abnormalities of ventilation characteristic of many congenital and acquired paediatric respiratory diseases, such as diaphragmatic hernia, pulmonary sequestration, bronchopulmonary dysplasia, foreign body inhalation and bronchiectasis. It improves diagnostic accuracy, aids clinical decision making and is used to monitor the progress of disease and response to therapy (Godfrey and Mackenzie 1977, Gordon, Helms and Fazio 1981, Wong Y-C and Silverman 1982, Gordon and

Helms 1982).

Theoretical analysis of the steady state Kr81m ventilation image (Fazio and Jones 1975) suggests that it may only reflect regional ventilation when specific ventilation (ventilation per unit volume of lung) is within or below the normal adult range (1-3 L/L/min). At higher values such as those seen in neonates and infants (8-15 L/L/min) Kr81m activity may reflect regional lung volume rather than ventilation, a conclusion supported by the studies of Ciofetta et al (Ciofetta et al 1980).

There is some controversy on this issue as animal studies (Modell and Graham 1982) have demonstrated that the Kr81m image reflects ventilation over a much wider range of specific ventilation (up to 13 L/L/min). A clinical study of sick infants and very young children (Heaf et al 1983) is in agreement with this animal work and suggests that the steady state Kr81m image still reflects regional ventilation in this age group.

The doubt cast on the interpretation of the Kr81m steady state image could limit the value of V/Q lung scans in following regional lung function through childhood, a period when specific ventilation is falling rapidly as the child grows. Therefore the first aim of this study was to examine the application of this theoretical model to children and determine whether the changing specific ventilation seen through childhood significantly alters the interpretation of the steady state Kr81m image. This is a necessary first step before conducting longitudinal studies of regional ventilation and perfusion in children.

The effect of posture on regional ventilation and perfusion in the adult human lung has been extensively studied. Radiotracer studies (West & Dollery 1960, Ball et al 1962, Milic-Emili 1966, Amis et al 1984) have consistently shown that both ventilation and perfusion are preferentially distributed to dependent lung regions during tidal breathing regardless of posture.

There is little published information concerning the pattern in children yet there are many differences in lung and chest wall mechanics of children and adults (Naimark and Cherniak 1960, Fisher et al 1980) which, along with clinical observation, have led to the hypothesis that the pattern of regional ventilation observed in adults may not be seen in children. Recent reports of regional ventilation in infants and very young children (Heaf et al 1983 Davies et al 1985) have provided support for this theory. The paper of Heaf et al demonstrated that these differences may in certain circumstances be clinically important. It is not clear however at what age children adopt the "adult pattern of ventilation".

In addition to the problems referred to above, attenuation of Kr81m activity as it passes through the chest wall and the changing geometry of the chest during tidal breathing have made quantitative analysis of the image difficult (Jones 1978) although fractional ventilation and perfusion to each lung can be calculated from the steady state image. In clinical practise, therefore, ventilation and perfusion are usually assessed by

inspection of the steady state image.

The aims of the present study were therefore:

1. To critically assess Kr81m ventilation and Tc99m MAA perfusion images in children.

2. To derive fractional ventilation and perfusion to each lung in children with normal chest radiography and homogeneous distribution of the radionuclides.

3. To conduct further studies into the effects of gravity on regional lung function.

4. To apply the technique in clinical practise.

5. To attempt to improve quantitation of the Kr81m ventilation image.

## ABBREVIATIONS

| | |
|---|---|
| AP | Anterior posterior |
| CV | Coefficient of variation |
| DS | Dead Space |
| FB | Foreign Body |
| FRC | Functional Residual Capacity |
| FRC(PLETH) | Functional Residual capacity determined by plethysmography |
| FVC | Forced Vital Capacity |
| HSC | Hospital for Sick Children |
| I131 | Iodine 131 |
| KR81M | Krypton 81m |
| MAA | Macroaggregates of human albumin |
| Mo99 | Molybdenum 99 |
| N13 | Nitrogen 13 |
| 015 | Oxygen 15 |
| PaO2 | Arterial partial pressure of oxygen |
| QFL | Fractional perfusion to the left lung |
| QFR | Fractional perfusion to the right lung |
| ROI | Region of Interest |
| RR | Respiratory rate |
| RV | Residual lung volume |
| SP. V.) V/Vol ) | Specific ventilation (Ventilation per unit volume of lung) |
| TC99M | Technetium 99m |
| TCPO2 | Trans cutaneous partial pressure of oxygen |
| TGV | Thoracic gas volume |
| TLC | Total lung capacity |

| | |
|---|---|
| TV | Tidal Volume |
| VFL | Fractional ventilation to the left lung |
| VFR | Fractional ventilation to the right lung |
| V/Q | Ventilation/perfusion |
| XE133 | Xenon 133 |

ACKNOWLEDGEMENTS

This work was conducted at The Hospital for Sick Children during my tenure of a Respiratory Unit Fellowship. It involved the co-operation of the Respiratory Unit and the Department of Radiology and was completed under the supervision of Dr P J Helms, Honorary Consultant in the Respiratory Unit and Dr I Gordon, Consultant Radiologist. It is to them that I owe a huge debt of gratitude. At the inception of the work they stimulated my interest in the subject and provided early guidance. They have always offered constructive criticism and often provided suggestions for future work. They have helped in the preparation of the thesis and kindly given their free time to read it through.

I also wish to thank Dr D J Matthew and Dr R Dinwiddie, Consultant Respiratory Paediatricians at The Hospital for Sick Children for allowing me to study patients under their care in addition to the staff of the Respiratory Unit who have contributed in many different ways to this project, particularly Miss Leigh Stanger who has typed much of the manuscript. Throughout the two and a half years all the members of both units have provided help and friendship.

This work would not have been possible without the co-operation and advice from many radiographers working in the Nuclear Medicine Unit in the Department of Radiology. To them I must also express my gratitude.

This thesis represents, I hope, a continuation of the research tradition in the Respiratory Unit and the Department of Radiology. From "cotside" observation to clinical studies these units have demonstrated that the pattern of regional lung function is different in adults and children and that these differences have clinical importance in managing critically ill patients.

My largest debt of gratitude is to my family, Irene, Oliver and Chloe for their help and contributions while I conducted the experimental work and wrote the thesis. They have tolerated my long absences and always provided support and encouragement. Finally my father showed an enthusiastic interest and made many constructive criticisms during the first two years. Unfortunately he did not live to see its completion. I dedicate this thesis to my family and his memory.

# CHAPTER 1

# HISTORICAL REVIEW

The proposal that inspired air is unevenly distributed throughout the lungs is now more than 150 years old (Laennec RTL 1830). Physicians in the nineteenth century suggested that the lung apices were both relatively hypoventilated and hypoperfused and that these regional differences between the top and bottom of the lungs in the erect position might explain the typical apical localisation of tuberculous infection.

This has been born out by experiments using expired gas analysis which have shown that ventilation is not uniform (Krogh and Lindhard 1917, Fowler et al 1952), although the topographical nature of this inhomogeneity could not be demonstrated until bronchospirometric techniques were able to quantify ventilation to individual lungs and lung regions. Workers using these latter techniques showed that both regional functional residual capacity (FRC) and ventilation were affected by posture (Bergan 1957, Lillington 1959, Svanberg 1957, Vaccarezza 1943). When the right lung was placed dependent its FRC fell from 55% to 45% of total FRC while ventilation to the right lung rose from approximately 55% to 65%. These changes have been further confirmed by studies of multibreath nitrogen washout from individual lungs in different postures. Disease seemed to have little effect on this redistribution (Carlens et al 1961).

The first report of the noninvasive assessment of regional

ventilation using the gaseous radioisotope Xe133 was published in 1955 (Knipping et al 1955). The purpose of their paper was to demonstrate the value of this technique in the preoperative assessment of patients undergoing lobectomy or pneumonectomy for malignant disease. Xe133 ventilation imaging, in conjunction with standard pulmonary function tests permitted examination of regional lung function and preoperative prediction of postoperative respiratory function.

The first physiological studies of regional ventilation were performed using the short lived isotope of oxygen, O15, produced in a nearby cyclotron (Dyson et al 1960, West and Dollery 1960). Emitted activity was detected by scintillation counters positioned over the chest wall and using the isotope as O2, carbon dioxide or carbon monoxide, profiles of regional activity during inhalation and breatholding were constructed in normal subjects erect, supine, decubitus both at rest and after exercise (Figure 1). Measurement of initial regional activity after inhaling the isotope allowed assessment of distribution of the isotope and hence regional ventilation while the subsequent fall in radioactivity during breathholding was a measure of regional clearance and as such represented the ratelimiting process (perfusion or diffusion of the gas from the field of view of the scintillation counter). These studies demonstrated a vertical gradient of ventilation with maximal values in the most dependent lung regions regardless of posture. This gradient was abolished by exercise.

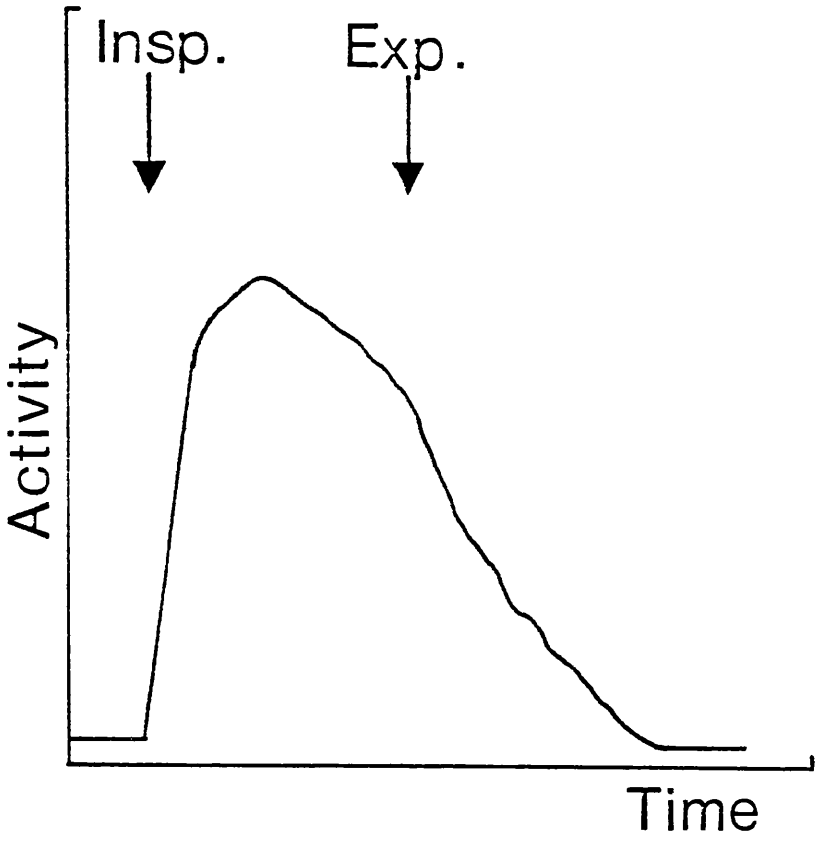


FIGURE 1

Profile of regional activity detected by single scintillation counter. (After Dyson et al 1960)

The subject is switched into a respiratory circuit containing radiotracer at "Insp" and then holds his breath. Peak activity is proportional to regional ventilation. The subsequent fall in activity while the subject breathholds will be an index of radioactive decay and diffusion if the isotope is CO2 or perfusion if CO. At "Exp" the subject breaths out.

These techniques, however, have several limitations. Measurements are made under static conditions and absolute quantification is impossible. In addition regional clearance of the isotope is dependent on radioactive decay, regional perfusion and diffusion of the tracer from the field of view of the counter making interpretation of the results less clear. Nevertheless, despite these criticisms subsequent studies have repeatedly confirmed their findings.

Within two years Ball et al working in Montreal reported a technique using the more readily available isotope, Xenon 133 (Xe133), that allowed quantification of regional ventilation and volume (Ball et al 1962). In this technique subjects were settled and scintillation counters attached to the chest wall. They were asked to breath out fully before being switched into a closed respiratory circuit containing a known quantity of Xe133. They then inhaled stepwise from residual volume to total lung capacity (TLC) breathholding at each step for sufficient counts to be recorded. As the isotope was uniformly distributed in the inspired air, absolute activity detected by the counters at each step was taken to be a measure of the distribution of ventilation to the underlying regions of lung.

This procedure was repeated after the subject had equilibrated with the Xe133 in the respiratory circuit. Regional activity was recorded at identical lung volumes as in the first part of the study. The authors argued that at equilibrium the Xe133 concentration in alveolar gas and spirometer would be identical and it would thus be possible to

calculate the detection efficiency of external counters at each lung volume and quantify regional ventilation.

Using a similar technique it was found that uppermost lung regions had a relatively larger regional residual volume (RV) and smaller forced vital capacity (FVC) when compared to dependent lung regions (Milic Emili et al 1966) . This group also demonstrated that ventilation was preferentially distributed to upper lung regions from RV to 40% TLC but that this pattern was reversed from 40% TLC to 100% TLC. In the normal tidal volume range ventilation was preferentially distributed to dependent lung regions.

Although these studies were performed under static conditions, it has been shown that distribution of ventilation is similar under dynamic conditions (Amis et al 1984) . Regional ventilation was determined during continuous inhalation of the gaseous radioisotope of the element Krypton, Kr81m (Fazio and Jones 1975) while regional volume was derived from Kr85m images, a radionuclide of Krypton with a half life of four hours. There was little difference between their results and those of earlier workers studying ventilation under static conditions. Posture had similar effects on regional ventilation, in supine and left and right decubitus positions, with ventilation being preferentially distributed to dependent lung regions. They were unable however to demonstrate this gradient in the prone position.

Dock (Dock 1946) proposed that the distribution of pulmonary perfusion must be uneven. Oxygen uptake studies using bronchospirometric techniques provided direct support for this hypothesis and demonstrated that the inequality is dependent on gravity. Using these techniques Mattson and Carlens (Mattson and Carlens 1955) and Martin and Young (Martin and Young 1957) have shown that pulmonary blood flow is greater in dependent lung regions.

The first noninvasive measurements of regional pulmonary blood flow were made by West and Dollery (West and Dollery 1960) using CO2, labelled with O15. Their methodology was described earlier in this chapter. Assuming that clearance of this isotope is a measure of regional blood flow, these authors were able to show that blood flow was greatest in the base of the upright lungs, falling toward the apex.

Bryan et al (Bryan et al 1964) measured distribution of perfusion after an intravenous injection of a bolus of Xe133 dissolved in normal saline along the lines of the study conducted by Ball et al investigating regional ventilation. Xe133 was injected into a peripheral vein while the subject breathheld at predetermined lung volumes. The isotope rapidly diffuses into the alveoli from the pulmonary capillary bed and regional activity during breathholding will represent regional perfusion of expanded lung regions. In the subjects studied, (aged from 22

to 44 years) mean perfusion indices (the observed regional concentration expressed as a percentage of the predicted concentration if the injected isotope were uniformly distributed through the lungs) varied from 41% in uppermost lung regions to 133% in dependent zones. This gradient was reversed in the supine position, attributed to the fact that in this posture the apex of the lungs are lower than the bases as the buttocks tend to tilt the body head down.

Kaneko et al (Kaneko et al 1966) were able to show that this gradient of perfusion was magnified in either decubitus posture. In these positions perfusion per alveolus was relatively constant in the lower two thirds of the thorax but then decreased progressively in the upper third.

Udea et al (Udea et al 1966) studied blood flow using macroaggregates labelled with the isotope of Iodine, I131. These authors demonstrated that the pattern of distribution of activity was dependent on the subject's position at the time of injection. When supine, the isotope was uniformly distributed but when upright, activity was greatest at the bases.

## PAEDIATRIC APPLICATIONS OF RADIOTRACER TECHNIQUES

Clinical application of the techniques outlined above was initially limited. Although suitable for physiological studies the scintillation counters used in early studies could not

provide two dimensional images of the inhaled tracer. It was only with the advent of the collimated gamma camera (Anger 1958) that radionuclide lung scanning gained widespread clinical acceptance. The gamma camera allows mapping of regional ventilation and perfusion and can provide clinicians with high quality two dimensional images of the lungs that may be used to assess the pathophysiological consequences of disease.

## 1. VENTILATION

Xe133 has been widely used in adult practise (Secker Walker 1973). Clinical techniques are similar to those already described in this chapter. Patients are positioned in front of a gamma camera and breathe from a closed respiratory circuit. A bolus of Xe133 is injected into the circuit at end expiration and at the end of the subsequent inspiration the patient is asked to hold his breath for 20 seconds. This image represents the regional distribution of inhaled isotope. A further image is acquired once Xe133 has reached equilibrium with the resident lung volume. Subsequently the patient is switched out of the circuit and washout of the isotope from the lungs is recorded in short, timed frames using dynamic ventilation imaging. This latter technique can identify regions of hypoventilation which because of trapped Xe133 appear as areas of increased activity or "hot spots" on the images.

While ideally suited for use in cooperative adults the physical characteristics of Xe133 limit its use in paediatrics

although it can be used in older, more cooperative children (Treves et al 1974). These limitations are :-

1. The equilibration phase of Xe133 represents lung volume and not ventilation.

2. Presence of dissolved Xe133 in the chest wall and blood makes quantification of the washout studies difficult.

3. The low photopeak of Xe133 is unsuitable for gamma camera imaging, providing poor spatial resolution and interfering with perfusion imaging when Tc99m is used (Table 1).

4. Complex breath holding techniques are required usually beyond the ability of children.

5. Xe133 imaging involves a radiation dose higher than alternatives such as O15 or Kr81m.

6. The long half life (5.3 days) makes efficient waste disposal mandatory, either by using a leak free respiratory circuit or a powerful extractor fan both of which are poorly tolerated by young children.

As an alternative approach workers at the Royal Postgraduate Medical School in London have studied regional ventilation using short lived isotopes such as O15 or N13 generated by an on site cyclotron. Such isotopes have major advantages. The rapid decay can allow serial images in different positions, waste disposal is not a major problem and patient cooperation is not needed.

TABLE 1

Physical Characteristics of Radiopharmaceuticals used in Ventilation and Perfusion Imaging.

| Radiotracer | Half life | Energy emitted |
|---|---|---|
| Xe133 | 5.3 days | 81 kEV |
| Xe127 | 36.4 days | 72 kEV<br>203 kEV<br>375 kEV |
| Kr81m | 13 secs | 190 kEV |
| Tc99m | 6 hours | 140 kEV |
| O15 | 2 mins | 511 kEV |
| N13 | 10 mins | 511 kEV |

Godfrey and McKenzie assessed the value of N13 (half-life 10 minutes) radioisotope lung scanning in their paediatric practise (Godfrey and Mackenzie 1977). This was not a randomly selected group and reflected the interests of the department (cystic fibrosis, congenital heart disease and musculoskeletal problems). They found the tests to be of most value in children between the age of 6 months and 5 years when normal lung function tests were difficult or impossible to perform. Below this age infant plethysmography could provide detailed information while above the age of 5 children could cooperate to perform standard respiratory manoeuvres. They identified particular diseases in which lung scanning proved useful regardless of age; unilateral hyperlucent lung, cystic fibrosis (particularly for preoperative assessment if lobectomy was being considered) and pulmonary vascular disease. They reported separately on its value in distinguishing between coexistent pulmonary and cardiac pathology (Godfrey et al 1975).

Although most units are too far from a cyclotron to make use of these isotopes, short lived isotopes or nuclides can be used further afield if there is a suitable generator with a longer living "parent" that decays to provide a short lived "daughter" radiotracer (Chandra R 1982). The useful life of such generators depends on the half life of the parent rather than the daughter.

The demand of respiratory physicians for accurate assessment of regional ventilation led to the development of the Rubidium

81m (Rb81m) generator from which the short lived gaseous nuclide Krypton 81m (half life 13 seconds) can be eluted. Rb81m has a half life of 4 hours and adequate quantities of Kr81m may be extracted from this generator up to 12 hours after production. Kr81m is a highly insoluble gas that provides excellent functional images (Jones 1978). The similar energy of the emitted gamma rays to those of Technetium 99m (190 and 140 kEV respectively) along with its rapid decay makes it ideal when Tc99m is used to image perfusion. Since the first report of its use by continuous inhalation in clinical practise (Fazio and Jones 1975) it has gained widespread acceptance. A good agreement between Kr81m and Xe133 ventilation images has been demonstrated but the higher energy of Kr81m provides a more detailed image and better localisation of disease (Li et al 1979). These workers performed both Kr81m and Xe133 ventilation lung scans on 14 children attending the Boston Children's Hospital. Three children showed no ventilatory abnormalities on either examination and all 11 with abnormal Xe133 scans had abnormalities on the Kr81m image. In 5 patients Kr81m was superior in localising disease and defined a greater number of focal defects. The authors reported that this was mainly due to the use of multiple views with Kr81m. In 2 patients Xe133 washout showed delayed clearance from an entire lung while Kr81m imaging could only show focal defects. Kr81m had the additional advantage of a significantly reduced radiation dose to lungs and gonads.

## 2. PERFUSION

Early clinical techniques assessing regional pulmonary perfusion used Xe133 dissolved in normal saline, injected into a suitable vein while the patient sat in front of a gamma camera, holding his breath at FRC (functional residual capacity). There are major theoretical disadvantages to this technique. It depends on the passage of Xe133 into the alveoli and can only assess perfusion in expanded areas of lung. It will therefore underestimate ventilation/perfusion mismatching. As this is one of the major reasons for performing V/Q lung scans in clinical practise, the technique is unsuitable for routine use. There are additional technical disadvantages similar to those of Xe133 ventilation imaging. The subject cooperation necessary limits its value in paediatric practise.

In 1964 Wagner et al described a technique for the measurement of regional pulmonary perfusion using I131 labelled macroaggregates of human albumin (MAA) that lodged in the pulmonary capillaries (Wagner et al 1964). Cardiovascular effects of capillary embolisation with macro aggregates of albumin were initially investigated in rats and dogs. LD (0) (dose required to kill all animals) was determined in rats and found to be 5000 times the dose subsequently used in human studies. Ten mg/kg were administered to dogs with no measurable effects on systemic or pulmonary blood pressure nor on pulse or respiratory rate. Histological examination of lungs of rats given similar doses of MAA could not separate them from normal

controls one week after injection.

Toxicity studies demonstrated an allergic reaction in 1 of 300 human subjects injected with MAA. This was not investigated further. Thyroid irradiation by the injected I131 was limited by prior block of iodine uptake into the gland by administration of Lugols iodine.

## THE TC99M MAA PERFUSION IMAGE

The validity of the Tc99m MAA perfusion image depends on the assumption that after intravenous injection of labelled macroaggregates regional Tc99m activity will be proportional to regional pulmonary blood flow. Tc99m macroaggregates must therefore be evenly distributed in blood ejected from the right ventricle, Tc99m must be tightly bound to the macroaggregates to prevent recirculation into the systemic blood supply of the lungs and chest wall and the macroaggregates should not be metabolised and removed from the lungs during the imaging procedure.

While these assumptions have not been tested, the accuracy of the technique has been confirmed in animals and human subjects. Wagner et al (Wagner et al 1964) produced experimental pulmonary emboli in laboratory dogs by floating radio-opaque balloon catheters into the pulmonary circulation. Subsequent perfusion imaging correctly identified the position of the "emboli" in all 90 cases. In the same paper the authors reported the results of the first 100 perfusion scans performed at their

hospital. 14 had evidence of perfusion defects on radioisotope scanning, all of which were confirmed either by angiography, operative exploration or post mortem examination. False negative results were not reported.

Garnett et al (Garnett et al 1969) studied the accuracy of the technique in a group of 20 patients suffering from either carcinoma or bullous emphysema. Fractional perfusion to each lung was determined by regional bronchospirometry and I131 MAA imaging. Fractional perfusion to the right lung varied from 10% to 90% and there was close agreement between the techniques. Technetium 99m with its better imaging properties is now used in preference to I131. The shorter half life of Tc99m reduces the dose needed for imaging and it can be eluted from the inexpensive Mo99m, Tc99m generator. It obviously presents much less risk of thyroid damage.

McNeil and Adelstein (McNeil and Adelstein 1978) estimated that a standard dose of $2*10^5$ to $10^6$ particles will temporarily occlude approximately 1 in 100,000 capillaries in an adult. The absolute number of alveoli in the human newborn is disputed and figures vary from 17,000,000 to 71,000,000 (Dunnill 1962, Angus and Thurlbeck 1972, Davies and Reid 1970). Thurlbeck and Angus (Thurlbeck and Angus 1972) have shown that there is similar variability in normal adults, the number of alveoli varying between 200 and 600 million. It would therefore seem reasonable to scale down the adult dose on the basis of weight or surface area.

This technique should not be used in known cases of severe pulmonary vascular disease where major pulmonary arteries are narrowed and may thus be embolised, nor should it be used without careful consideration in patients where a major right to left shunt exists as systemic embolisation may occur in these subjects. When lung function is severely compromised this technique may place excessive strain on the patients condition (Bjure et al 1970) and again caution should be exercised in such children.

## PAEDIATRIC CLINICAL APPLICATIONS OF KR81M/TC99M MACROAGGREGATE VENTILATION PERFUSION SCANS

There is now considerable experience in the acquisition, interpretation and clinical value of Kr81m ventilation and Tc99m MAA perfusion images in paediatric practise. It is generally agreed that for clinical purposes visual inspection of the steady state image in conjunction with a recent chest radiograph suffices and that mathematical analysis usually provides little further useful clinical information. Small areas of hypoventilation contain too few radioactive counts for reliable quantitative analysis while they can be identified by simple visual inspection of the image (Wong and Silverman 1982).

The role of Kr81m ventilation imaging in paediatrics has been defined over the last decade (Gordon, Helms and Fazio 1981,

Wong and Silverman 1982). It acts as a supplementary investigation to radiography, delineating abnormalities of regional pulmonary function. While radiography can define the structure of the lungs and anatomical abnormalities, derangement of function can only be inferred from chest Xrays. It has been clearly demonstrated that major abnormalities of ventilation can exist with only minimal radiographic changes.

Recent studies have confirmed its particular value in the uncooperative infant and young child. Wong and Silverman concluded that Kr81m ventilation imaging provides a simple, safe and sensitive means for the follow up of children recovering from the respiratory distress syndrome. There was good agreement between the conclusions drawn from this technique and those of infant plethysmography. These authors suggested that ventilation imaging alone could be used as it was less time consuming and not as prone to technical failure (Wong and Silverman 1981).

Gordon, Helms and Fazio reviewed the first 100 scans performed at the Hospital for Sick Children, London (Gordon, Helms and Fazio 1981). They defined 3 areas in which V/Q lung scans contributed to the management of children with pulmonary disease. In 10 of the 86 patients a diagnosis could be made on the basis of the scan. In 7 patients a normal scan disproved the presumptive diagnosis. In another group of children V/Q scans demonstrated the extent of disease and in 2 of 3 children with pulmonary hypoplasia unsuspected function was demonstrated in the affected lung. Perfusion scans were of particular value in

assessing the state of the pulmonary circulation and measuring the effect of surgical intervention. Furthermore the absence of perfusion with preserved ventilation in paediatric practise was virtually diagnostic of pulmonary sequestration, a normal scan excluded the diagnosis.

Gordon and Helms reported separately on the value of V/Q scanning in the diagnosis of children with unilateral lung disease (Gordon and Helms 1982). In 18 such children aged 1 week to 13 years the V/Q scan contributed to all assessments. They confirmed Godfrey and Mackenzie's observation (Godfrey and Mackenzie 1977) that a unilateral small normally functioning image is virtually diagnostic of pulmonary hypoplasia and that further more invasive tests are unwarranted.

However with such a sensitive technique it is important to identify transient rather than persistent abnormalities. These are most frequently seen in patients with bronchial hyper-reactivity. Fazio et al clearly demonstrated marked functional abnormalities in asthmatic patients that could be reversed by bronchodilator therapy (Fazio et al 1979). It is therefore important to perform ventilation imaging after bronchodilator therapy if there is a history of airway hyper-reactivity before fixed ventilation defects can be confidently diagnosed.

One of the continuing aims of nuclear medicine must be to minimise radiation exposure during diagnostic procedures while ensuring sufficient isotope is administered to produce high quality images that can provide useful clinical information. One of the major advantages of Kr81m over Xe133 that has led to its widespread use is the smaller radiation dose administered to the patient. Li (Li et al 1979) calculated the absorbed radiation dose of a Kr81m image for a 1 year old to be 0.75 milliSieverts (mSv) while that of a Xe133 study would be 7.3 mSv. Gonadal doses would be approximately 0.04 and 0.90 mSv respecively. For a 15 year old Kr81m absorbed radiation dose would be 0.15 mSv per image and 3.0 mSv for a Xe133 study. Gonadal doses would be 0.0078 and 0.20 mSv respectively.

Although the output of Kr81m generators may be measured under standard conditions, it is rarely constant and administered activity is difficult to quantify precisely. Furthermore the length of administration is flexible, usually continued until a satisfactory image has been acquired.

Myers (Myers 1981) has therefore suggested that the absorbed dose from short lived isotopes should be calculated as "absorbed radiation dose per image count". This depends on the degree of attenuation of the emitted radiation as it passes through the lungs and chest wall and also on the detection efficiency of the imaging equipment (collimator and camera). Calibration using

Kr81m is obviously difficult for reasons stated above and therefore Myers chose an indirect method using Tc99m and subsequently allowing for different camera and collimator efficiencies, different energy spectra analysed for each radionuclide and number of available gamma photons from each radioactive decay. Attenuation within the lungs and chest wall were calculated from studies of 15 adults with normal distribution of activity while attenuation in children was derived from in vitro studies using 1 cm plastic discs of different diameters stacked in different configurations to simulate the lung. From these data absorbed dose per unit of image counts can be calculated for adults and children (Figure 2).

Calculation of absorbed radiation dose from Tc99m perfusion imaging is much simpler as the activity administered is known. Whole body absorbed dose resulting from injection of 100 MBq Tc99m MAA in an adult is 1 mSv (Department of Health Handbook of Absorbed Doses from Internally Administered Isotopes). Paediatric dosimetry is less certain but it is generally agreed that the adult dose should be scaled down according to weight or surface area.

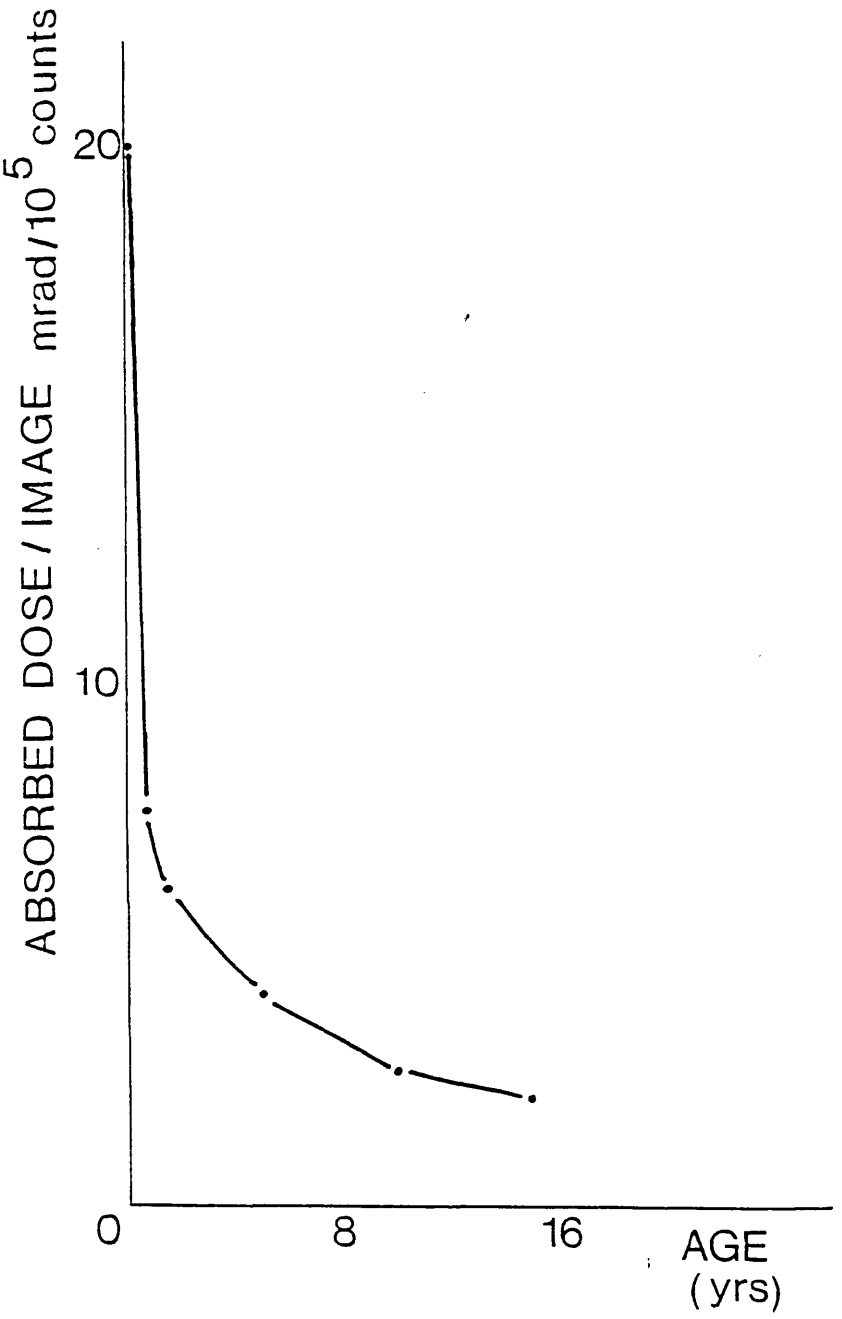


FIGURE 2

Calculated absorbed radiation dose from a 100,000 count Kr81m ventilation image (vertical axis) at different ages (horizontal axis). Data from Myers 1981.

1 mRad = 0.01 mSv

## SUMMARY

Radionuclides have made a major contribution to the understanding of pulmonary physiology and are now an important part of the investigation of lung disease. They provide the only noninvasive means of assessing regional lung function, and require little patient cooperation, making them ideal for use in paediatric practise. Radiation doses are well within acceptable limits for diagnostic imaging.

# CHAPTER 2

# APPARATUS AND METHODS

The Nuclear Medicine Unit is part of the Department of Radiology at the Hospital for Sick Children. V/Q scans performed in this unit are supervised by a Research Fellow from the Respiratory Unit. Radiographers have both paediatric and nuclear medicine training.

Kr81m generators are supplied by the MRC Cyclotron Unit, Royal Postgraduate Medical School, London. The parent radionuclide Rubidium 81m (Rb 81m) present in the generator is bound to an ion exchange column from which Kr81m can be eluted (Jones 1978). For ventilation studies this is done by passing humidified air through the generator at a constant flow (0.5 to 1.0 l/min). Useful activity can be extracted from the generator up to 12 hours after the Rb81m has been attached to the column.

This Kr81m/air mixture is delivered to the patient through a fine (1 mm) catheter to prevent significant decay of the radionuclide before inhalation. A suitably sized face mask (Rendell Baker Soucek) is gently held over the face. In the case of neonates or infants a cupped hand may be less threatening and is often used instead. An electric fan disperses exhaled Kr81m away from the camera face and minimises background activity.

Preparation of Tc99m is conducted under aseptic conditions in a designated radiopharmaceutical preparation area. Tc99m is

eluted from a Molybdenum 99m (Mo99m) generator (Technetium Sterile Generator Amatec, Amersham International plc) and attached to macroaggregates of human serum albumin (Human Albumin Macroaggregate Kit Sorin Biomedica). The macroaggregates are prepared from HIV and hepatitis B surface antigen negative human plasma. Aggregated albumin particles range from 10 to 100 microns in size.

Images are acquired using a Scintronix large field gamma camera with a parallel hole, high resolution collimator (thickness 22.5 mm, approximately 86,600 holes sized 1.18 mm of hexagonal configuration). The similar energy of gamma rays emitted by Tc99m and Kr81m allow both perfusion and ventilation images to be acquired using this collimator; diverging collimators are not used to enlarge the image in infants as resolution suffers. Images are stored both in an online computer (Informatek) for further analysis and on xray film for clinical reporting.

Lung scans are performed while the child lies on the face of the gammma camera which is appropriately reinforced with a glass fibre support sheet. The camera fits into a table which provides support for the child (Figure 3).

**EQUIPMENT FOR WARD STUDIES**

Ventilation studies were also performed on the wards using a mobile gamma camera and dedicated on line computer (Apex 215M Elscint) (Figure 4).

FIGURE 3

Posterior Kr81m ventilation imaging in progress.

Air from the cylinder is humidified and passed through the Kr81m generator. The resultant gas is delivered to the patient through a fine tube and mask. Kr81m is detected by the gamma camera on which the child is lying.

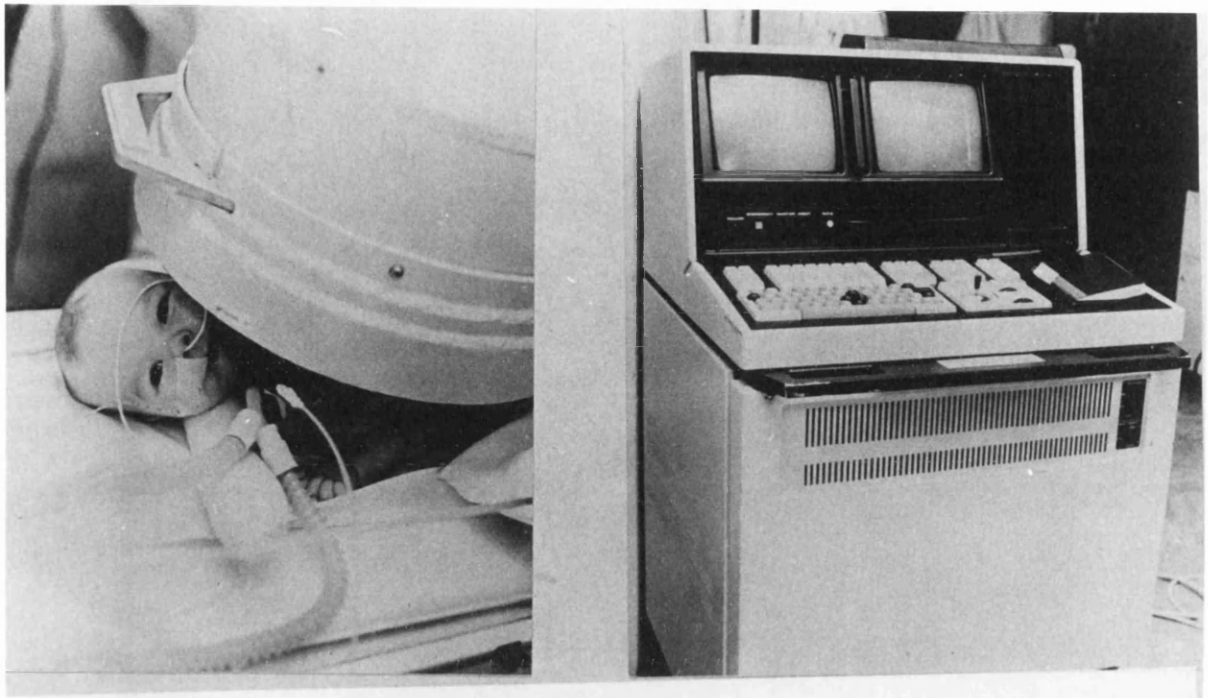

A B

FIGURE 4

A. Infant undergoing anterior Kr81m ventilation imaging using El Scint mobile gamma camera.

B. Dedicated mobile computer.

Kr81m image acquisition was identical to that described below. Images were analysed using similar programs stored within the dedicated mobile computer.

## CLINICAL METHODOLOGY

Children under 5 years of age are admitted to the respiratory ward for sedation (Chloral Hydrate 60-90 mg/kg) while those over five are studied without sedation and therefore attend the x-ray department at the time their investigation has been booked. Young children with evidence of upper airway narrowing are not sedated and infants are also occasionally studied without sedation while asleep after a feed.

One room of the department is dedicated to nuclear medicine. Parents are encouraged to help and reassure their children during the examination. Standard AP and lateral chest radiographs are taken either immediately before or after the V/Q lung scan.

The sequence of the study may be altered to suit the individual patient. If asleep the injection of Tc99m is delayed until completion of the ventilation study. Alternatively in older children or infants not fully sedated, the injection is administered and the child gently restrained when necessary while ventilation and perfusion images are acquired.

Tc99m MAA is injected while the patient is supine to minimise inequality of perfusion caused by gravity. It is

injected as a bolus into a suitable vein through a 25 gauge butterfly needle (Venisystem Abbot). Isotope and blood are not allowed to mix in the tubing as this may cause the macroaggregates to "clump" and give an artefactual mal-distribution of isotope in the lungs. Once the isotope is injected the needle is withdrawn.

With the window of the camera set at 140 kEV (+/-10%) the child is positioned so that the lung apices are near one edge of the collimator to minise background activity in subsequent Kr81m ventilation studies. Once satisfactorily positioned acquisition of a posterior perfusion image is started and continued until a predetermined number of radioactive counts, (200 kilocounts in older children and 150 kilocounts in infants) has been recorded.

The energy window of the camera is then changed to 190 KEV (+/-10%). Once the position has been checked and background activity reduced to an absolute minimum a posterior steady state ventilation image is acquired during continuous inhalation of Kr81m. Ventilation and perfusion studies are repeated in four positions, posterior, right posterior oblique, left posterior oblique and anterior.

Functional abnormality in the right middle lobe or lingula of the left lung may be missed if only these standard positions are used . If pathology is suspected in these lung regions right or left anterior oblique perfusion and ventilation images are

acquired.

## IMAGE ANALYSIS

### 1. QUALITATIVE

For clinical purposes ventilation and perfusion images in the 4 standard views (posterior, right posterior oblique, left posterior oblique and anterior) are recorded on x-ray film and assessed subjectively in conjunction with an AP and lateral chest radiograph taken on the same day. Scans are inspected to identify areas of abnormal ventilation or perfusion and determine whether they are matched (similar defects in both ventilation and perfusion) or unmatched defects (discrepancy between ventilation and perfusion image). Spatial resolution of the imaging procedure allows localisation of the defect to lobar segments and a qualitative report of regional ventilation and perfusion is provided.

### 2. QUANTITATIVE

Quantification of the steady state image is accomplished using interactive computer programs that allow comparison of ventilation or perfusion to either lung or any lung region. Images are stored in the computer as 64*64 matrices which can be interpolated to 256*256 matrices and displayed on screen (Figure 5). Using a "Region of Interest" program, areas of any size or shape within this image can be defined. Kr81m or Tc99m activity

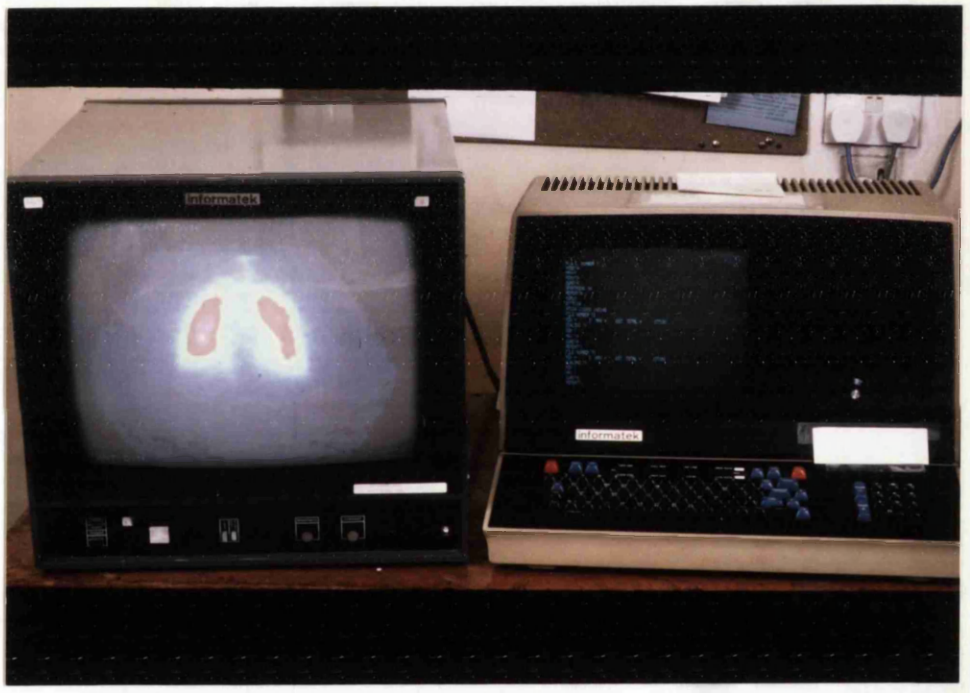


FIGURE 5

Dedicated computer and TV screen

within these areas can then be displayed by a separate program. Using this information fractional ventilation or perfusion to any lung or lung region, defined as:

$$\frac{\text{Activity within region}}{\text{Total activity recorded over both lungs}} * 100\ (\%),$$

can be calculated.

## VENTILATION AND PERFUSION IMAGING IN DIFFERENT POSTURES

### 1 VENTILATION

The effects of posture on regional ventilation were studied using right and left lateral decubitus images. For these images the gamma camera head was rotated until vertical and the patient repositioned with his or her back against the camera face in either the left or right decubitus posture. Posterior steady state ventilation images of 150,000 or 200,000 counts were then acquired using the technique described above.

To examine postural changes in fractional ventilation (Vf) to either lung (proportion of ventilation distributed to one lung), Kr81m activity recorded over the lung was calculated and expressed as a percentage of the activity from both lungs using the computer programs described above. This was calculated for the different postures.

## 2 PERFUSION

As the macroaggregates impact in pulmonary capillaries Tc99m MAA imaging allows the assessment of regional perfusion in only one posture. Repositioning the patient will not alter the distribution of activity and it was therefore necessary to use a different study design to investigate the effect of posture on regional perfusion.

One third of the calculated dose of Tc99m macroaggregates was injected into a peripheral vein with the child in the supine posture. The dosage used was based on an adult dose of 37 MBq, scaled down according to surface area of the child (Chandra et al 1973). Once the child was settled a posterior 100 kilocount Tc99m perfusion image was acquired.

The child was then positioned in the lateral decubitus posture. The remaining Tc99m macroaggregates were then injected and once no further activity was visible in the arm the child was returned to the supine position and a second Tc99m perfusion image of the same length as the first was acquired.

All images were stored on the dedicated computer. Pulmonary perfusion was calculated using these two images from the distribution of the isotopes .

Regions of interest corresponding to right and left lung were identified and activity within each was calculated. The distribution of perfusion to the right lung (QfR) was expressed

as:

$$\frac{\text{Counts in right lung}}{\text{Counts in right lung + counts in left lung}} * 100\ \%$$

The distribution of perfusion in the supine position was calculated using the first image. As the macroaggregates lodge in the capillaries and the Tc99m half life is 6 hours, the second perfusion image represents the sum of activity in the lung injected in both supine and lateral decubitus postures. To allow for this activity detected within each lung in the first perfusion image was subtracted from the activity in the same lung in the second perfusion image. This provided the distribution of the radionuclide injected in the lateral decubitus posture alone and QfR in the lateral decubitus posture was then calculated.

If the two images are acquired over the same field of view of the gamma camera (i.e. the child is repositioned in the identical place for the second image) a separate program can be used which directly subtracts activity within one image from that of another.

This is illustrated in Figure 6. As this was only possible in cooperative children it was not universally adopted.

SUPINE RIGHT DECUBITUS

PERFUSION

VENTILATION

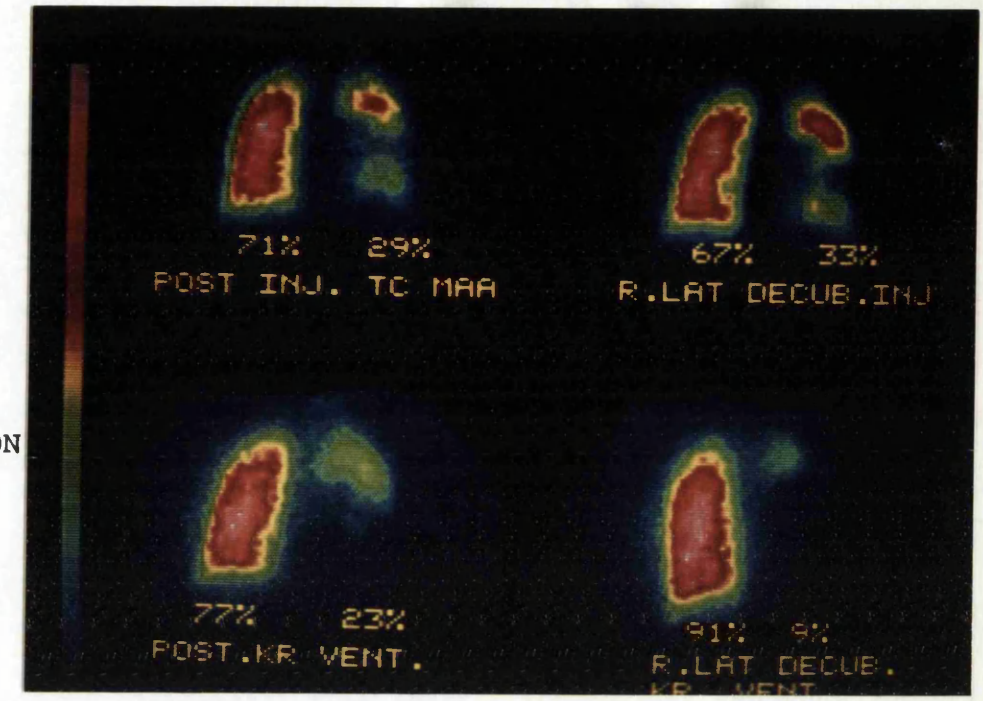


FIGURE 6

Supine and right lateral decubitus steady state perfusion and ventilation images in an eight year old child with residual lung damage after pertussis infection.
A posterior perfusion image was first acquired after injection of one third of the total dose of Tc99m MAA while the child was supine (left upper image). After turning the child onto her right side the remaining radionuclide was injected. She was then repositioned over exactly the same area of the camera face and a second perfusion image acquired (not shown). Using an image subtraction program the first image was subtracted from the second, thus constructing a third (right upper image) which represents the distribution of perfusion in the decubitus posture. Fractional perfusion was calculated from these two images.
Fractional ventilation was calculated from supine (left lower image) and right decubitus (right lower image) steady state images.
Note that ventilation and perfusion are redistributed in the opposite direction when the child is repositioned.

In steady state ventilation images Kr81m activity is stored in a single frame or matrix, acquisition being terminated when a predetermined number of counts has been acquired. A suite of computer programs allows acquisition and storage of the Kr81m activity in sequential timed frames, whose length can be adjusted to match the respiratory frequency of the patient. Frame speeds varied from 5 per second in neonates to 1 frame per second in older children. Each dynamic image varied in length but characteristically 50 or 100 frames were acquired. Activity may be acquired in this way during continuous inhalation of Kr81m (dynamic steady state imaging) or during washout of the radionuclide (dynamic washout imaging) or during a forced vital capacity manoeuvre.

## DYNAMIC IMAGE ANALYSIS

Dynamic steady state and washout ventilation images were analysed in an identical manner to provide activity/time curves for either lung or any lung region.

Kr81m activity in all frames of the dynamic series was summated and stored separately to provide a single steady state image. This image was displayed and using a line drawing program, regions of interest defined (Figure 7). Using the original sequential frames and the regions of interest defined on the summated image, activity/time curves were created for predefined

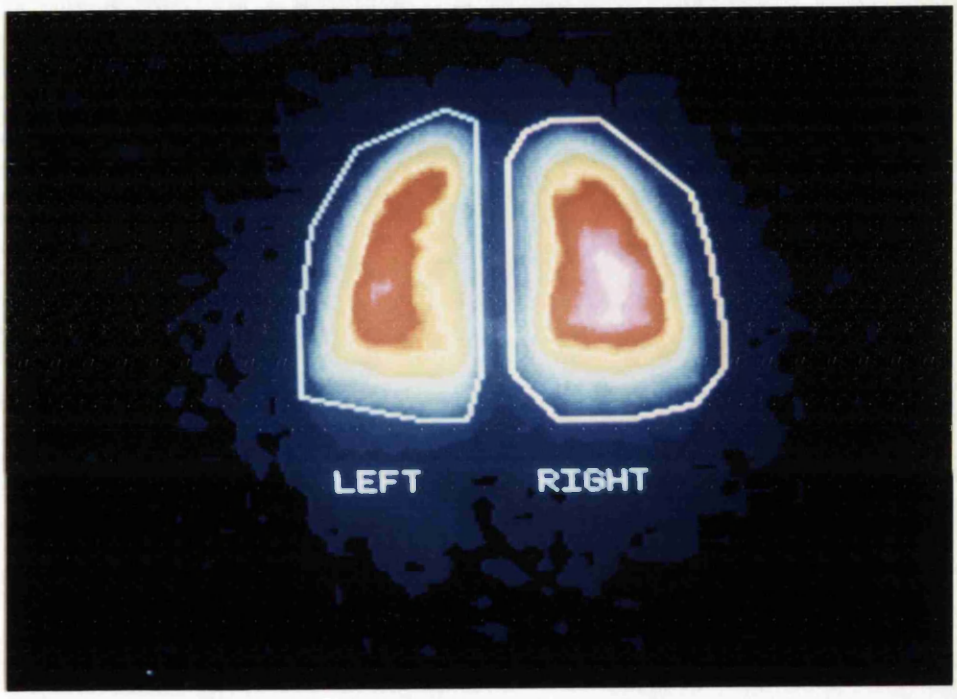


FIGURE 7

Posterior ventilation image created by adding together all dynamic frames. "Regions of Interest" corresponding to left and right lung drawn in.

lung regions (Figure 14 page 75).

## SPIROMETRIC RECORDING DURING VENTILATION IMAGING.

### 1. TIDAL BREATHING

Cooperative children and adults breathed through a mouthpiece attached to a differential pressure pneumotachograph (Fleisch 1) while infants were sedated and breathed through a closely fitting mask which was gently applied and kept in place using therapeutic putty (Carters Westbury WILTS UK). Tidal volume was derived by integrating the flow signal.

### 2. FORCED VITAL CAPACITY MANOEUVRE

Forced Vital capacity (VC) was recorded using either a dry wedge spirometer (Vitalograph, Buckingham,UK) or a Fleisch size 3 pneumotachograph.

## CALIBRATION OF EQUIPMENT

### PNEUMOTACHOGRAPHS

Volume signals were recorded by electronic integration of flow signals from the pneumotachograph and subsequently recorded on magnetic tape (Racal STO 4 four channel tape recorder). An electronic digitimer (Digitimer UK, Welwyn Garden City) provided

a time scale for synchronisation of Kr81m activity and tidal volume traces. Linearity of both pneumotachographs was confirmed prior to use and flow rates in each study were calculated to ensure they fell within the linear range.

Volume calibration was performed prior to each respiratory manoeuvre using a 50ml calibrated syringe.

DRY WEDGE SPIROMETER

Volume calibration was performed prior to use with a calibrated 3 litre syringe (Vitalograph Buckingham England).

| | | 1 LITRE | 1.5 LITRE | 3 LITRE |
|---|---|---|---|---|
| Spirometer reading | 1. | 0.93 | 1.43 | 2.98 |
| | 2. | 0.98 | 1.47 | 3.01 |
| | 3. | 0.95 | 1.50 | 2.96 |
| Mean error (%) | | 3.67 | 2.22 | 0.78 |

**SIMULTANEOUS NITROGEN AND KR81M WASHOUT STUDIES**

Subjects were positioned in front of the gamma camera and breathed from a respiratory circuit containing a differential pressure pneumotachograph (Fleisch '1') and continuous N2 meter (H-P Model 47302A Hewlett Packard Waltham MASS USA). A switch on

the inspiratory limb of this circuit allowed delivery of either an air and Krypton 81m mixture or 100% oxygen.

Calibration of the N2 meter showed a mean bias of - 4.35% (SD 2.49)

Tidal volume was recorded by electronic integration of the flow signal from the pneumotachograph and exhaled N2 concentration was recorded continuously by the N2 meter. Both signals were stored on magnetic tape using a four channel tape recorder (Racal Sto 4). Dynamic posterior Krypton 81m ventilation images were stored in the computer. An electronic digital time signal provided synchronisation between tape recorder and dynamic ventilation image.

When the subject was satisfactorily positioned Kr81m was added to the inspired air and after a further minute to allow Kr81m levels to plateau, recording of tidal volume and exhaled N2 concentration was commenced. After Kr81m activity had stabilised the dynamic Kr81m ventilation image was started. At subsequent end expiration, Kr81m and N2 washout were started by switching the subject into the circuit containing 100% O2. Clearance of Krypton 81m and N2 were recorded for a minimum of 30 seconds. At the same time as the withdrawal of Kr81m the electronic time signal was commenced in order to align the 2 separate signals. Tidal volume and nitrogen traces were subsequently replayed onto paper using a Gould brushpen 2600s recorder. The first 20 seconds of each trace were used. Calculation of the time for

Kr81m activity and N2 concentration to fall to half initial value (t0.5) was calculated using a linear regression programme after logarithmic transformation of the data.

# CHAPTER 3

## THEORETICAL ANALYSIS OF KR81M VENTILATION IMAGES

## 1. THE STEADY STATE IMAGE

Current interpretation of the steady state Kr81m ventilation image is based on the theoretical analysis of Fazio and Jones (Fazio and Jones 1975).

In their report, Fazio and Jones suggested that Krypton 81m activity would only reflect regional ventilation if inspired and alveolar Kr81m did not reach equilibrium. When ventilatory turnover is high (greater than 3 $min^{-1}$) and equilibrium has been reached their model predicted that regional activity would reflect regional lung volume rather than ventilation (Figure 8).

This would have important implications in paediatric practice. Specific ventilation (Sp. V.) is typically much higher in infants ( 5-10 $min^{-1}$) declining to normal adult values in the second decade of life (Polgar and Promadhat, 1971). Values as high as 15-20 $min^{-1}$ (calculated from Kr81m dynamic washout studies) have been recorded in lung regions of sick neonates (Wong and Silverman 1981). If the meaning of the steady state image changes because of changing Sp. V. during childhood the use of this nuclide to monitor progress and therapeutic response of pulmonary disease would be limited.

The mathematical analysis of Fazio and Jones was based on a uni compartment model in which gas mixing would be instantaneous and Kr81m would be uniformly distributed. In such a case:

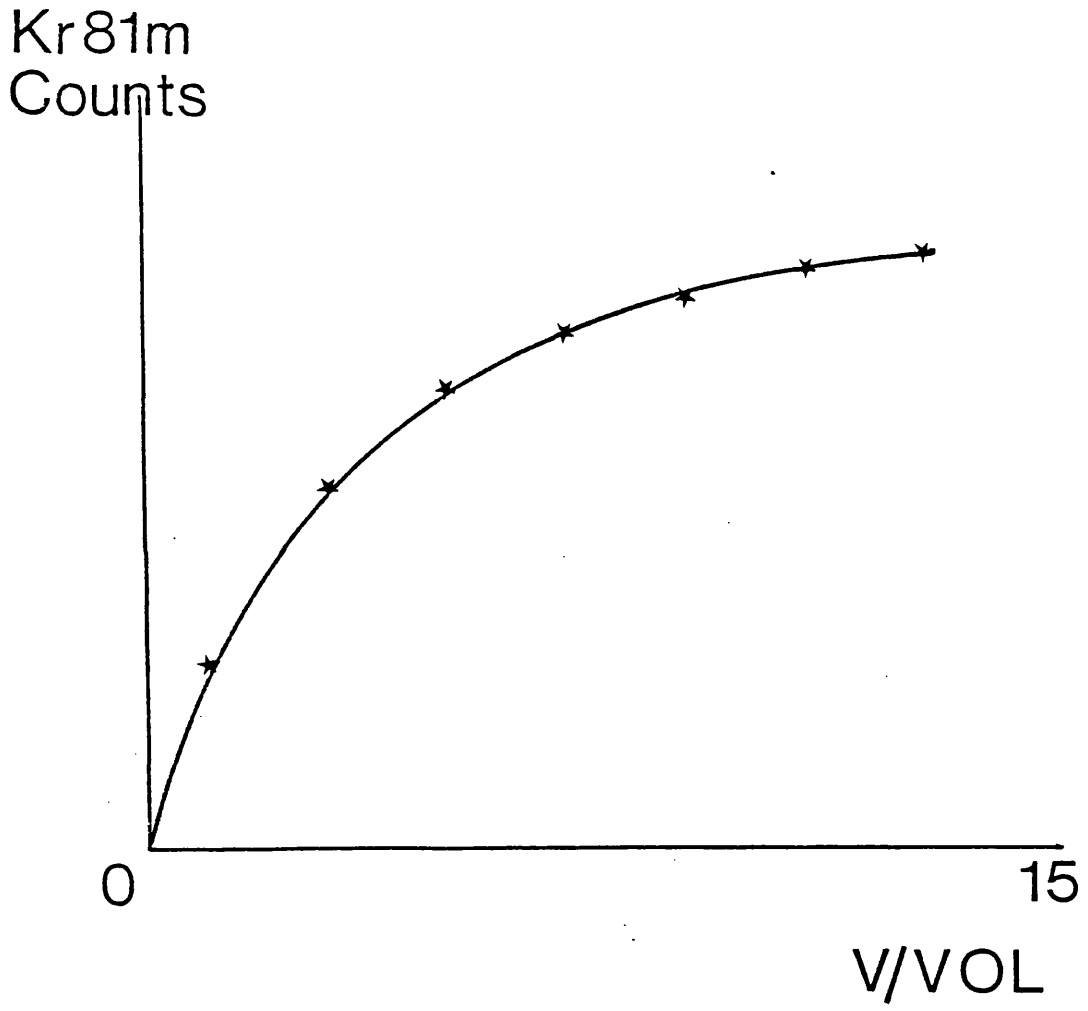


FIGURE 8

Predicted relationship between Kr81m activity (N81) (ordinate) and specific ventilation (abscissa) using the equation derived by Fazio and Jones (see text):

INSPIRED ACTIVITY = EXHALED ACTIVITY + ACTIVITY DECAYED

i.e.

$$Vi * Ci(81) = Ve*Cl(81) + lambda * N(81) \quad (1)$$

Where

Vi - Volume of gas inhaled

Ci(81) - Concentration of Kr81m in inhaled gas

Ve - Expired volume

Cl(81) - Kr81m concentration in expired gas

Lambda - Radioactive decay constant of Kr81m ($3.2\ min^{-1}$)

N(81) - Regional Kr81m activity

Concentration of Kr81m can be expressed as regional activity divided by volume of the compartment, ie N(81)/Vol where Vol is regional volume.

Substituting N(81)/Vol for Cl(81):

$$Vi * Ci(81) = Ve*N(81)/Vol + lambda * N(81)$$

Rearranging :

$$N(81) = \frac{Vi * Ci(81)}{Ve/Vol + lambda}$$

Inspired and expired volumes will be identical (Ve = Vi) and therefore

$$N(81) = \frac{V * Ci(81)}{V/Vol + Lambda}$$

A proportion of emitted activity will not be detected by external counting so a factor, K(81) needs to be introduced to allow for camera efficiency and tissue attenuation. The expression becomes:

$$N(81) = K(81) * \frac{V * Ci(81)}{V/Vol + Lambda} \qquad \text{Equation 1}$$

Fazio and Jones argued that while V/Vol is within or below the normal adult range (1-3 $min^{-1}$), the denominator will effectively be lambda. Hence as other expressions are constant, regional Kr81m activity will be proportional to ventilation and uninfluenced by regional lung volume. However when ventilatory turnover increases the denominator will be more dependent on V/Vol rather than lambda and the equation can be simplified to:

$$\text{Kr81m activity} = \frac{V * Ci(81)}{V/Vol}$$

or $$= Vol * Ci(81).$$

Hence regional Kr81m activity will be proportional to volume rather than ventilation.

Using this mathematical model they calculated the relationship between regional Kr81m activity and Sp V for changing values of ventilation (Figure 8). This suggests that Kr81m activity and ventilation are only linearly related when specific ventilation is below 4 $min^{-1}$. Above this value the

Kr81m static image will be relatively insensitive to changes in ventilation. This theoretical analysis therefore questions whether the steady state image can be used to monitor pulmonary disease through childhood. If it is to be an accurate reflection of regional ventilation it must be shown that Kr81m activity is sensitive to changing ventilation at all ages.

Using published values for Tidal Volume (TV), Functional Residual Capacity (FRC), respiratory rate (RR) and Dead Space (DS) (Polgar and Promadhat 1971) for different body weights (and hence ages) the theoretical relationship between ventilation and Kr81m activity has been calculated for a neonate of 3.5 kg, a child of 20 kg and an older child of 50 kg (Appendix 1). The relationship between SpV and calculated Kr81m activity using the model of Fazio and Jones is displayed in Figure 9.

To allow comparison specific ventilation and Kr81m activity have been expressed as a percentage of that calculated at the predicted mean respiratory rate for children of that weight.

The relationship is alinear in the three groups; as specific ventilation increases the rate of change of Kr81m activity falls. In the smaller children the method is theoretically less sensitive, the slope of the graph is flatter, a fixed change in ventilation causing a smaller alteration in Kr81m activity. However the model suggests that even in 3 kg infants Kr81m activity increases as specific ventilation rises, up to values of 10.0 $min.^{-1}$

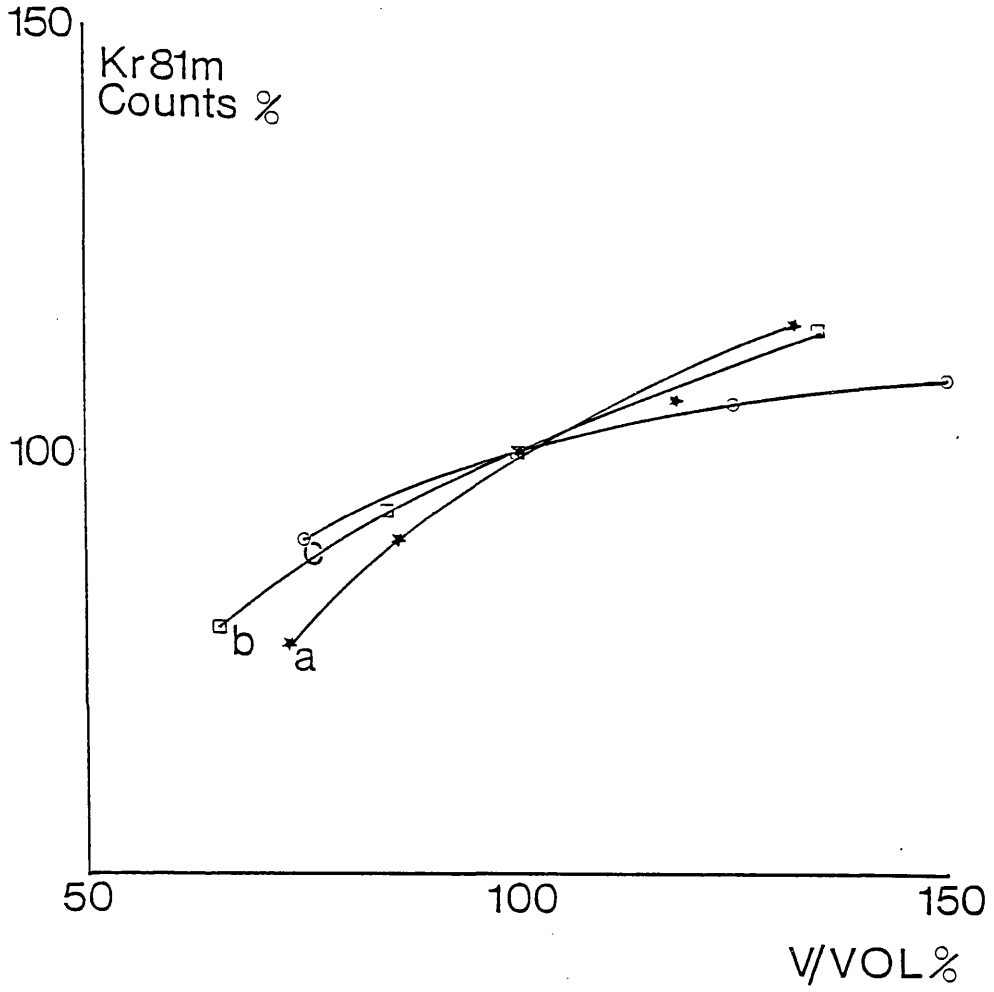


FIGURE 9

Predicted relationship between Kr81m activity and specific ventilation using theoretical model of Fazio and Jones.

Each line represents the effect on Kr81m activity of changing ventilation at mean lung volume for :-
a) Child of 50 kg (12 year old)
b) Child of 20 kg (6 year old)
c) Infant of 3.5 kg (term infant)
It can be seen from this model that Kr81m activity increases in all cases but the changes are smaller in the infant

This is in agreement with clinical experience of V/Q scanning. Individual ventilation images in infants with high specific ventilation can demonstrate that Kr81m activity is sensitive to changes in regional ventilation.

A clinical example serves to illustrate this point.

DM was a 3 month old child with the diagnosis of the fetal valproate syndrome referred for investigation of persistent respiratory symptoms. She had had a persistent patent ductus arteriosus ligated in the neonatal period. Simultaneous tidal volume monitoring during a Kr81m ventilation scan gave a minute alveolar ventilation of 1578 mls/min. Thoracic gas volume of 125mls derived by plethysmography (113.5 corrected for anatomical deadspace) gave a value for Sp V during ventilation imaging of 13.9 $min.^{-1}$ This is well above the values at which the theoretical model predicts that Kr81m activity would reflect regional ventilation. Inspection of the right posterior oblique (RPO) steady state image and chest radiograph (Figure 10) clearly demonstrates regions of expanded lung with reduced Kr81m activity indicating that Kr81m ventilation imaging can identify expanded yet hypoventilating regions of lung even at this high Sp V of 13.9 $min.^{-1}$

These findings are in agreement with the work of Modell and Graham (Modell and Graham 1982) who have studied the effect of changing ventilation on the steady state Kr81m image in anaesthetised, ventilated dogs. Ventilation was altered by adjustment of either respiratory rate or tidal volume. Steady

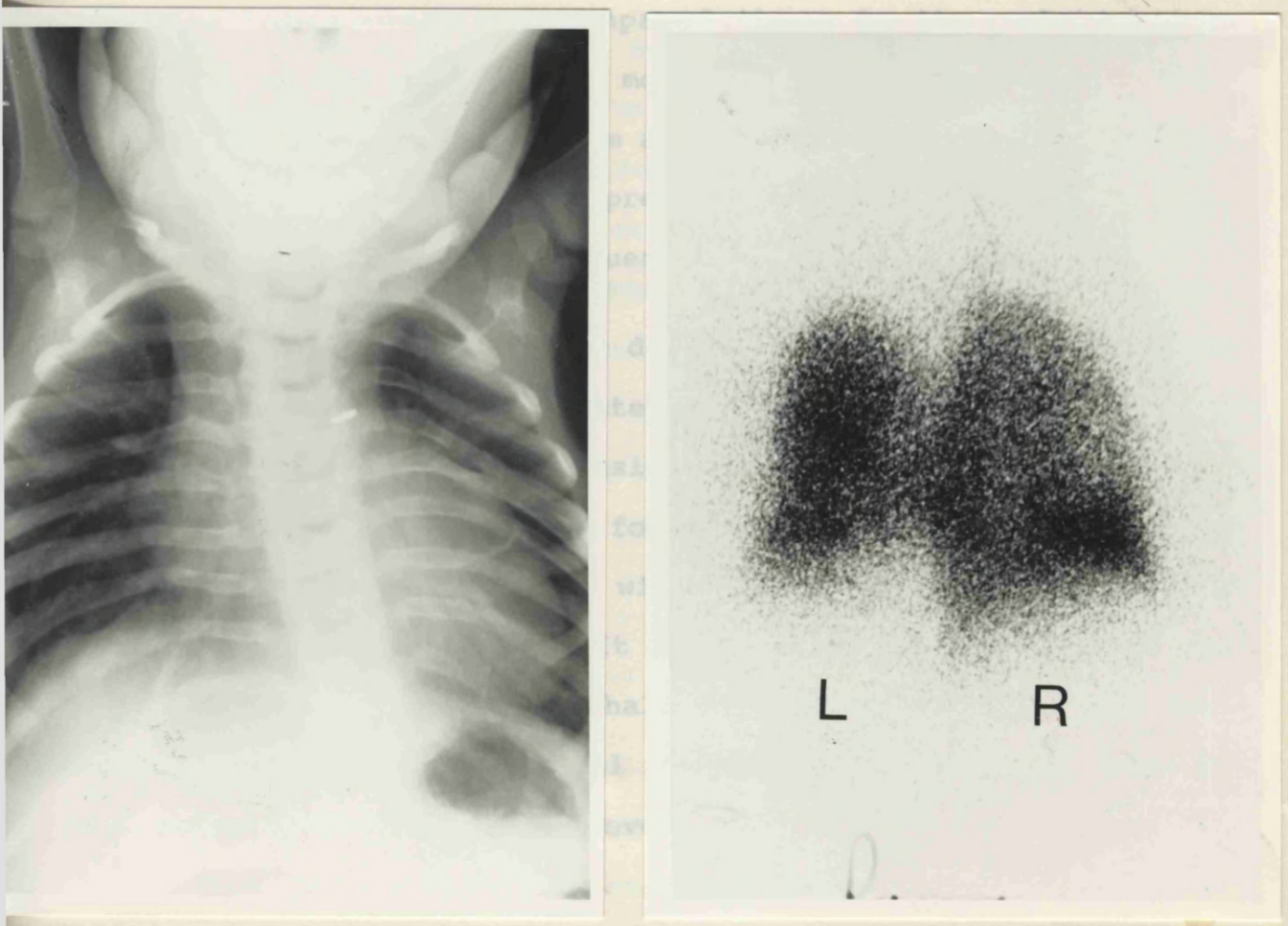


FIGURE 10

AP Chest Xray and Right Posterior Oblique ventilation scan of DM. Note the varying regional Kr81m activity in expanded areas of upper zone of the right lung.

state Kr81m images were acquired for 100-200 seconds. End expiratory volume was either estimated from published data on the basis of body weight or obtained directly by a Xe133 dilution technique.

They determined the relationship between Kr81m activity and specific ventilation and compared these to the relationship predicted by the theoretical model of Fazio and Jones. They demonstrated that in vivo Kr81m activity is more linearly related to ventilation than the model predicts and this linearity is seen up to specific ventilation values of 12-15 $min^{-1}$.

They postulated that this discrepancy could be explained if Kr81m was not evenly distributed throughout the end expiratory lung volume. Previous work using N2 (Fowler et al 1952) has clearly demonstrated that a foreign gas does not equilibrate immediately with resident gas within the lungs, even in healthy subjects with normal lungs. It is therefore unlikely that a gas such as Kr81m with a short half life of only 13 seconds can equilibrate with the functional residual capacity (FRC), even at high rates of ventilatory turnover.

If the volume of distribution of Kr81m (Vol) is not constant and rises as ventilation increases (V), the term V/Vol in the denominator of equation 1 will remain relatively constant.

$$N(81) = K(81) \times \frac{V \times Ci(81)}{V/Vol + Lambda} \qquad \text{Equation 1}$$

Modell and Graham proposed that as ventilation increases so will the volume of distribution of Kr81m (Vol). If this is so the denominator in equation 1 will not be dominated by V/vol at high rates of ventilatory turnover and a more linear relationship between ventilation and Kr81m activity would be predicted.

To test this hypothesis Modell and Graham compared the volume of distribution of Kr81m in a 3 litre gas bag where gas mixing would be instantaneous and in anaesthetised dogs ventilated at different respiratory rates and tidal volumes. End expiratory volume of distribution of Kr81m was determined using a different experimental technique. Twenty eight gated ventilation images were acquired during each breath. As the dogs were paralysed and ventilated, each breath was identical and activity in each image could be added to the appropriate image in the previous breath to provide a "summated" picture. They argued that:

$$\frac{A(peak)}{A(min)} = \frac{Vi}{Vo}$$

A(peak) is Kr81m activity at end inspiration

A(min) is Kr81m activity at end expiration

Vi is volume of distribution at end inspiration

Vo is volume of distribution at end expiration

OR $$\frac{V_i}{V_0} = \frac{Vo + Vt}{Vo}$$

where Vt is tidal volume.

End expiratory volumes measured directly or independently derived from published data were then compared with the calculated volume of distribution of Kr81m. While these agreed closely for the 3 L balloon demonstrating that Kr81m was evenly distributed in the 3 litre bags, there was a marked discrepancy in the case of the ventilated dogs. This discrepancy was less at higher ventilatory turnover. Kr81m was distributed in a greater proportion of the resident lung volume as SpV rose, but was never consistently distributed throughout the resident lung volume.

## SUMMARY

Modell and Graham's data suggest that in vivo the volume of Kr81m distribution may rise as ventilatory turnover increases. The term V/Vol may remain more constant than the theoretical model developed by Fazio and Jones would predict and the steady state Kr81m ventilation image will therefore be a more accurate reflection of regional ventilation than the model would predict. Kr81m activity will still be a measure of regional ventilation when specific ventilation has risen to values as high as 10 $min.^{-1}$

## 2. KRYPTON 81M WASHOUT IMAGES

The difficulties in quantifying the steady state image have led workers to investigate Kr81m washout or clearance studies as a means of determining regional specific ventilation (Ciofetta et al 1980).

The rate of fall of Kr81m activity once inhalation of the radiotracer ceases will depend upon clearance by continuing ventilation and natural radioactive decay. Dynamic ventilation imaging allows quantification of this process. Kr81m activity recorded over the lungs is stored in sequential frames of predetermined length and subsequently analysed to provide time activity plots for predefined regions of lung. These can be used to calculate regional specific ventilation (V/Vol) using the equation :-.

$$V/Vol = \ln 2 / t(0.5) - \lambda_{Kr81m} \qquad \text{Equation 2}$$

where V = minute ventilation
t(0.5) = half life of Kr81m washout from the lung or lung region
Vol = volume of distribution of Kr81m
lambda Kr81m = the decay constant of Kr81m (3.2).
ln2 = log(natural)2

t(0.5) is calculated from the clearance curve, and V/Vol a quantitative index of ventilation, can then be calculated. If ventilation (V) is simultaneously recorded during washout of the nuclide, the volume of distribution of Kr81m can be calculated.

Wong and Silverman have used this technique to study regional ventilation in infants recovering from the respiratory distress syndrome (Wong and Silverman 1982). In 11 infants lung function tests and Kr81m ventilation lung scans were performed under light sedation with chloral hydrate. Specific ventilation was calculated from tidal volume measured by electronic integration of the signal from a differential pressure pneumotachograph and functional residual capacity measured by plethysmography (FRC pleth). After these tests, under the same sedation, steady state Kr81m ventilation scans and Kr81m washout studies were acquired.

They found close agreement between specific ventilation determined by respiratory function tests and dynamic Kr81m washout. Assuming that alveolar ventilation would be similar during each study they concluded that the volume of distribution of Kr81m and FRC (pleth) were practically identical. The Kr81m steady state image in these infants would therefore reflect regional lung volume rather than ventilation, supporting the theoretical analysis of Fazio and Jones. However, in 8 of the 13 subjects studied, specific ventilation measured during the plethysmographic study was greater than specific ventilation derived from Kr81m washout. If the pattern of ventilation during the two studies was identical these results suggest that the volume of distribution of Kr81m was larger than FRC (pleth), a result that is plainly impossible.

In view of this inconsistency the study was repeated. Using identical techniques 10 infants attending the Hospital for Sick Children for the investigation of respiratory symptoms were studied. Specific ventilation was determined in an identical fashion to that of Wong and Silverman.

Details of children studied are included in Table 2. Mean age was 6.3 months (6 weeks to 1 year 1 month) and mean specific ventilation (V/Vol) was 7.2 (4 - 11), slightly lower than the range in subjects studied by Wong and Silverman. The relationship between the volume of distribution of Kr81m and FRC pleth can be expressed by dividing V/Vol (pleth) by V/Vol Kr81m (A/B). If ventilation is assumed to be the same during each investigation this fraction becomes Vol Kr81m / FRC(pleth), ie the fraction of FRC in which Kr81m is distributed.

## RESULTS

Mean V/Vol determined from Kr81m washout was 13.3 (range 5.8 - 20.1) whereas mean V/Vol determined by plethysmography was 7.2 (range 4.0-11). In all cases V/Vol determined from Kr81m washout studies was greater than that determined by lung function tests. The volume of distribution of Kr81m had a mean value of 56% FRC(pleth), similar to that determined by Modell and Graham in laboratory animals (Modell and Graham 1982). The relationship between this fraction and V/Vol determined by plethysmography is depicted in Figure 11. There is no clear relationship between the two parameters although the graph sugggests that as V/Vol increases so does the fraction Kr81m VOL/ FRC(pleth).

TABLE 2

Comparison of specific ventilation (V/Vol) derived from plethysmography and Kr81m washout.

| | SEX | DIAGNOSIS | AGE (months) | A V/VOL (pleth) | B V/VOL (Kr81m washout) |
|---|---|---|---|---|---|
| 1 | M | C.F. | 7 | 11.0 | 20.1 |
| 2 | M | C.F. | 8 | 4.0 | 13.8 |
| 3 | M | Post Pneumonia | 1 | 5.9 | 10.9 |
| 4 | F | C.F. | 5 | 6.8 | 12.4 |
| 5 | M | C.F. | 13 | 6.8 | 16.5 |
| 6 | M | V.S.D. | 4 | 7.3 | 12.3 |
| 7 | F | C.D.H. | 2 | 8.0 | 12.8 |
| 8 | M | Aspiration Pneumonia | 2 | 4.4 | 5.8 |
| 9 | F | C.F. | 9 | 8.9 | 11.9 |
| 10 | M | Wilson-Mikity | 2 | 9.0 | 16.8 |
| | | | MEAN | 7.2 | 13.3 |

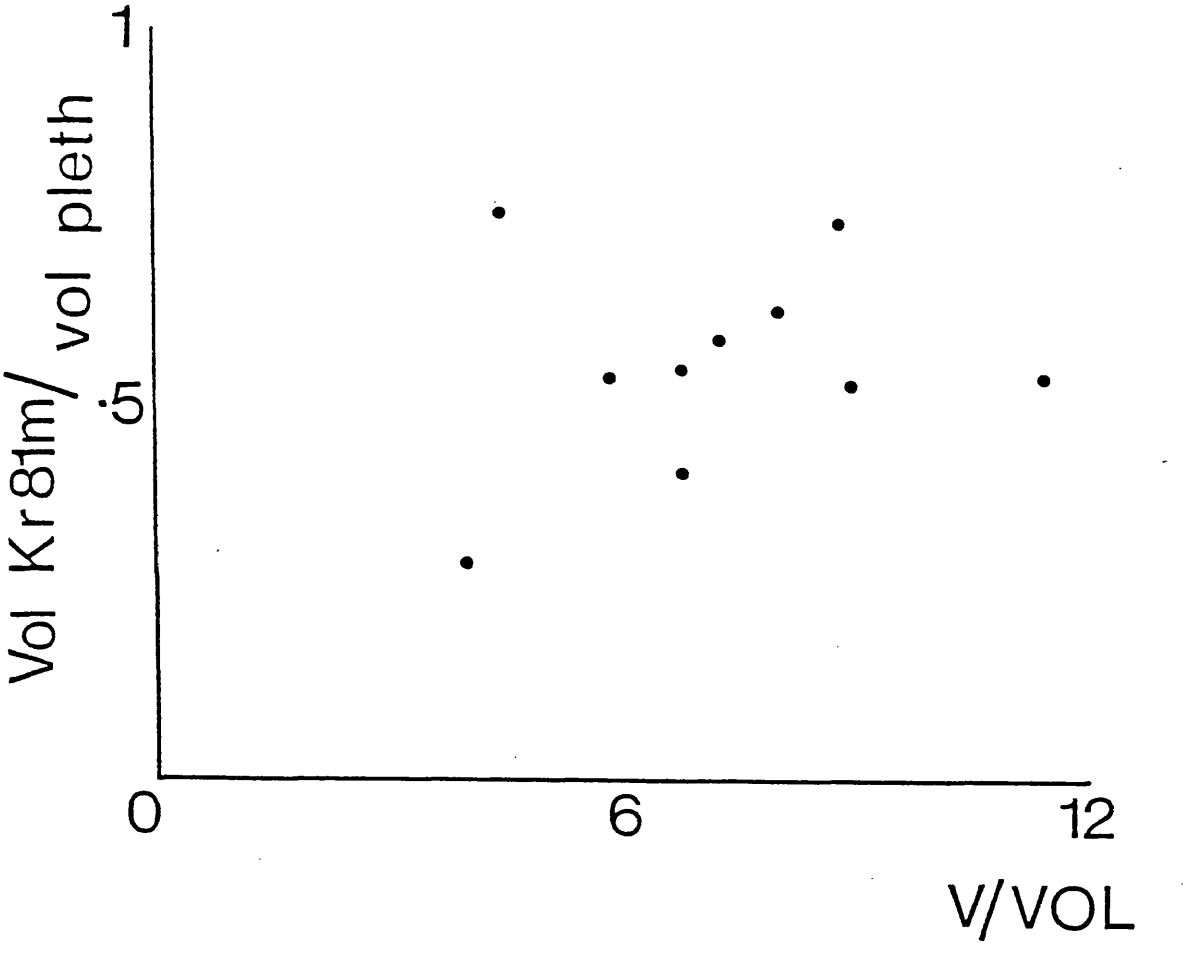


FIGURE 11

Relationship between specific ventilation (horizontal axis) and proportion of FRC(pleth) in which Kr81m is distributed (Vol Kr81m/vol pleth) (vertical axis). Data suggest that Kr81m is not distributed throughout FRC although as V/Vol increases it is distributed through a greater proportion.

This is in line with Modell and Graham's animal experiments that inspired and resident Kr81m do not reach equilibrium in the range of specific ventilations of 4 to 11 $min.^{-1}$ Kr81m may however be distributed through a larger fraction of FRC as specific ventilation increases.

Although attractive this method has theoretical limits to its accuracy that raise questions about its clinical application.

1. The short half life of Kr81m results in rapid decay to background levels of radioactivity so the washout period is very short, in some cases lasting only 5 to 10 seconds (Figure 12). Consequently any irregularity of respiration during the period of Kr81m washout could affect the results.

2. Kr81m images are acquired as sequential frames of a predetermined length and activity within these frames fluctuates with respiration, rising during inspiration and falling during expiration. This is illustrated by a clinical example (Figure 12). Kr81m was withdrawn at B. Inhalation of the remaining Kr81m in the dead space resulted in a small rise in activity within the lungs falling rapidly with expiration. The rate of fall in activity slowed at the next inspiration as remaining activity within the dead space was inhaled again. Calculation of t(0.5) from peak activity (end inspiration or A) would yield a value of 2.67 $min^{-1}$ for specific ventilation while calculation from the true end expiration point (B) to correspond with washout from the end tidal volume gives the very different value of 0.93

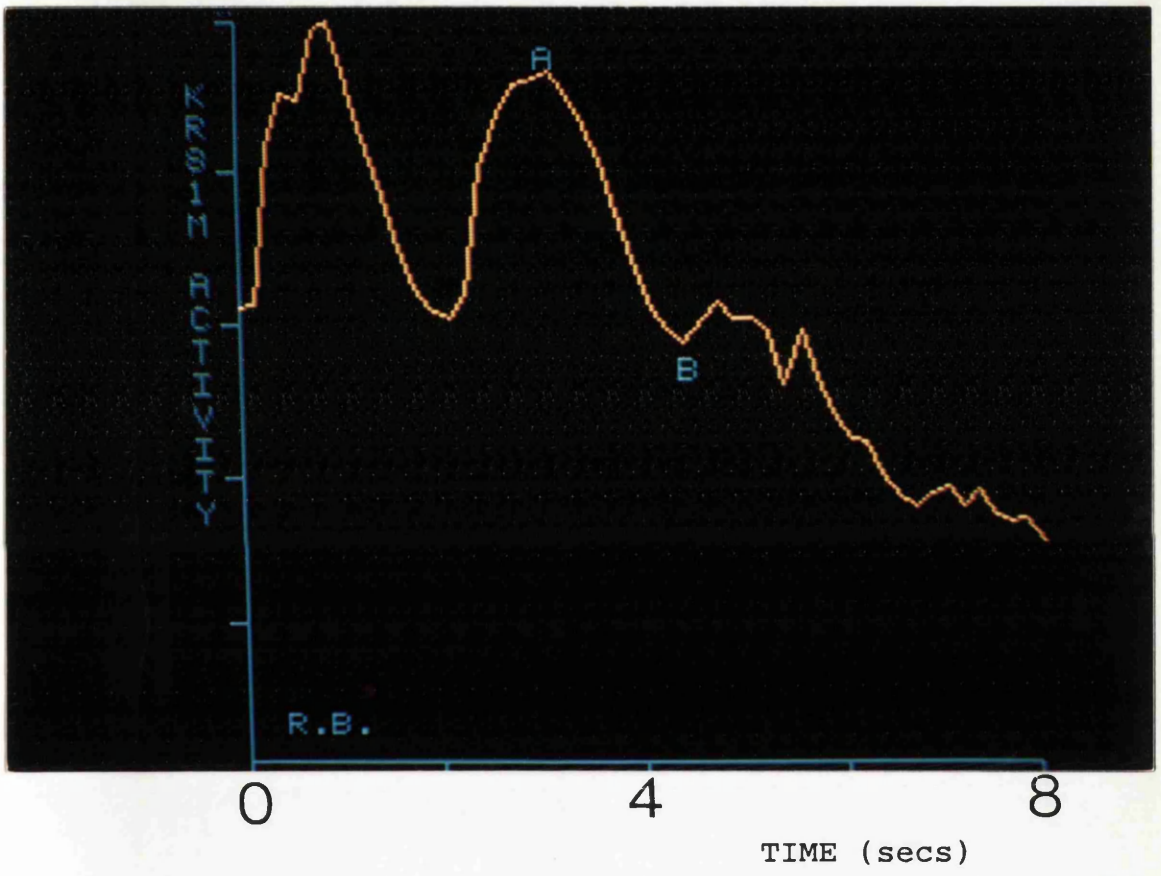


FIGURE 12

Dynamic wash out ventilation image in a healthy adult volunteer.

Time is on the horizontal axis, Kr81m activity on the vertical axis. Kr81m is withdrawn at "B". Activity initially rises as fresh Kr81m is inhaled from the dead space and then falls rapidly. Calculation of V/Vol from peak activity "A" or "B" gives very different results (see text).

$min^{-1}$, a difference of 287%.

The point at which Kr81m washout is deemed to begin is therefore critically important. Previous studies have not recorded this and their conclusions must therefore be questioned.

## COMPARISON OF KR81M AND N2 WASHOUT IN COOPERATIVE SUBJECTS

As an alternative and more accurate technique the volume of Kr81m distribution can be compared with that of a resident gas such as nitrogen (N2). Simultaneous Kr81m and N2 washout studies allow direct comparison of the volumes of distribution and clearance of both gases.

Seven adult volunteers aged 20 to 40 were studied. Simultaneous Kr81m and N2 washout studies were performed (Chapter 2). Subjects breathed an air/Kr81m mixture until detected activity fluctuated from a constant end expiratory level. At end expiration they were switched out of this circuit into 100% 02 with no Kr81m.

## RESULTS

V/Vol determined on the first 20 seconds of N2 clearance varied from 0.78 to 3.56. (Table 3) Mean ratio of SpVs was 0.73 (range 0.35 - 1.48) and no consistent relationship was found between ventilatory turnover and volume of distribution of Kr81m. In 3 studies (PH1, PH2 and HD1) the volume of distribution

TABLE 3

Specific ventilation calculated from N2 and Kr81m washout

| | SPECIFIC VENTILATION calculated from 1 | 2 | |
|---|---|---|---|
| NAME | N2 washout | Kr81m washout | 1/2 |
| PH1 | 0.95 | 0.70 | 1.36 |
| PH2 | 0.93 | 0.63 | 1.48 |
| PH3 | 1.01 | 1.29 | 0.78 |
| JA1 | 3.56 | 5.12 | 0.69 |
| JA2 | 4.37 | 9.35 | 0.47 |
| MP | 0.78 | 0.89 | 0.88 |
| HD1 | 1.50 | 1.05 | 1.43 |
| HD2 | 1.36 | 2.09 | 0.65 |
| UN | 1.43 | 2.05 | 0.70 |
| GB | 2.73 | 3.99 | 0.68 |
| MO | 1.38 | 3.89 | 0.35 |

of Kr81m was greater than that of N2.

## DISCUSSION

The mean ratio of SpVs (0.72) supports the work of Modell and Graham (Modell and Graham 1982). In 9 studies Kr81m had a smaller volume of distribution than resident N2; in the other studies where Kr81m was distributed throughout the resident lung volume SpV was within the normal adult range.

These studies could not demonstrate a consistent relationship between V/Vol and volume of Kr81m distribution within this range of specific ventilation (0.78 to 3.56 $min^{-1}$) suggesting that the steady state Kr81m image is more sensitive to change in ventilation at high specific ventilation than the theoretical analysis of Fazio and Jones would predict. Within this range Kr81m does not equilibrate with FRC and therefore Kr81m activity is a reflection of regional ventilation rather than volume.

However, carefully controlled simultaneous N2 and Kr81m washout studies still produced 3 results that could not be explained, similar to 8 of the 13 studies in the work reported by Wong and Silverman (Wong and Silverman 1982). It is plainly impossible for Kr81m to be distributed in a volume greater than the volume of distribution of Nitrogen and in view of these criticisms the reproducibility of this technique was critically examined.

## METHODS

6 infants aged 0.3 to 11 months were studied. All were inpatients in the HSC for respiratory investigations. Studies were performed on the wards using an Elscint mobile gamma camera (Chapter 2).

When the infants were settled three Kr81m washout studies were performed within 5 minutes of each other. The rate of washout of Kr81m was calculated separately for right and left lungs and from these figures the specific ventilation of each lung was calculated, as outlined above.

The reproducibility of the method within individuals was examined by calculating the coefficient of variation (CV) between the three studies for right and left lungs (Table 4). The ratio of specific ventilation of right to left lung was calculated and compared for each study (Table 5).

## RESULTS

Mean coefficient of variation of specific ventilation was 25% (10.8-38.1) for the right lung and 33% (19.5-51.7) for the left lung. If these results were used to calculate the volume of distribution of Kr81m, each study would yield very different answers, yet they were performed within 5 minutes of each other while the child rested on the gamma camera.

TABLE 4

REPRODUCIBILITY OF Kr81m WASHOUT STUDIES

Reproducibility of specific ventilation of right and left lung from three consecutive studies in 6 infants.

CV = Coefficient of variation

| | SEX | AGE (months) | | V/VOL RIGHT LUNG | CV% | V/VOL LEFT LUNG | CV% |
|---|---|---|---|---|---|---|---|
| 1 | M | 3 | a | 6.1 | | 6.0 | |
| | | | b | 8.3 | 20.0 | 8.3 | 19.5 |
| | | | c | 9.2 | | 8.7 | |
| 2 | F | 0.3 | a | 2.8 | | 2.1 | |
| | | | b | 1.4 | 35.0 | 2.4 | 37.9 |
| | | | c | 1.8 | | 4.2 | |
| 3 | M | 8.5 | a | 4.9 | | 4.6 | |
| | | | b | 6.1 | 13.7 | 7.1 | 27.8 |
| | | | c | 6.3 | | 4.4 | |
| 4 | M | 4 | a | 9.2 | | 9.0 | |
| | | | b | 8.3 | 10.8 | 6.0 | 19.7 |
| | | | c | 7.4 | | 7.7 | |
| 5 | F | 11 | a | 8.5 | | 4.9 | |
| | | | b | 7.9 | 38.1 | 7.5 | 51.7 |
| | | | c | 15.1 | | 13.7 | |
| 6 | M | 6 | a | 7.7 | | 4.7 | |
| | | | b | 4.5 | 31.6 | 4.7 | 42.1 |
| | | | c | 4.8 | | 2.0 | |

TABLE 5

REPRODUCIBILITY OF Kr81m WASHOUT STUDIES

IN DETERMINING RATIO OF V/VOL (RIGHT LUNG): V/VOL (LEFT LUNG)

| PATIENT | AGE (months) | | A V/VOL RIGHT LUNG | B V/VOL LEFT LUNG | A/B |
|---|---|---|---|---|---|
| 1 | 3 | a | 6.1 | 6.0 | 1.02 |
| | | b | 8.3 | 8.3 | 1.00 |
| | | c | 9.2 | 8.7 | 1.06 |
| 2 | 0.3 | a | 2.8 | 2.1 | 1.33 |
| | | b | 1.4 | 2.4 | 0.58 |
| | | c | 1.8 | 4.2 | 0.43 |
| 3 | 8.5 | a | 4.9 | 4.6 | 1.07 |
| | | b | 6.1 | 7.1 | 0.86 |
| | | c | 6.3 | 4.4 | 1.43 |
| 4 | 4 | a | 9.2 | 9.0 | 1.02 |
| | | b | 8.3 | 6.0 | 1.38 |
| | | c | 7.4 | 7.7 | 0.96 |
| 5 | 11 | a | 8.5 | 4.9 | 1.73 |
| | | b | 7.9 | 7.5 | 1.05 |
| | | c | 15.1 | 13.7 | 1.01 |
| 6 | 6 | a | 7.7 | 4.7 | 1.64 |
| | | b | 4.5 | 4.7 | 0.96 |
| | | c | 4.8 | 2.0 | 2.40 |

One of the primary purposes of ventilation imaging is to compare ventilation to individual lung regions, yet there is considerable variability when V/vol to right and left lungs are compared (Table 5).

## DISCUSSION

This study must cast doubts on the reproducibility of the washout technique when Kr81m, a radionuclide with a very short half life is used. It demonstrates that methods appropriate for longer lived isotopes such as Xe133 are unsuitable for short lived isotopes or nuclides. Xe133 washout takes several minutes and any transitory irregularities in the respiratory pattern are unlikely to materially affect the results. The result is that the variability of washouts for either lung or both lungs combined is unacceptably high and results may be unreliable. Even more disturbing is the observation that relative specific ventilation of right and left lungs is very variable. In only one case (pt 1) was there close agreement between the picture of regional lung function derived from the three studies (1.02, 1.00, 1.06).

Results of studies designed to look at the distribution of Kr81m using the dynamic washout technique must therefore be suspect unless the breathing pattern is regular. Furthermore during analysis the tidal waveform prior to withdrawal of the nuclide must be identified and t(0.5) calculated from an end expiratory point.

Nevertheless the present study in infants and adults is in broad agreement with that of Modell and Graham in laboratory dogs. Values for the volume of distribution of Kr81m when related to the volume of distribution of N2 were similar to those reported by Modell and Graham. The work suggested that distribution of Kr81m within the FRC rose as specific ventilation increased. It is difficult to determine the relationship between ventilation and Kr81m activity above specific ventilations of 12 to 15 $min^{-1}$ as such high rates of specific ventilation are uncommon. Hence over the range of specific ventilations seen in most infants and children the steady state Krypton 81m image reflects the distribution of ventilation.

SUMMARY

Using previously published normal paediatric data the equation derived from the theoretical model of Fazio and Jones predicts that Kr81m activity will reflect regional ventilation up to values of specific ventilation of 15 $min.^{-1}$ This is in agreement with the animal work of Modell and Graham and clinical experience of V/Q scanning. Simultaneous N2 and Kr81m washout studies offer broad support but must be interpreted with caution as the reproducibility of this technique is poor.

# CHAPTER 4

# DYNAMIC STEADY STATE VENTILATION IMAGING

## BACKGROUND

In routine clinical practise regional lung function is assessed by inspection of steady state Kr81m ventilation images and a chest radiograph. This technique has the advantages of speed and simplicity. It provides an image of regional ventilation whose value has been established (Gordon, Helms, and Fazio 1981; Gordon and Helms 1982). Nevertheless much potentially valuable information is lost.

Activity of a gaseous radiotracer within the lungs fluctuates with respiration, rising during inspiration as fresh radionuclide is inhaled and falling during expiration (Figure 13). This information can be recorded by dynamic imaging, a technique that has already been used experimentally in respiratory practise to investigate the volume of distribution of Kr81m (Ciofetta et al 1980) and has also been used in cardiological practise to quantify right ventricular function.

## METHODOLOGY

### A. IMAGE ACQUISITION

Subjects were positioned in front of the gamma camera and when settled started breathing from a continuous supply of Kr81m. Once a steady state was reached and Kr81m activity fluctuated above a constant end expiratory level (10 to 20 seconds) a dynamic Kr81m ventilation image was acquired.

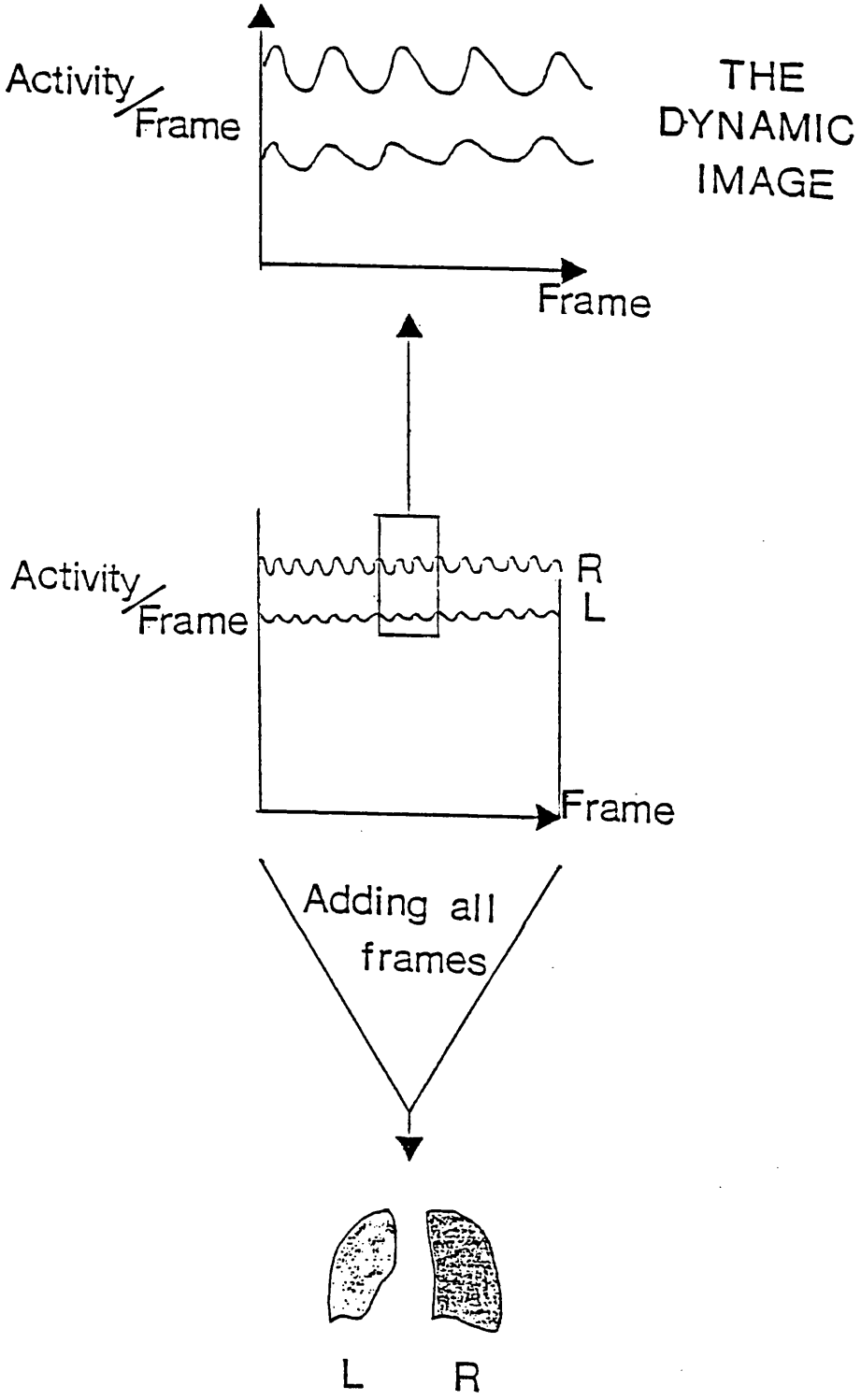


FIGURE 13

During scanning activity within each lung fluctuates with time (middle image). The steady state image is created by storing all activity within one frame (lower image). The dynamic image (upper picture) is created by storing activity in short sequential frames.

Two dimensional images of Kr81m activity were stored in 50 to 100 short sequential frames, whose length was adjusted to match the subjects respiratory pattern. The maximum permitted frame rate on the equipment used was 5 frames per second. This was used for infants and young children with respiratory rates of 30 or more breaths per minute. Slower frame rates were used for older children.

### B. IMAGE MANIPULATION

The images of Kr81m activity in each frame were superimposed and added together to produce a single steady state image. This composite image was subsequently displayed on a colour monitor and using a line drawing program, "regions of interest (ROIs)" were created corresponding to individual lungs or regions of lung. Recalling the original frames of the dynamic image, a curve drawing program was used to create activity time profiles for any predefined "ROI" as shown in Figure 14.

## THEORETICAL ANALYSIS OF THE DYNAMIC STEADY STATE VENTILATION IMAGE

Once a steady state has been reached, Kr81m activity fluctuates above an end expiratory level (Figure 15) and a line joining all end expiratory points will divide the dynamic image into two parts. Activity above this line is inhaled during inhalation and subsequently exhaled, i.e. tidally exchanged.

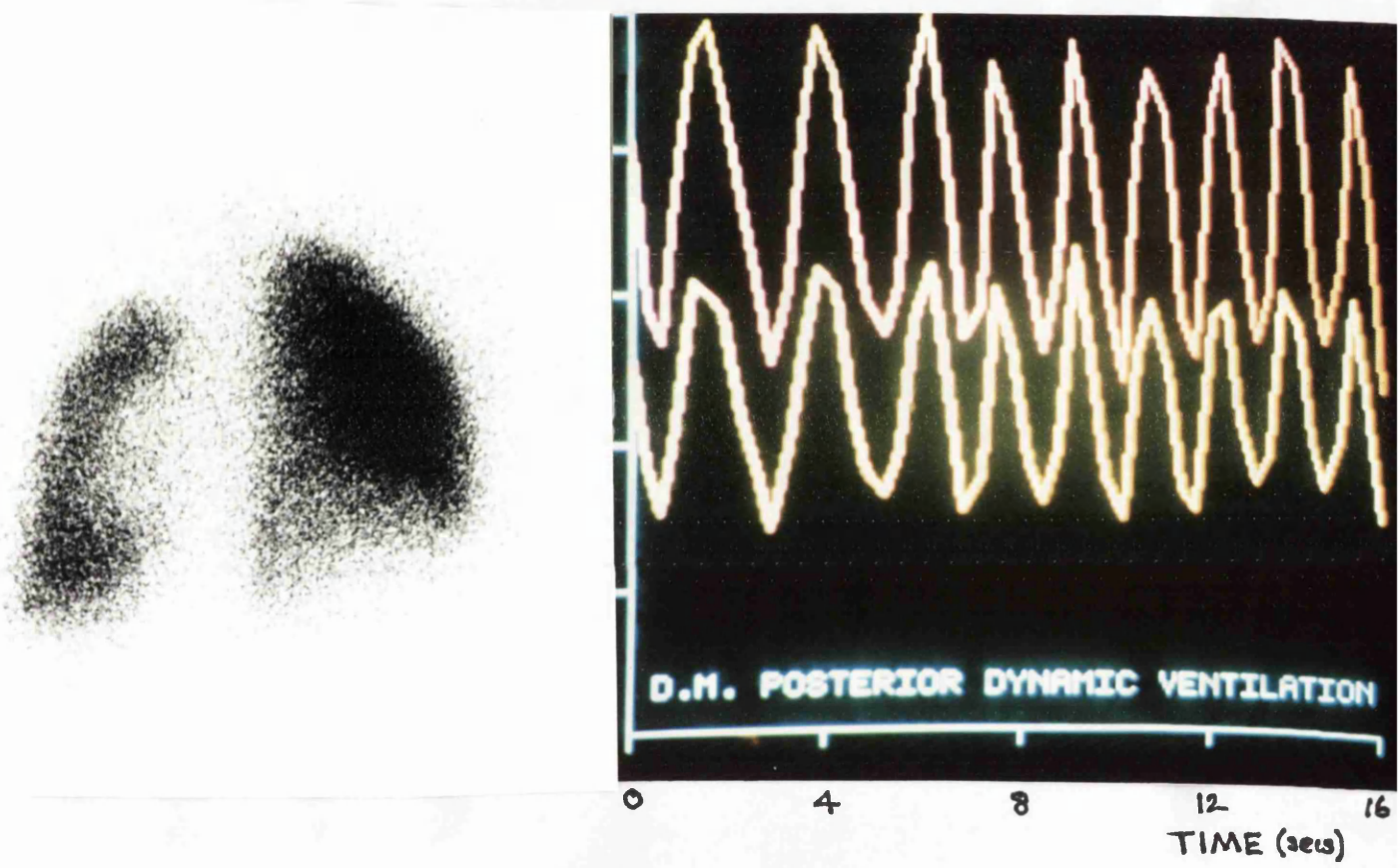


FIGURE 14

D.M. was a six month infant with a provisional diagnosis of Poland's anomaly. A ventilation/perfusion lung scan was performed to delineate the consequence of the marked chest assymetry on regional pulmonary function.

A. Steady state posterior Kr81m ventilation image.

B. Dynamic ventilation image of right and left lung created using "regions of interest" defined on image A.
Time is recorded on the horizontal axis. Activity per frame is on the vertical axis.

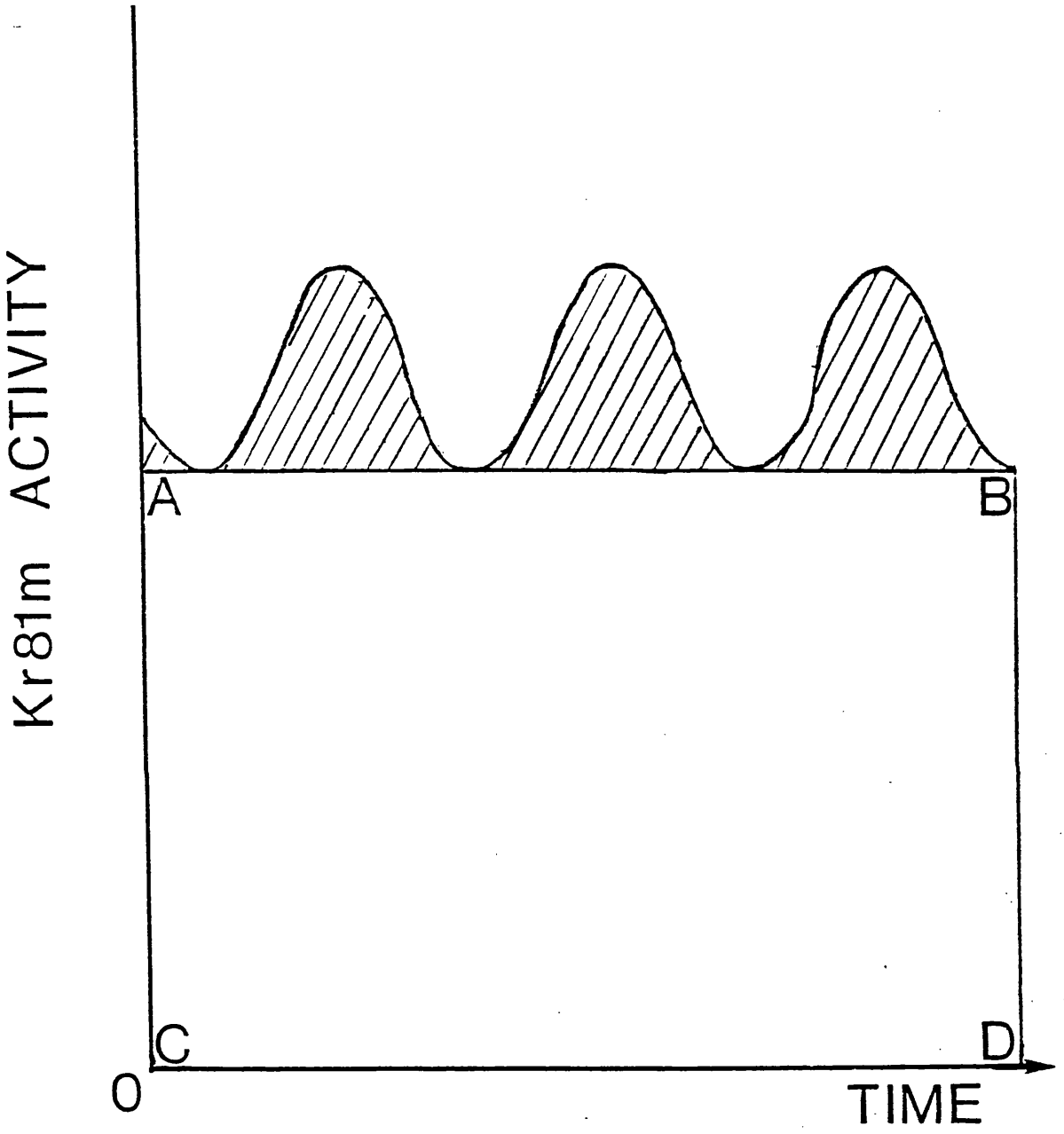


FIGURE 15

Theoretical Kr81m dynamic steady state ventilation image. Total Kr81m activity is represented by the area under the curve, resident Kr81m by the area ABCD and tidally exchanged Kr81m by the hatched area.

Provided the radiotracer is evenly distributed in the inspired air this activity, represented by the area between the end expiratory plateau and the fluctuating Kr81m profile will be proportional to its ventilation.

Kr81m activity below the end expiratory level (represented by rectangle ABCD) could be described as "resident" rather than tidally exchanged. This fraction has equilibrated with part of the resident lung volume. As Kr81m rapidly decays, a portion of tidally exchanged Kr81m must be added to the resident Kr81m with each breath to maintain a constant end expiratory plateau.

## QUANTIFICATION OF THE DYNAMIC IMAGE

Total Kr81m activity in defined lung regions was calculated in the summated single image of the dynamic image. Resident Kr81m activity was derived by multiplying the mean end expiratory level by the number of frames in the dynamic image. Tidally exchanged Kr81m activity was calculated as the difference between the two.

As Kr81m has such a short half life a proportion of inhaled Kr81m must be distributed in the resident activity if the end expiratory level is to remain constant. Inhaled Kr81m activity must therefore be greater than that simply represented by the area above the end expiratory plateau. This is best illustrated by following the sequence of events after Kr81m is withdrawn

(Figure 16).

Once inhalation of Kr81m has ceased activity will fall as a result of its natural decay. Levels of the radiotracer will depend upon the initial activity and the rate of radioactive decay of the radionuclide.

The level at the end of the subsequent breath will also depend on the respiratory rate, the longer the respiratory cycle, the lower the Kr81m activity. The area of triangle ABC represents the activity lost during one breath and is the amount of activity that must be redistributed from the tidally exchanged Kr81m to maintain a constant end expiratory plateau.

$$\text{Area ABC} = 0.5(AB*BC)$$

$$AB = 60/R \text{ seconds or } 60/(R*Z) \text{ frames}$$

$$BC = N(0)-N(t)$$

where

R = Respiratory frequency (breaths per minute)

Z = Frame length (seconds)

N(0) = End expiratory plateau (counts per frame)

N(t) = Activity predicted should no activity be inhaled

t = Time for one breath (mins)

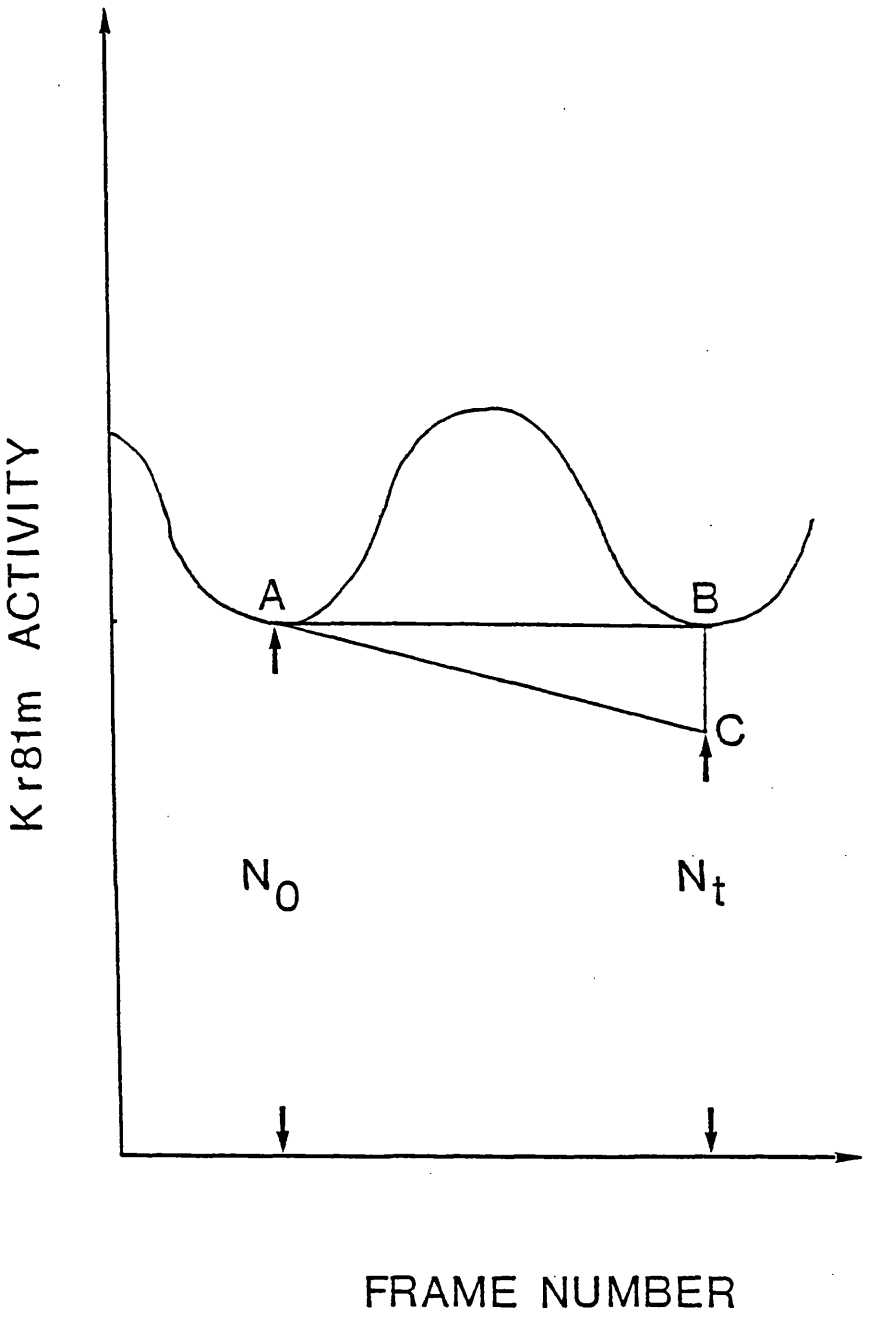


FIGURE 16

Theoretical analysis of dynamic Kr81m image (see text for explanation)

$$\text{Now } N(t) = N(0) * e^{-\text{lambda} * t}$$

OR

$$= N(0) * e^{-\text{lambda} * 1/R}$$

where lambda = decay constant for Kr81m

$$\text{Hence area ABC} = \frac{30}{(R*Z)} * N(0) * (1 - e^{-\text{lambda} * (1/R)})$$

Theoretical calculations for this Kr81m activity were derived using this equation for differing respiratory rates, frame speeds and end expiratory levels and are presented in Appendix 2. They demonstrate that decay correction at any respiratory frequency was a fixed proportion of resident Kr81m. Comparisons of regional tidally exchanged Kr81m within ROIs on one scan are therefore unaffected by this correction.

## THE ACCURACY OF DYNAMIC STEADY STATE IMAGING IN ASSESSING REGIONAL VENTILATION

### IN VITRO

The accuracy of this technique can only be assessed by comparison with an independent, previously validated method for the measurement of regional ventilation, such as bronchospirometry or an alternative well established radiotracer (Xe133), neither of which is feasible in children. The former is an invasive measurement that could only be

accomplished under a general anaesthetic while the latter involves further radiation exposure, both unethical in paediatric practise.

A two compartment lung model was therefore constructed to determine the accuracy of dynamic imaging and the analysis described previously (Figure 17). The apparatus consisted of two 500 ml rubber anaesthetic bags (compartments 1 and 2) inside an airtight perspex box. The mouths of the bags were attached to two ports drilled in the side of the box, connected outside to differential pressure pneumotachographs (Fleisch size "0") and a Y connector. A continuous suction pump maintained a constant vaccuum within the box to maintain the bags at a constant level of inflation while ventilation of the two bags was achieved using a sine wave pump whose frequency and stroke volume could be varied. The distribution of ventilation to each bag was altered using fine wire mesh resistances inserted between the pneumotachographs and the ports in the perspex box.

Flow signals from the two pneumotachographs were electronically integrated to provide a tidal volume tracing, recorded on a 4 channel tape recorder (RACAL STO 4). Flow linearity was confirmed for each pneumotachograph and volume calibrations were performed with a 50 ml syringe prior to each run.

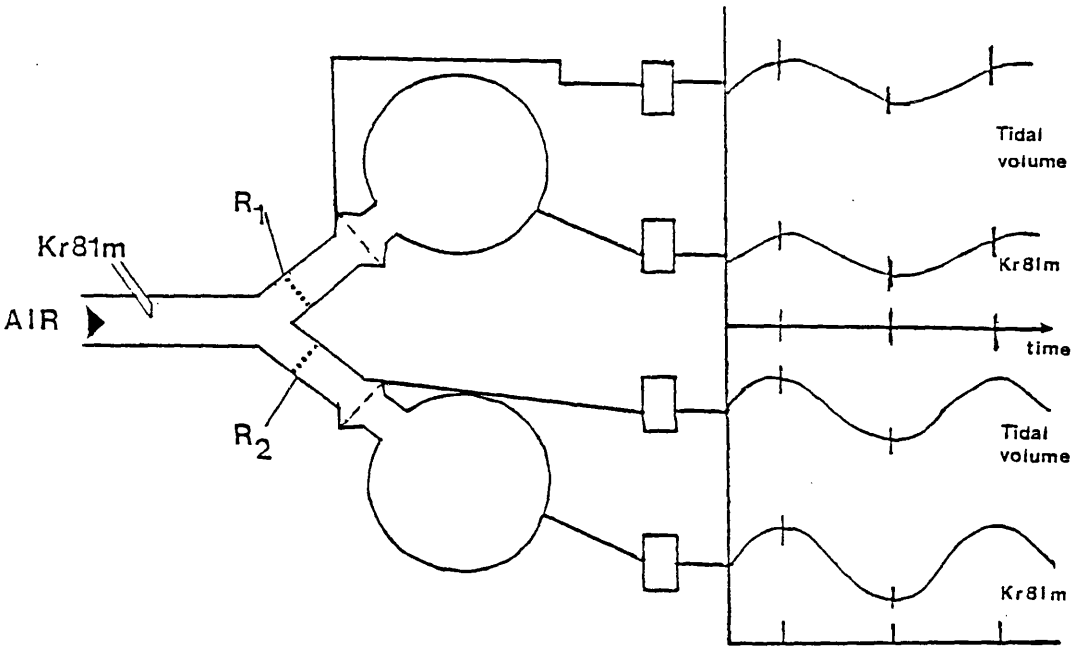


FIGURE 17

Diagramatic representation of two compartment lung model with variable resistances R1 and R2 (see text).

Kr81m was bled into the model via a fine catheter inserted into the Y tubing. Tidal volume and Kr81m traces were synchronised by a digital electronic signal which was simultaneously recorded on the 4 channel magnetic tape.

Once the end expiratory volumes of the compartments were stable, Kr81m was bled into the Y piece and after 10 to 20 seconds a dynamic ventilation image of 100 frames was acquired.

Ventilation was stopped at end expiration and resident volume determined by allowing the bags to deflate and recording the volume of air flowing through the pneumotachographs. A small positive pressure was applied to ensure complete emptying.

The integrated flow signal from the pneumotachograph was replayed on a Gould 6000 6 channel pen recorder and tidal volume to each bag was read directly from this. Distribution of ventilation was expressed as the ratio:

Tidal Volume (Bag 1): Tidal volume (Bag 2)

OR

TV(1):(2)

The dynamic images of Kr81m activity were summed to produce a single steady state image. This was subsequently displayed and "ROIs" were drawn corresponding to the two compartments. Activity time plots were then generated for each ROI similar to those in figure 14. Total and tidal Kr81m activity detected over each compartment were calculated as described above.

Distribution of total Kr81m activity was described as the ratio:

Kr81m activity (Bag 1) : Kr81m activity (Bag 2)

OR

Kr81m(1) : (2)

Distribution of tidally exchanged Kr81m was similarly described:

Kr81m activity (tidal) (Bag 1) : Kr81m activity (tidal) (Bag 2)

OR

Kr81m (Tidal) (1) : (2)

RESULTS (Appendix 3)

Steady state Kr81m images (ie total Kr81m activity) provided an accurate picture of the distribution of minute ventilation to the two compartments. The ratio of total Kr81m activity recorded over each bag, (Kr81m (1):(2)), was related to the distribution of ventilation (TV(1):(2)) (Figure 18). There is, however, some scatter of the data points with one experiment showing poor agreement. If agreement were perfect the expression

$$\frac{Kr81m(1):(2)}{TV(1):(2)}$$

would be 1 while the observed value was 1.10 with large 95% confidence interval (0.21-1.99).

Tidally exchanged Kr81m (Kr81m(Tidal)) agreed more closely

with relative ventilation (Figure 19). Mean value for

$$\frac{Kr81m(Tidal)(1):(2)}{TV(1):(2)}$$

was closer to 1.0 (1.03) with tighter 95% confidence interval (0.73 and 1.33).

## DISCUSSION

While distribution of total Kr81m activity was related to the distribution of minute volume, it grossly misrepresented relative ventilation on one occasion. In this case there was a large difference in the residual volumes of the two bags (220 mls and 400 mls (ratio 0.55)) with ventilation being preferentially distributed to the smaller bag (TV(1):(2)=3.05). The ratio of Kr81m(1):(2) was 1.35, lying between these two values, suggesting that in a unicompartment model total Kr81m activity, as a composite signal of tidally exchanged and resident Kr81m, was significantly affected by residual volume. Tidally exchanged Kr81m gave a more accurate picture. The ratio of tidally exchanged Kr81m (Kr81m(tidal)(1):(2)) was 2.94.

These studies demonstrated that both total and tidal Kr81m give an estimate of regional ventilation although there may be a more accurate agreement with the latter. When there is a gross discrepancy between ventilation to one compartment and its volume, total Kr81m activity may be an unreliable guide to ventilation and in these cases tidal Kr81m will be more accurate.

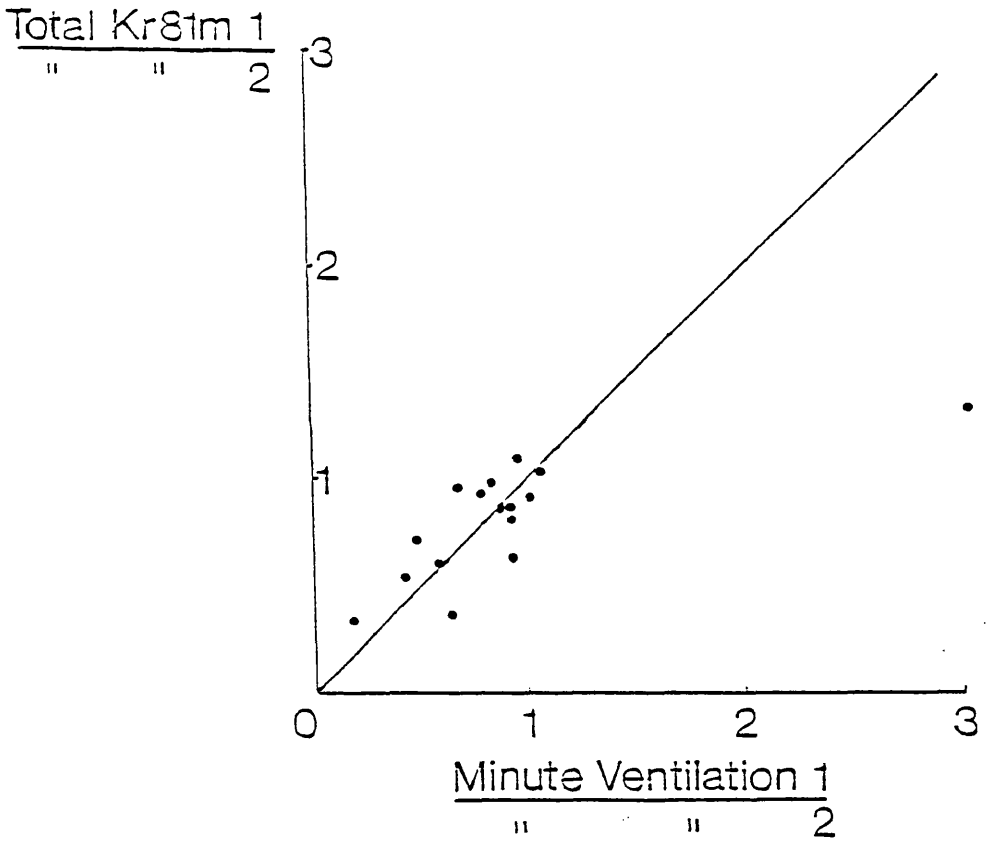


FIGURE 18

Comparison of relative minute ventilation to each compartment (horizontal axis) and relative distribution of total Kr81m activity (vertical axis).
Note the scatter and single outlying point.

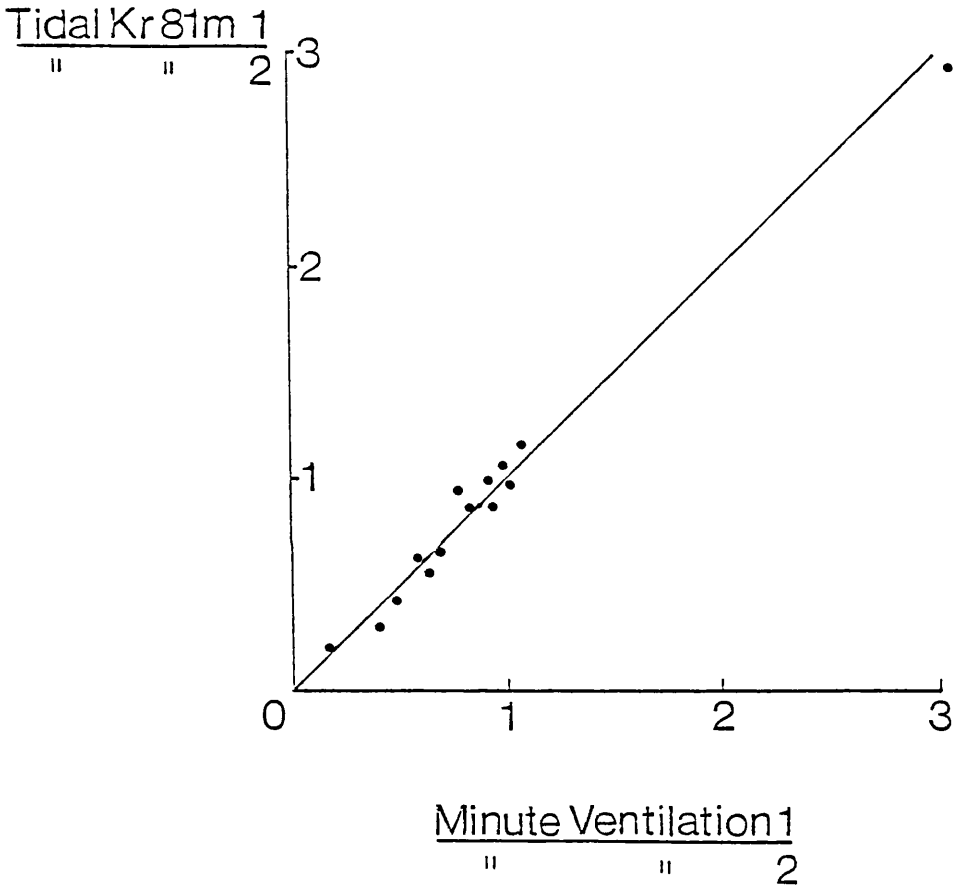


FIGURE 19

Comparison of relative minute ventilation to each compartment (horizontal axis) and relative distribution of tidally exchanged Kr81m activity (vertical axis).
Note closer agreement when compared with Figure 18.

The model however is not a true representation of the human lung. The bags may be considered a perfect gas mixing model in which Kr81m is distributed evenly in the end expiratory volume. The human lung even in health does not behave like this (Fowler et al 1952). It may be considered to be a series of individual compartments with slightly different rates of ventilatory turnover. Kr81m will not therefore equilibrate with the end expiratory volume and observations made in a perfect gas mixing model may not be applicable. Further investigations were therefore conducted in children and adult volunteers.

## COMPARISON OF STEADY STATE AND DYNAMIC IMAGING IN CHILDREN AND ADULTS

Dynamic ventilation images were acquired in a group of children and adult volunteers. Distribution of minute ventilation to each lung was determined using total Kr81m activity (the traditional steady state ventilation image) and tidally exchanged Kr81m. These were compared to assess the agreement between the two techniques.

### PATIENTS AND METHODS

Dynamic posterior steady state Kr81m ventilation scans were performed during quiet tidal breathing in 22 subjects, age range 0.03 - 38.6 years (Appendix 4). Twenty seven studies were performed, 3 subjects had two studies and one had three.

Activity/time curves for right and left lungs were derived from these scans as already detailed. These were subsequently analysed to derive tidal, resident and total Kr81m detected over each lung. The distribution of tidal and total Kr81m to right and left lung were calculated and expressed as ratios.

## RESULTS

Values for fractional ventilation calculated using either total or tidally exchanged Kr81m were similar ( Figure 20). This can be demonstrated by comparing the relative distribution of the radionuclide to the right lung (VfR) calculated using total and tidal Kr81m activity. The value of the ratio

$$\frac{\text{VfR (Total Kr81m)}}{\text{VfR (Tidal Kr81m)}}$$

was 1.05 with 95% confidence limits of 0.88 - 1.20. Tidally exchanged Kr81m activity in the right lung was slightly lower than total Kr81m. Mean difference between VfR (total Kr81m) and VfR (tidal Kr81m) was 2.15 (-12.1 to +6.3), probably accountable in all but one case by the normal variability of radioactive decay. Similar difference was seen in both normal (VfR>45%) and abnormal (VfR<45%) lungs. No effect of age was apparent.

## DISCUSSION

There was good agreement between these two methods of assessing fractional ventilation. Although this evidence of its own cannot prove the accuracy of the technique when examining smaller lung volumes when taken with the evidence of Li et al

FRACTIONAL VENTILATION TO RIGHT LUNG

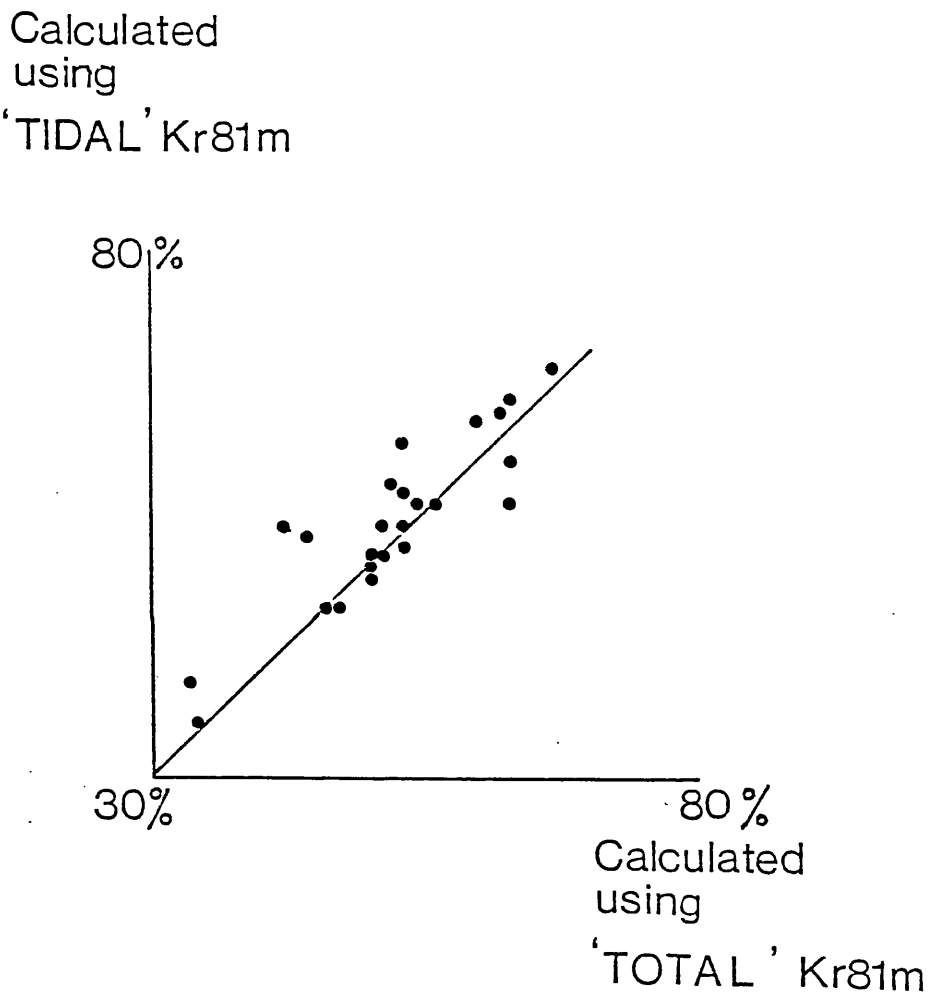


FIGURE 20

Relationship between fractional ventilation to the right lung calculated from total Kr81m activity (abscissa) and tidally exchanged Kr81m (ordinate).

and Gordon et al (Li et al 1979, Gordon et al 1981) it is strongly suggestive that both tidal and total Kr81m activity provide an accurate reflection of regional ventilation. There was a persistent and marked discrepancy between the two techniques in one child and detailed examination illustrates the limitations of using total Kr81m activity to determine regional ventilation.

T.D. was a 20 day old neonate referred for the investigation of persistent respiratory symptoms. He was born by elective Caesarian section at 36 weeks. Apgar scores were 3 at 1 minute, 6 at 5 minutes and 8 at 10 minutes. He required intubation for 7 minutes but after extubation remained tachypnoeic, requiring supplemental oxygen. Chest radiography showed hyperlucency of the left upper lobe and a diagnosis of congenital lobar emphysema of the left upper lobe was made (Figure 21). Whole body plethysmography demonstrated hyperinflation. FRC (pleth) was 320 ml (predicted normal range 110-210) and airway resistance was increased compatible with the diagnosis. However steady state V/Q scan (Figure 21) showed equal activity in the right and left upper lobe with decreased perfusion to the left, uncharacteristic of congenital lobar emphysema.

Analysis of the dynamic ventilation image (Figure 21) demonstrated a discrepancy between the distribution of ventilation calculated using total and tidally exchanged Kr81m. Fifty eight percent of TOTAL Kr81m activity was distributed to the hyperinflated left lung whereas only 46% of TIDALLY EXCHANGED activity was recorded over the left lung. V/Q lung scan was repeated one month later with similar results ( Vf(L) calculated

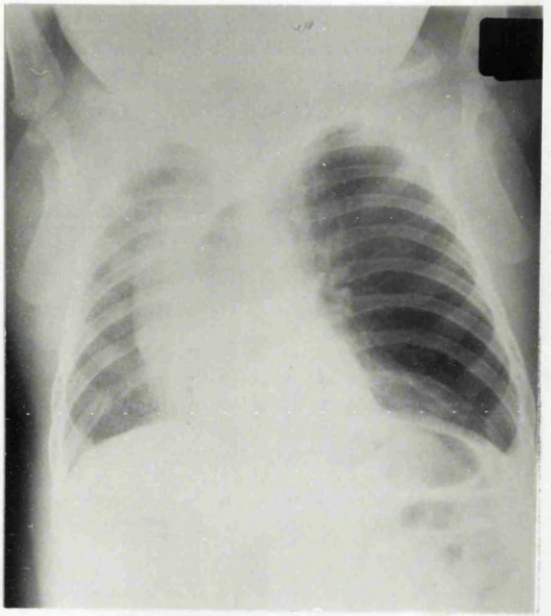

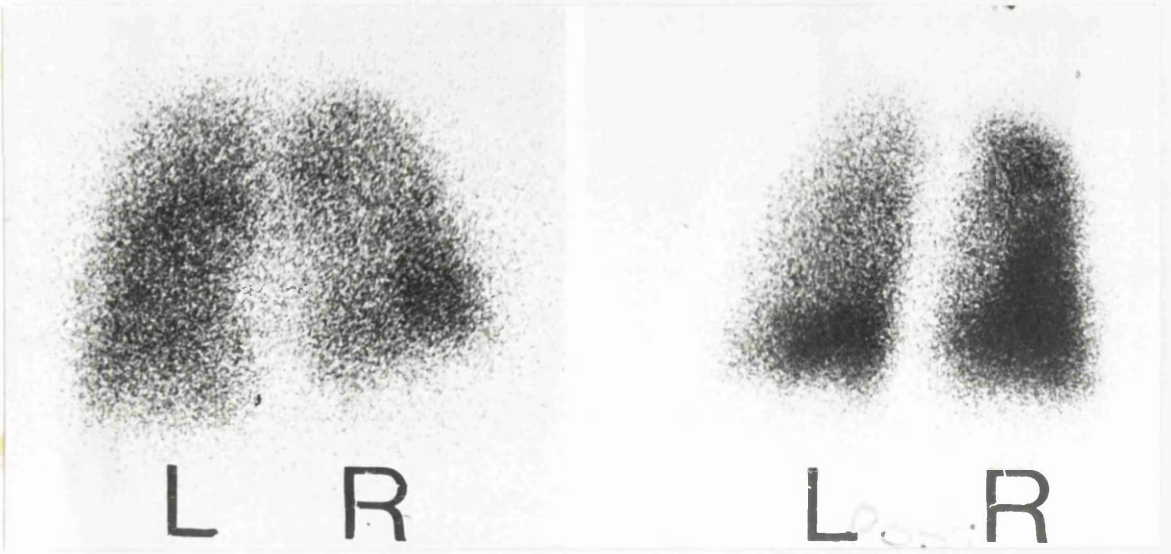


VENTILATION PERFUSION

FIGURE 21

Initial chest radiograph and steady state V/Q scan of T.D.

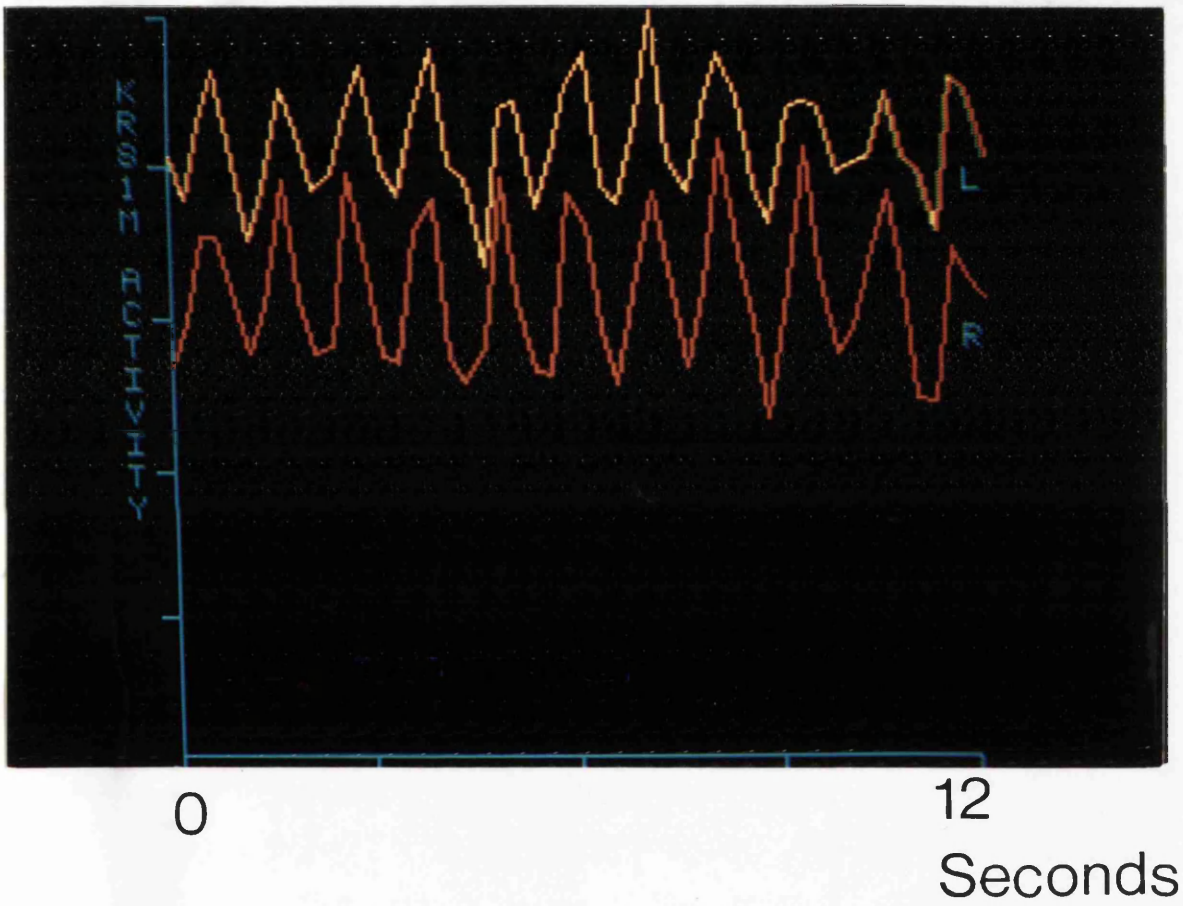


FIGURE 21A

Dynamic Kr81m Ventilation image of TD

Note that while the overall activity in the right lung is diminished, tidal fluctuations within this lung are greater.

from total Kr81m was 55.8% compared with 44.2% using tidally exchanged activity). This case suggests that what was observed in the model may also be seen in vivo. When there is gross disparity between resident volume and ventilation, ie a hyperinflated yet relatively underventilated region of lung, total Kr81m (the steady state image) may give a false impression of regional ventilation as it includes the volume of distribution of Kr81m as well as the tidally exchanged Kr81m. In this infant the increased activity of the abnormal left lung seen on the steady state image was a reflection of the increased volume of that lung rather than ventilation. The model demonstrated that tidally exchanged Kr81m activity gave a truer picture of distribution of ventilation. It is obviously much more difficult to prove this in vivo, but the distribution of ventilation calculated from the dynamic scan would seem more in keeping with clinical and radiographic findings in this case.

## EXAMINATION OF THE MODEL OF FAZIO AND JONES USING TIDALLY EXCHANGED AND RESIDENT KR81M ACTIVITY.

If the theoretical analysis of Fazio and Jones (Fazio and Jones 1975) is correct resident Kr81m should make a larger contribution to total Kr81m at the higher ventilatory turnover rates seen in infants and very young children. Separation of these two components can therefore be used to test Fazio and Jones hypothesis.

Using data from the same group of children and adults this technique was used to study the relative contribution of tidal and resident Kr81m activity to the steady state image through childhood and into adult life.

Scans were analysed as described above and the ratio of tidally exchanged to total Kr81m calculated for each subject.

## RESULTS (Appendix 3)

The proportion of total Kr81m activity that was "resident" did not change with age and therefore by implication, specific ventilation, nor was there any discernible relationship between age and the fraction of total Kr81m that was tidally exchanged (Figure 22).

## DISCUSSION

These findings are in agreement with the theoretical analysis described earlier where a clear relationship between ventilation and theoretically derived Kr81m activity was demonstrated (Chapter 3). Thus the volume of distribution of Kr81m seems to be a similar proportion of FRC in children and adults again suggesting that Kr81m ventilation images can be used throughout childhood to monitor respiratory disease. The only exceptions are likely to be subjects with gross disparity between regional lung volume and ventilation. In such cases dynamic imaging may provide a more accurate representation of regional ventilation.

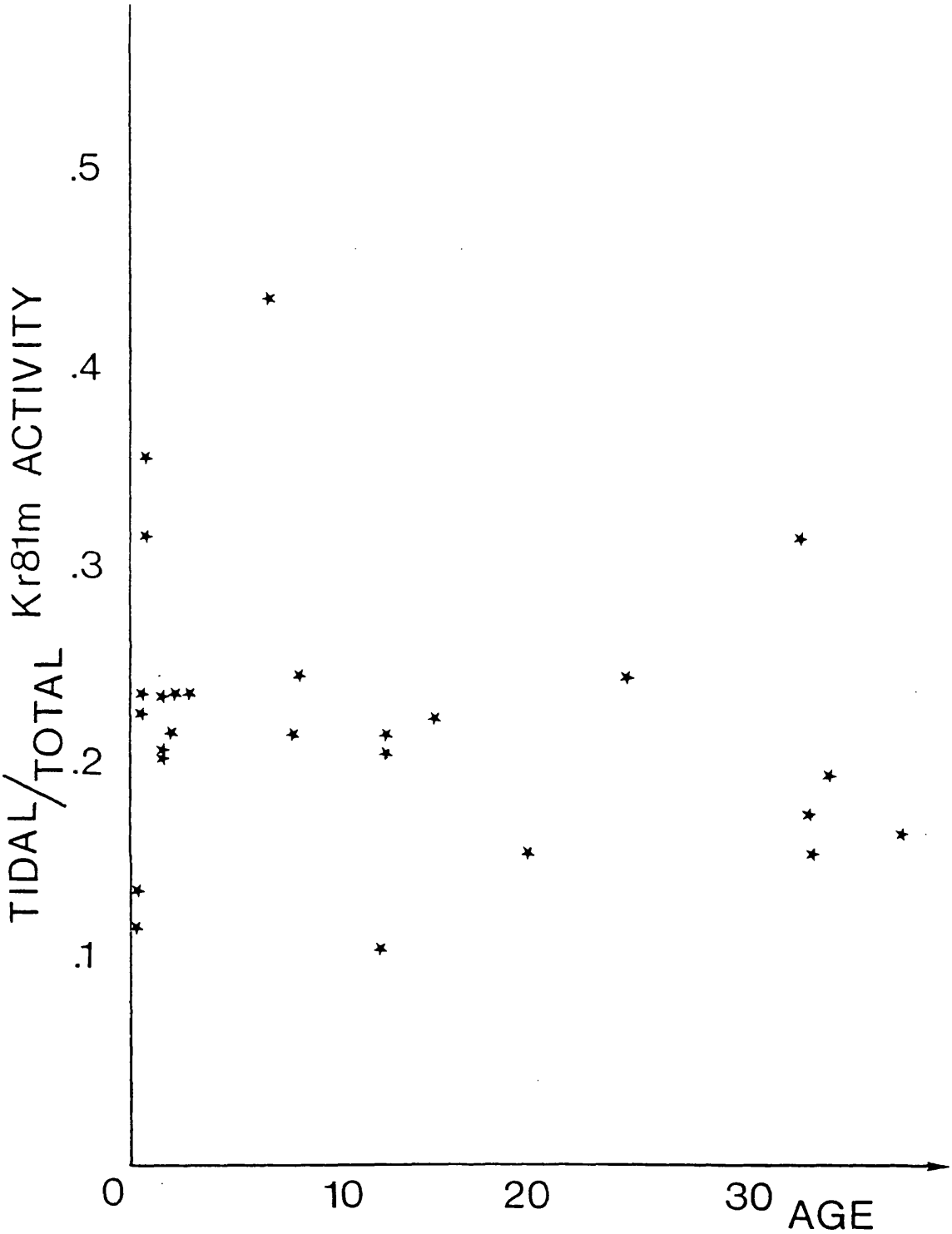


FIGURE 22

Relationship between age (horizontal axis)and fraction of total Kr81m that is tidally exchanged (vertical axis) i.e. contribution of TIDAL Kr81m to TOTAL Kr81m activity.

1. Kr81m dynamic ventilation imaging is feasible in paediatric practise provided background activity is minimised. This is of particular importance in younger children where faster frame rates are needed to capture the pattern of ventilation.

2. The dynamic steady state ventilation image can be analysed to separate tidally exchanged and resident Kr81m. This allows separation of the confounding effects of regional ventilation and volume.

3. In vitro total and tidal Kr81m activity recorded over a single compartment provide an accurate reflection of regional ventilation. Tidally exchanged Kr81m provides a better picture, particularly when there is marked discrepancy between ventilation and volume .

4. There was little difference between regional ventilation calculated by either tidal or total Kr81m activity. In one case where there was gross disparity between regional ventilation and volume tidal Kr81m provided a picture of regional ventilation that was more consistent with the clinical and radiographic findings.

5. The theoretical analysis described earlier and experimental work in infants, children and adults add further support to the contention that the contribution of resident Kr81m to total activity is similar in all age groups. Steady state Kr81m images can therefore be used throughout childhood to monitor the progress of paediatric respiratory disease.

# CHAPTER 5

# CLINICAL STUDIES

## 1.ESTIMATION OF TC99M SPILLOVER INTO THE KR81M IMAGE

One of the advantages of Kr81m is that the energy emitted is similar to that of Tc99m (190 and 140 kEV respectively). Ventilation and perfusion images can therefore be acquired using the same collimator.

Kr81m decays very rapidly and will not interfere with the Tc99m perfusion image. The 6 hour half life of Tc99m, however, means activity emitted from this nuclide may spillover into subsequent Kr81m ventilation images . A study was therefore conducted to determine whether continuing emission of Tc99m activity clouded the ventilation images.

### PATIENTS AND METHODS

Eight children were studied. A standard 200 kilocount posterior Tc99m perfusion image was acquired after injection of the radionuclide with the camera window set at 140 kEV. The time taken to acquire this image was noted and a further image acquired for an identical time with the energy window of the camera readjusted to 190 kEV. Care was taken to keep the child in the identical position so that images could be superimposed. No Kr81m was administered during this time. Images were stored in the online computer for subsequent analysis.

The first image was displayed and used to define a region encompassing both right and left lungs. Activity within this region was determined and recorded. The second image was then displayed and the activity within the identical region of interest in this image noted. While activity in the first image will represent perfusion to both lungs,the number of counts in the second image will be a combination of background activity and Tc99m "spillover" into the Kr81m window. By dividing this activity in the second image by the time of image acquisition a "rate of background acquisition" was determined.

RESULTS (TABLE 6)

Tc99m perfusion images took between 70 and 144 seconds to acquire. In one case (pt 8), a small neonate, a shorter image of only 60,000 counts was acquired. Spatial resolution depends on count density rather than total counts and therefore the reduced activity acquired will not affect the resolution of the smaller image.

Activity in the second image ranged between 730 and 3269 counts. Mean rate of background acquisition was 15.7 counts per second (range 6 to 47).

DISCUSSION

Kr 81m ventilation images usually take between 50 and 200 seconds, depending on the activity of the generator, hence Tc 99m

TABLE 6

Tc99m MAA spillover and background activity through energy window of 190 kEV. (Figures in brackets represent percentage contribution of background and spillover to Kr81m activity.)

| PT | TIME (secs) | COUNTS ACQUIRED at 140 KEV (+-10%) | COUNTS ACQUIRED at 190 KEV (+-10%) | BACKGROUND COUNTS/ SECOND |
|---|---|---|---|---|
| 1. | 70 | 200,000 | 3269 (1.6%) | 47 |
| 2 | 113 | 185,472 | 1276 (0. %) | 11 |
| 3. | 90 | 194,163 | 808 (0.4%) | 9 |
| 4. | 88 | 194,028 | 1191 (0.6%) | 14 |
| 5. | 70 | 193,729 | 1419 (0.7%) | 20 |
| 6. | 102 | 194,260 | 1294 (0.7%) | 13 |
| 7. | 144 | 189,663 | 885 (0.5%) | 6 |
| 8. | 107 | 59,487 | 730 (1.2%) | 7 |

would contribute 300 to 9,400 counts (0.1% to 4.7%) to the Kr81m ventilation image, a small fraction of the total activity recorded. In one case (patient 1) a much higher rate of background activity was noticed (47 counts per second). As all others were considerably smaller ( < 20 counts per second) it seems unlikely that this disparity was attributable to Tc99m activity alone. It may rather be due to fluctuations in the radioactive background in the room.

Spillover of Tc 99m activity therefore is small and need not be considered when analysing the ventilation image.

## 2. PATTERN OF KR81M DISTRIBUTION USING DIFFERENT ADMINISTRATION SYSTEMS.

The administration system used in this study does not provide a reservoir of Kr81m that allows even distribution of the tracer in the tidal volume. Hence most will be inhaled during the early part of inspiration. Milic Emili et al have demonstrated that the distribution of Xe133 depends on the point at which this isotope is inhaled (Milic Emili et al 1966). Starting from residual volume, the first 40% is distributed preferentially to the lung apices but subsequently the bases are better ventilated. It is unkown whether this affects the mal-distribution of ventilation seen during tidal breathing in patients with respiratory illnesses although previously published work (Amis and Jones 1980, Mostafa et al 1985) suggest that it

has little or no effect in normal individuals. The aim of this study was to compare ventilation images acquired with and without a Kr81m reservoir in the respiratory circuit.

## PATIENTS AND METHODS

Five children with obvious inhomogeneities of regional ventilation were studied (Table 7).

TABLE 7

Patients studied

| NAME | AGE (years) | DIAGNOSIS |
|---|---|---|
| NC | 12.5 | POST PERTUSSIS |
| JC | 10.3 | CYSTIC FIBROSIS |
| JA | 10.3 | CYSTIC FIBROSIS |
| ST | 8.7 | OBLITERATIVE BRONCHIOLITIS |
| AP | 9.3 | CYSTIC FIBROSIS |

An erect posterior ventilation image was acquired using a small face mask with a volume less than a single tidal volume (estimated on the basis of body weight (Polgar et al 1971)). A similar image was then acquired while the subject breathed from a 1 litre "reservoir" anaesthetic gas bag containing a mixture of

air and Kr 81m. Flow to this bag was adjusted to maintain a small volume of gas within it throughout the respiratory cycle thus providing a continuous supply of Kr 81m during tidal breathing.

The two images were stored in the online computer for analysis. Each was divided into either 6 or 8 identical regions dependent on the image size and their fractional activity determined using computer programs previously described (Chapter 2).

## RESULTS

Distribution of ventilation to each region was similar in the two scans and no consistent differences emerged. The apices were slightly prefentially ventilated when the reservoir was used, although this was not a universal finding and the differences were small. In none could the two images be clearly distinguished (Figure 23).

## DISCUSSION

As these scans were acquired erect, it might be expected that ventilation would be preferentially distributed to the uppermost lung regions when inhaling Kr81m from the administration set without a reservoir (Chapter 6). Such a pattern was not seen. Mean variation between regions was 1.35%

FIGURE 23

Regional distribution of Kr81m when administered with and without a reservoir.

(Figures are % ventilation to each region)

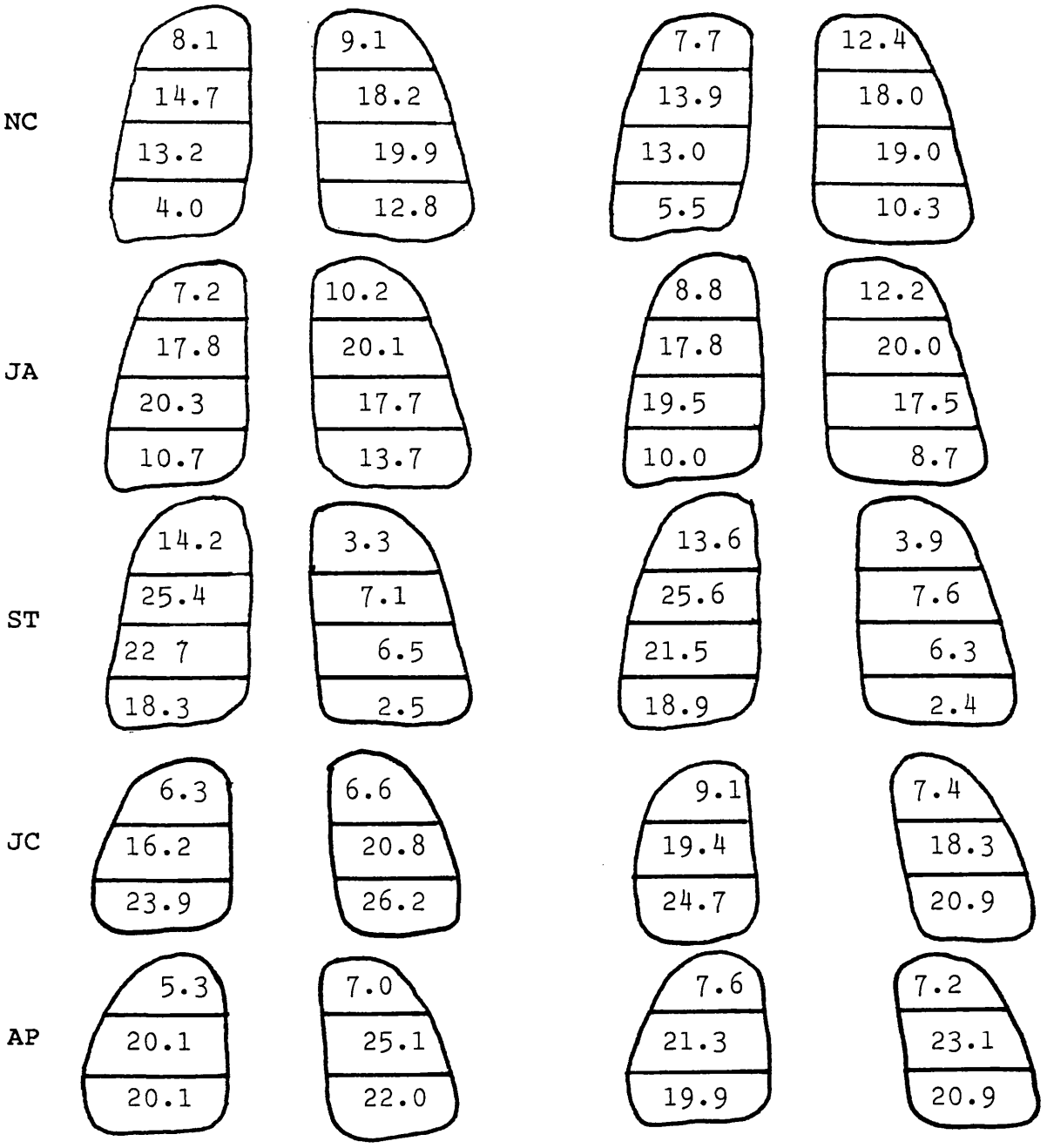

(0-5.3) and it was impossible to separate the two images by simple inspection. As the small face mask is simpler and more easily tolerated and indeed the only way of administering the radiotracer in very young children unless asleep this method was adopted in routine clinical practise.

## 3. THE NORMAL DISTRIBUTION OF VENTILATION AND PERFUSION

### INTRODUCTION

Data on normal regional lung function are limited as ethical considerations prevent the administration of radionuclides to normal children and the use of invasive techniques such as bronchospirometry. Godfrey and Mackenzie and Ciofetta et al (Godfrey and Mackenzie 1977, Ciofetta et al 1980) attempted to circumvent this problem by investigating washout of an administered radiotracer from radiologically normal areas of lung in children attending hospital for assessment of respiratory symptoms, although the accuracy of this technique must be questioned when Kr81m is used as the radiotracer (Chapter 3).

The distribution of ventilation and perfusion to each lung may be derived from steady state images. In an attempt to provide such data V/Q lung scans of all children with normal chest radiography and homogeneous distribution of Kr81m and Tc99m MAA were used to calculate fractional ventilation and perfusion to right and left lungs. To provide similar data in adults Kr81m

ventilation scans of healthy adult volunteers were also analysed.

## PATIENTS AND METHODS

28 children, mean age 3.29 years (range 0.01 to 10.86) fulfilled these criteria. Ventilation scans were also acquired on 22 adult volunteers mean age 29.6 (range 18.92 to 50.17). Fractional ventilation to right (VfR) and left lung (VfL) were calculated as described in Chapter 2 from posterior ventilation images in all children and adults. Fractional perfusion (QfR and QfL) were calculated in those children who underwent perfusion imaging. Anterior ventilation and perfusion images were acquired in 15 children and fractional ventilation and perfusion similarly analysed in these images.

## RESULTS

### 1. POSTERIOR IMAGES (Appendix 6, Figure 24)

In the posterior images relative ventilation (VfR/VfL) ranged from 1.00 to 1.50 (mean 1.16, 54% / 46%). The largest disparity between right and left lung was 60% / 40% (pts 2, 6, 8).

For adult volunteers relative ventilation varied from 1.00 to 1.22 (mean 1.09, 52% /48%, mode 1.08).

In none of the 50 cases was the left lung preferentially ventilated, the lowest value being 1.00 (50% / 50%).

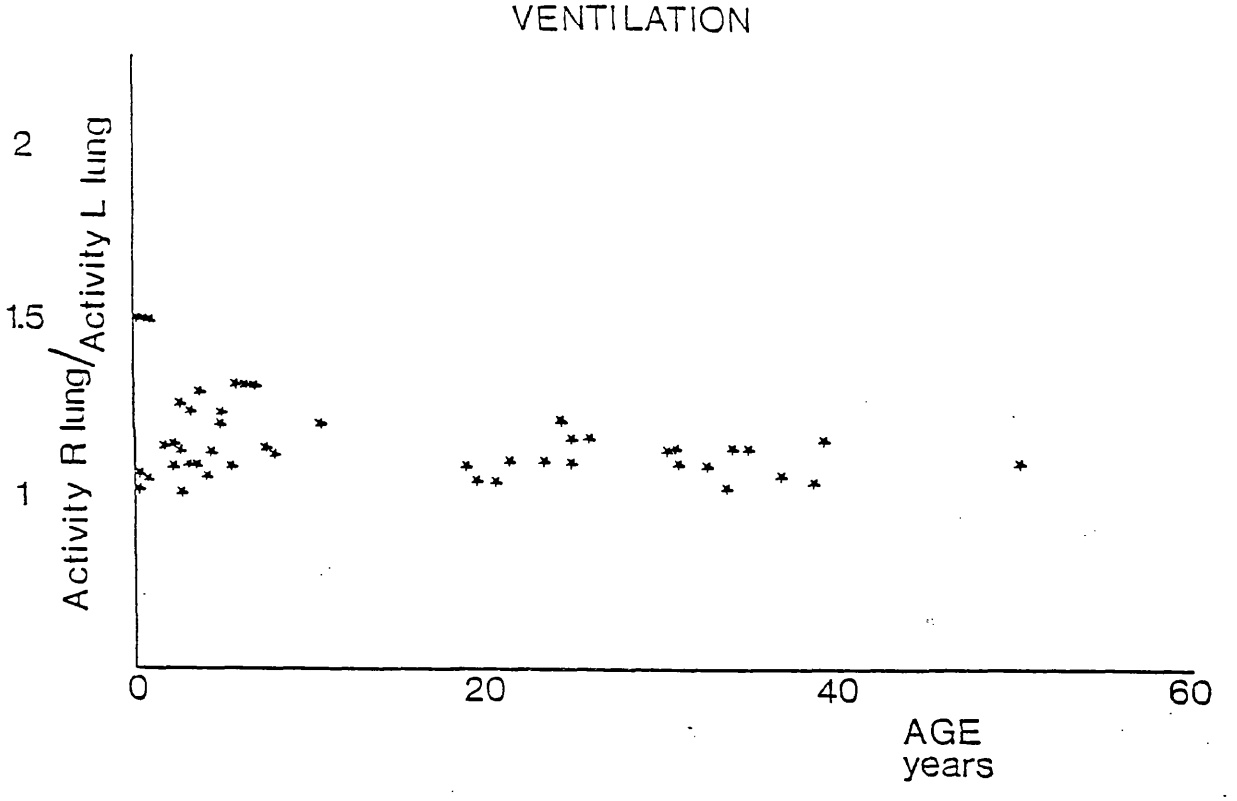


FIGURE 24

Relative distribution of Kr81m activity to right and left lung determined from posterior image (vertical axis) plotted against age (years) (horizontal axis).

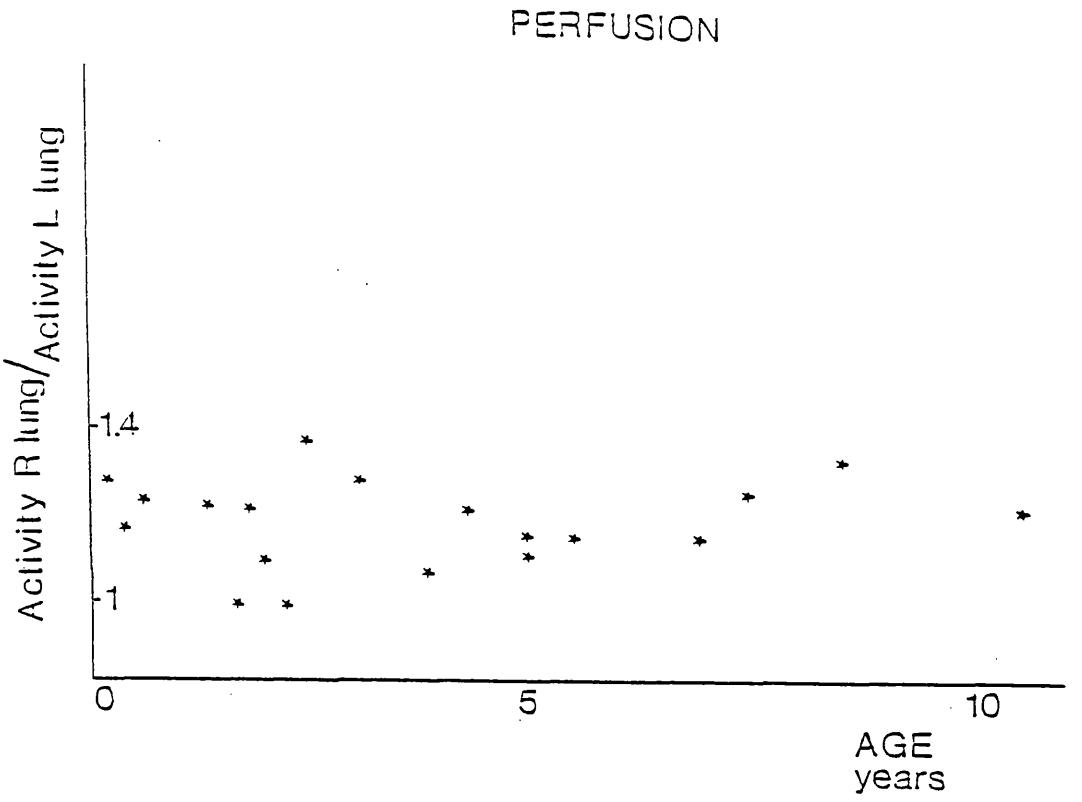


FIGURE 25

Relative distribution of Tc99m MAA activity to right and left lung determined from posterior image (vertical axis) plotted against age (years) (horizontal axis).

Values for relative perfusion (QfR/QfL) were similar. They ranged from 0.82 (45% / 55%) to 1.36 (58% / 42%) (mean value 1.13, 53% / 47%). In 3 cases the left lung was preferentially perfused, but in two of these relative perfusion was very close to unity (0.98 and 0.98). Perfusion scans were not performed in the adult volunteers.

The relationships between age and fractional ventilation and perfusion determined from the posterior images are shown in Figures 24 and 25. Although there is greater scatter in the results in the infants and very young children there is a suggestion that fractional ventilation to the right lung was greater in the younger age group. The distribution of perfusion did not appear to change.

2. ANTERIOR IMAGES (Appendix 6)

These ratios of fractional ventilation and perfusion (VfR/VfL and QfR/QfL) were consistently higher in the anterior images, 1.29 (1.04 to 1.55) and 1.29 (1.02 to 1.5) respectively. In no cases was the left lung preferentially perfused or ventilated. This persistent bias of the anterior image is depicted in Figure 26. Fractional ventilation to the right lung derived from the anterior image was greater than that derived from the posterior image in all but 4 cases. In 2 of these the difference was small ( less than 0.3%)

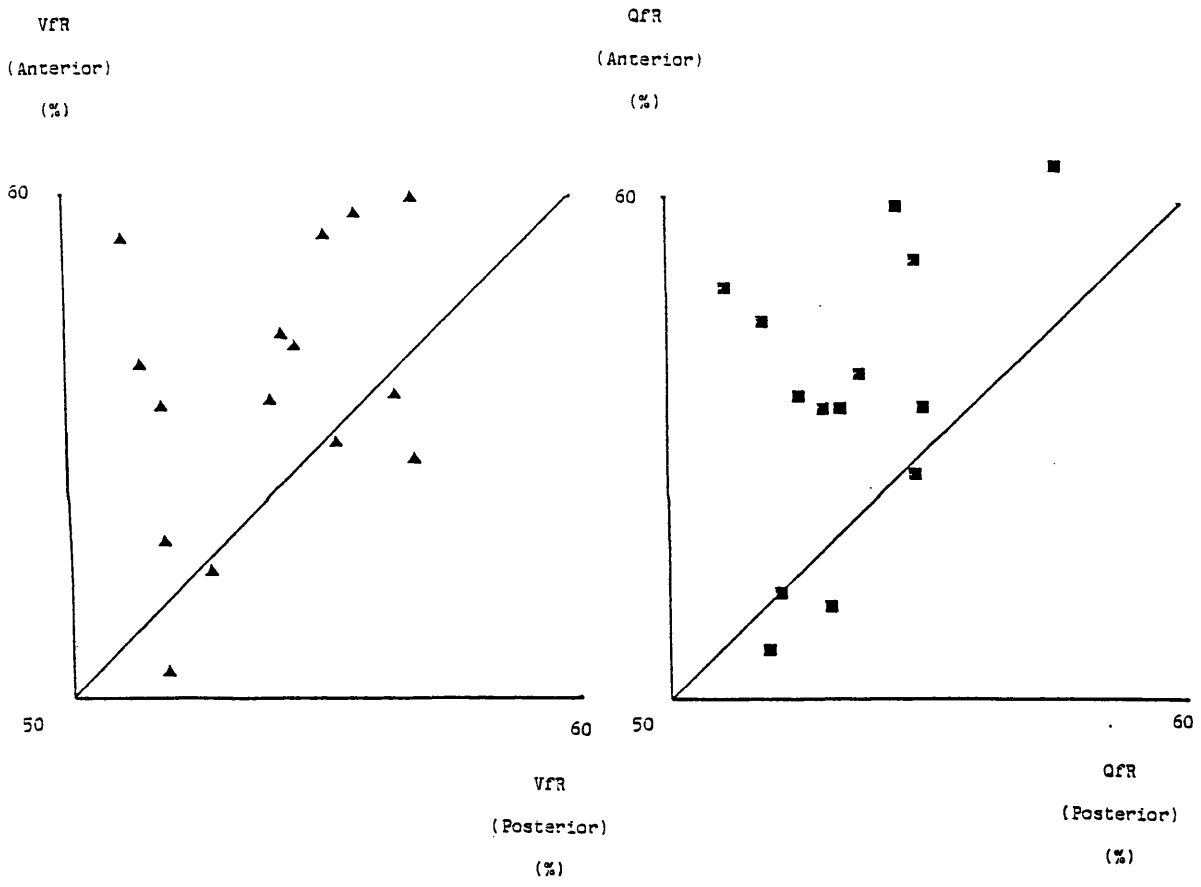


FIGURE 26

A. Comparison of fractional VENTILATION to right lung calculated from posterior image (horizontal axis) and anterior image (vertical axis)

B. Comparison of fractional PERFUSION to right lung calculated from posterior image (horizontal axis) and anterior image (vertical axis)

while in the other two the differences were 1.4% and 2.1%. Similarly the fractional perfusion to the right lung derived from the anterior image was greater than the corresponding value derived from the posterior image in all but 3 cases.

## DISCUSSION

Analysis of posterior Kr81m ventilation images showed that the right lung received a greater proportion of ventilation in 48 of the 50 studies. In two cases ventilation was evenly distributed. In 20 of the 23 perfusion studies the right lung received a greater proportion of perfusion.

It is interesting to note that relative ventilation (1.10) seen in adults is very similar to the relative lung weights determined from post mortem examinations (Stowens 1966, Figure 27). The data suggest that the right lung receives a greater proportion of ventilation in infants and young children. Mean relative ventilation in the age group 0.01 to 4 years was 1.23 compared to 1.12 in older children and adults, a similar trend to the published data of Stowens which demonstrate that the ratio of lung weights falls from high values in infancy to normal adult values by the age of 4.

It is often quoted that the left lung appears relatively hypoperfused and ventilated in the anterior views. This may be due to the anterior position of the heart masking a region of the left lung from the camera. The data from this study confirm this

although the difference is small. The mean ratio QfR Posterior/Anterior was 0.88 (0.62-1.04) and VfR Posterior/Anterior 0.92 (0.72-1.09).

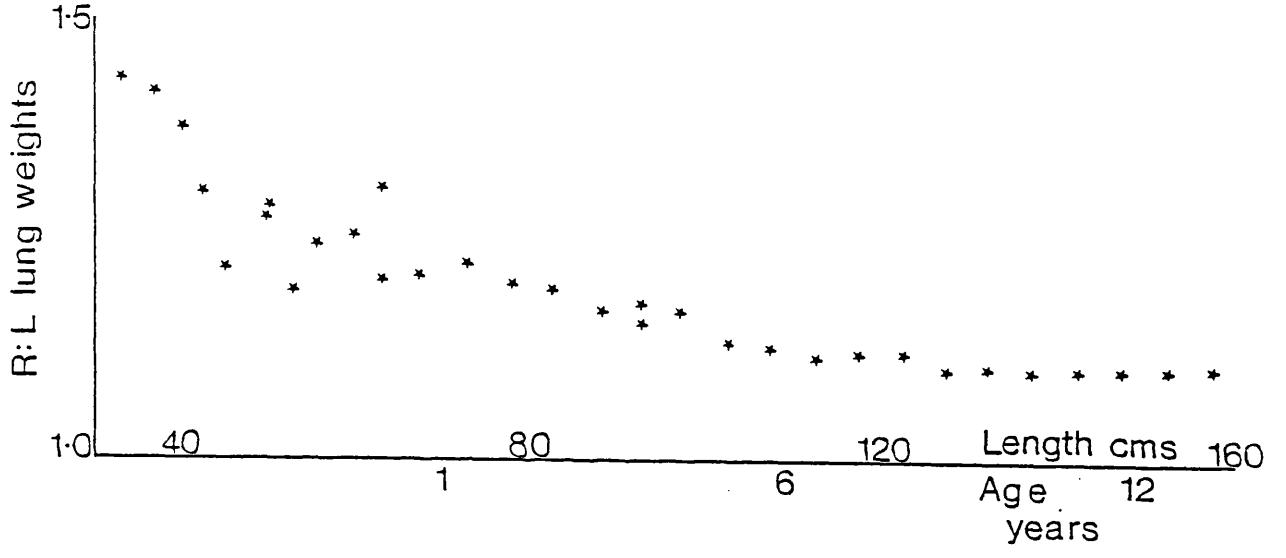


FIGURE 27

Post mortem relative lung weights (vertical axis) plotted against age (years). Data from Stowens (1966).

## INTRODUCTION

The incidence of foreign body inhalation reaches a peak in infancy and early childhood, a time of rapid lung growth when any significant insult might be expected to cause persistent lung damage. Despite this possibility most studies have concentrated on immediate rather than long term consequences (Abdulmaid et al 1976, Davis 1966, Harboyan et al 1970, In Guk Kim et al 1973, Norris 1948, Pyman 1971). These reports have assessed outcome by clinical examination and chest radiography, which can only be expected to detect the most severe sequaelae such as bronchiectasis, Macleods syndrome and persistent collapse/consolidation. Furthermore a reliable picture of regional pulmonary ventilation and perfusion may sometimes only be achieved noninvasively by radionuclide lung scanning (Gordon et al 1981). The studies in the earlier part of this chapter have clearly demonstrated that Kr 81m/Tc99m ventilation/perfusion imaging can provide accurate pictures of regional lung function. This is illustrated by one of the cases studied.

VC was an 18 month old child referred as an emergency with a 10 day history of acute paroxysmal coughing associated with severe cyanosis. Whooping cough had been diagnosed initially and she had been prescribed Erythromycin. However symptoms worsened and she was admitted with increasing respiratory difficulty. Chest radiography and screening did not show any gross

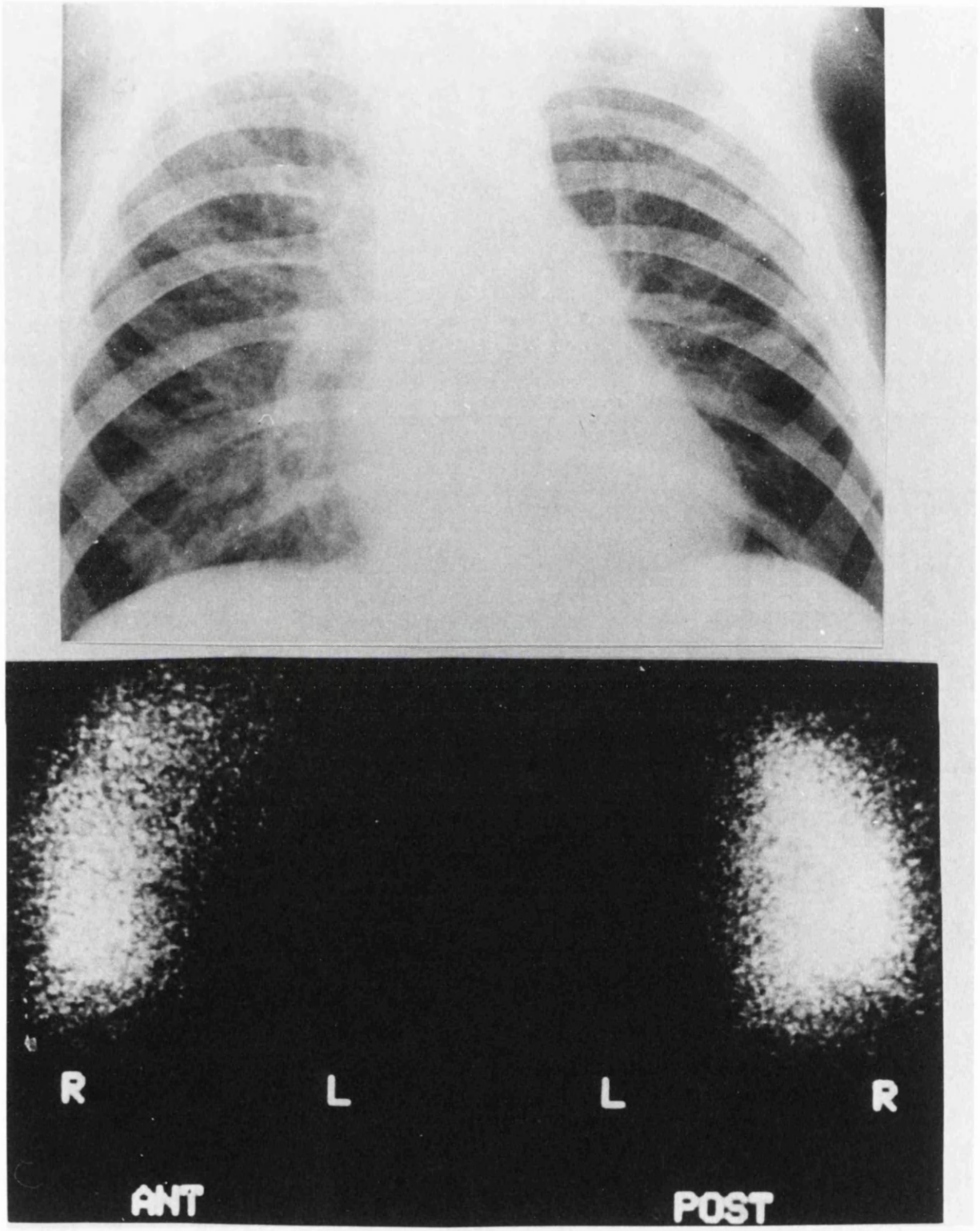


FIGURE 28

Chest xray and V/Q Scan of V.C. Note the complete absence of ventilation to the left lung while the chest Xray only suggests reduced pulmonary blood flow to that lung.

abnormality and bronchoscopy could not identify a foreign body. Symptoms continued and one week later there was clinical evidence of decreased ventilation to the left lung. A ventilation lung scan (Figure 28) demonstrated complete absence of ventilation to the left lung and at repeat bronchoscopy a foreign body was identified in the left main bronchus and removed. Symptoms resolved and repeat V/Q lung scan 10 months later showed complete resolution of the ventilatory defect.

In order to identify risk factors that may lead to chronic lung damage after foreign body inhalation all children who had presented to the Hospital for Sick Children over the five years 1979 to 1984 with bronchoscopically proven foreign body inhalation were reviewed. Outcome was assessed using clinical examination, chest radiography and Kr 81m ventilation/ Tc99m MAA perfusion lung scan (V/Q lung scan).

## PATIENTS AND METHODS

Review included symptomatic assessment (cough, wheeze, haemoptysis or repeated chest infections), clinical examination, chest radiography and standard four view (posteror, right posterior oblique, left posterior oblique and anterior) V/Q lung scan. Clinical details at presentation and subsequent treatment were obtained from the medical notes along with chest xrays taken prior to removal of the foreign body.

All radiographs were analysed in an identical manner following the recommendations of the European Society of Nuclear

Medicine (Paediatric Task Group, Piepz et al). Each lobe was defined as normal, emphysematous, collapsed, consolidated or collapsed/consolidated. The V/Q scans were scored using a semiquantitative method (Fazio et al 1978). Statistical analysis for significance of associations was by Chi squared test with correction for small numbers.

RESULTS

Twenty six children were identified of whom twenty one, 14 boys and 7 girls, mean age 2.16 years (range 1.03 to 5.65) returned for review. Four could not be traced and one failed to attend. Mean length of follow up was 2.05 years (range 0.38 to 4.79). All had inhaled a peanut except one who had inhaled a piece of coal and one who had inhaled a plastic peg (Table 8).

The foreign body was removed within one week in only 10 cases, in 5 between one and four weeks and in 6 removal was delayed beyond one month (Table 8). One lodged at the carina, eight in the right lung, and eleven in the left. In one child fragments of peanut were removed from both lungs. Nine children required more than one bronchoscopy for complete removal, (maximum number 4).

At follow up 14 were asymptomatic. Of the other 7, 2 complained of persistent cough, 1 of recurrent wheezing and 4 of cough and wheeze. Thirteen had normal chest radiography but only 7 had normal V/Q lung scans. All children with normal scans were asymptomatic and had normal chest radiographs.

| AGE | SEX | FB | SITE (LUNG) | DAYS BEFORE REMOVAL | INITIAL CHEST X-RAY | SYMPTOMS | FOLLOW UP CHEST X-RAY | V/Q LUNG SCAN | |
|---|---|---|---|---|---|---|---|---|---|
| | | | | | | | | LEFT | RIGHT |
| 1.0 | F | NUT | R | 6 | NORMAL | NONE | ABNORMAL | NORMAL | ABNORMAL |
| 1.1 | M | NUT | R | 10 | COLLAPSE | NONE | NORMAL | ABNORMAL | NORMAL |
| 1.2 | M | NUT | R | 30 | HYPERINFLATION | NONE | NORMAL | NORMAL | NORMAL |
| 1.3 | M | NUT | R | 4 | HYPERINFLATION | NONE | NORMAL | NORMAL | NORMAL |
| 1.3 | F | COAL | L | 150 | HYPERINFLATION | COUGH | ABNORMAL | ABNORMAL | NORMAL |
| 1.3 | F | NUT | R | 2 | COLLAPSE | COUGH/WHEEZE | ABNORMAL | ABNORMAL | ABNORMAL |
| 1.4 | M | NUT | R | 1 | HYPERINFLATION | NONE | NORMAL | NORMAL | NORMAL |
| 1.5 | M | NUT | L | 1 | COLLAPSE | NONE | NORMAL | ABNORMAL | ABNORMAL |
| 1.6 | M | NUT | R | 14 | HYPERINFLATION | COUGH | NORMAL | ABNORMAL | NORMAL |
| 1.6 | M | NUT | C | 7 | HYPERINFLATION | NONE | NORMAL | NORMAL | ABNORMAL |
| 1.7 | F | TOY | L | 28 | HYPERINFLATION | NONE | NORMAL | ABNORMAL | NORMAL |
| 1.9 | M | NUT | R | 1 | HYPERINFLATION | NONE | NORMAL | NORMAL | NORMAL |
| 2.0 | F | NUT | R+L | 1 | NORMAL | NONE | ABNORMAL | ABNORMAL | NORMAL |
| 2.2 | M | NUT | L | 75 | COLLAPSE | COUGH/WHEEZE | ABNORMAL | ABNORMAL | ABNORMAL |
| 2.2 | F | NUT | L | 2 | HYPERINFLATION | NONE | NORMAL | NORMAL | NORMAL |
| 2.2 | M | NUT | L | 1 | HYPERINFLATION | NONE | NORMAL | ABNORMAL | NORMAL |
| 2.4 | M | NUT | L | 21 | COLLAPSE | NONE | ABNORMAL | ABNORMAL | NORMAL |
| 2.8 | M | NUT | L | 42 | COLLAPSE/ CONSOLIDATION | WHEEZE | ABNORMAL | ABNORMAL | NORMAL |
| 2.9 | M | NUT | L | 21 | HYPERINFLATION | COUGH/WHEEZE | NORMAL | ABNORMAL | ABNORMAL |
| 5.3 | M | NUT | L | 30 | HYPERINFLATION | COUGH/WHEEZE | NORMAL | ABNORMAL | NORMAL |
| 5.7 | F | NUT | L | 120 | COLLAPSE | NONE | ABNORMAL | ABNORMAL | NORMAL |

TABLE 8

Patients studied

The incidence of abnormalities on V/Q scan was not higher in children reviewed early (before median length of follow up - 1.67 years), suggesting that abnormalities seen on scans were persistent. Four of eleven children reviewed before median follow up had normal V/Q scans, a similar proportion (3 out of 10) to those who were reviewed after 1.67 years.

Site of impaction, initial chest radiograph appearances and time before removal were identified as major adverse prognostic factors, the first of which reached statistical significance.

The FB impacted in the left lung in 12 children and of these 11 had an abnormal V/Q lung scan. Only 2 of the 9 in whom the foreign body lodged in the right lung showed persisting abnormality ($p<.05$).

SITE OF IMPACTION

(20 children, one excluded as FB impacted in the carina. In one child fragments removed from right and left lung. In this case the two lungs were analysed separately)

| | LEFT LUNG | RIGHT LUNG |
|---|---|---|
| NORMAL SCAN | 1 | 7 |
| ABNORMAL SCAN | 11 | 2 |

Collapse or consolidation of the affected lung on the initial chest xray carried a worse prognosis than hyperinflation. Of the seven children presenting with lobar collapse or collapse/consolidation only one (14%) had a normal V/Q scan at follow up. Eleven presented with hyperinflation on their chest xray and at follow up 6 had normal V/Q scans.

INITIAL RADIOGRAPHIC APPEARANCES OF AFFECTED LUNG

(Those children in whom initial radiograph reported as normal and child in whom FB impacted in carina excluded)

| | HYPERINFLATION | CONSOLIDATION/COLLAPSE |
|---|---|---|
| NORMAL SCAN | 6 | 1 |
| ABNORMAL SCAN | 5 | 6 |

Persistent defects of regional ventilation were commoner when removal was delayed beyond one week. Of 11 such children only 3 had a normal V/Q scan. When the foreign body was removed within one week four out of eight had a normal scan.

(1 child where FB impacted in carina excluded: in one child fragments were removed from both lungs, the lungs have been analysed separately in this case).

| | LESS THAN 7 DAYS | MORE THAN 7 DAYS |
|---|---|---|
| NORMAL SCAN | 5 | 3 |
| ABNORMAL SCAN | 5 | 8 |

## DISCUSSION

These results demonstrate that V/Q scanning provides a sensitive technique for the assessment of regional lung function after foreign body inhalation, more sensitive than either clinical review or chest radiography. However abnormalities of regional ventilation were seen on the non affected side in six cases. Two had histories suggestive of asthma, which is well known to produce abnormalities particularly in the lower lobes (Fazio et al 1979) and one had a respiratory infection at the time of the scan. In the other three children removal of the foreign body was noted to be incomplete suggesting these abnormalities represented the effect of fragmented material not seen or removed at bronchoscopy.

This study suggests that long term sequelae from foreign body inhalation are not uncommon. Fourteen had persisting abnormalities of regional ventilation, regardless of the time from inhalation to follow up. However the observed incidence of impaction in the left lung (57%) suggests that this sample may not be typical. Previous studies (Abdulmaid et al 1976, Davis 1966, Harboyan et al 1970, In Guk Kim et al 1973, Norris 1948, Pyman 1971) agree that the majority of foreign bodies lodge in the right lung and there is experimental pathological work to explain this (Lowe and Ross Russell 1984).

The bias may be explained by the role of the HSC as a tertiary referral centre treating what are likely to be the more complicated cases. In some cases removal had already been attempted at the referring hospital. It is therefore difficult to determine the overall incidence of long term sequelae although the high incidence of abnormality in our group has enabled identification of 3 adverse prognostic factors, impaction in the left lung, collapse or collapse/consolidation on the initial chest radiograph and delayed removal. Of these, the site of impaction appeared the most important, long term sequelae being more likely if the FB impacted in the left lung. It is difficult however to disentangle these factors and determine their relative importance. Both delayed removal and collapse/consolidation were commoner when the FB was in the left lung.

The accepted teaching that FBs most often impact in the right lung may partially explain the diagnostic delay when

impaction occurs in the left main bronchus. Furthermore collapse/consolidation in the left lower lobe may be hidden behind the heart and escape the notice of medical staff (Figure 29).

It is therefore important to recognise that foreign body inhalation may present with the radiographic picture of collapse/consolidation rather than the classical appearances of air trapping. Children who inhale a foreign body into the left lung with resultant collapse or consolidation are in the group at greater risk of long term sequelae. The data suggest that long term abnormalities of regional lung function in such children are not uncommon and that these children merit particularly close follow up.

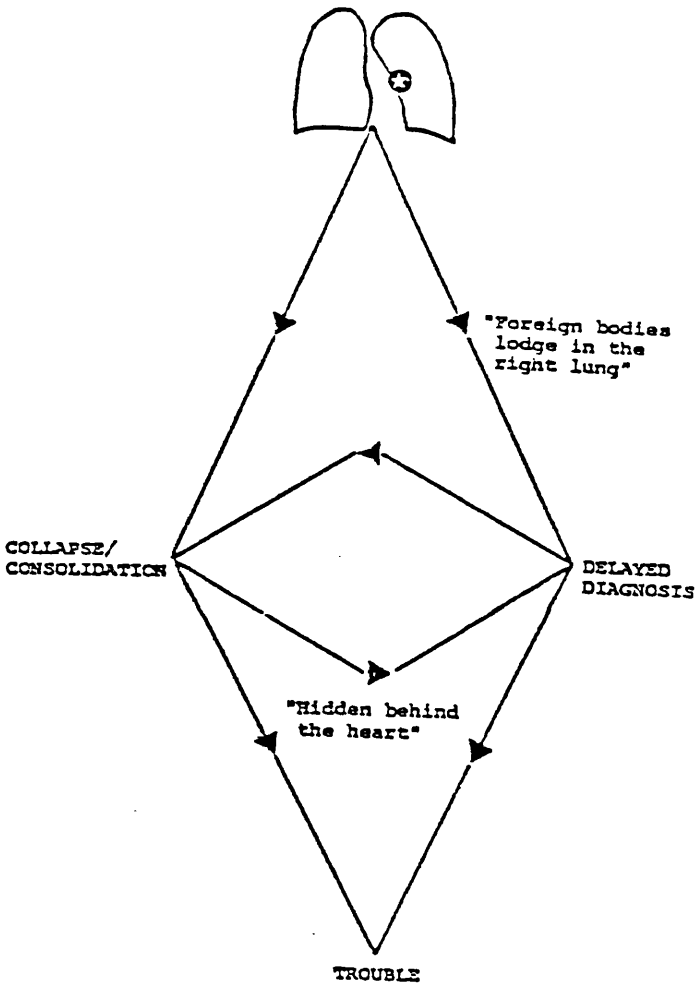


FIGURE 29

Sequence of possible events after inhaling a foreign body into the left lung.

# CHAPTER 6

# EFFECT OF POSTURE ON REGIONAL VENTILATION IN CHILDREN AND ADULTS

The distribution of ventilation and perfusion in the adult human lung has been extensively studied. Bronchospirometric (Svanberg 1957, Martin & Young 1957, Lillington et al 1959, Vaccarezza et al 1943) and radioactive gas methods (West & Dollery 1960, Ball et al 1962, Milic-Emili et al 1966, Amis et al 1984) have consistently shown that both ventilation and perfusion are preferentially distributed to dependent lung regions during tidal breathing and that this pattern is seen regardless of posture.

Remolina et al have demonstrated that the preferential distribution of ventilation to dependent lung regions is clinically important in managing adults with unilateral lung disease (Remolina et al 1981). Gas exchange improved in a group of 9 such adult patients when the good lung was dependent and deteriorated when it was uppermost (Figure 30). Mean arterial oxygen tension (PaO2) was 66.9 mm Hg supine, fell to 59.7 mm Hg when the good lung was uppermost and rose to 100.7 mm Hg when the good lung was dependent.

There is little published information concerning the pattern in children yet there are many differences in lung and chest wall mechanics in childhood which, along with clinical observation, have led to the hypothesis that the pattern of regional ventilation seen in adults may not be seen in children. The more compliant chest wall cannot fully support the underlying lung and functional residual capacity is therefore closer to residual

volume (Agostini 1959, Avery and Cook 1961). As a result airway closure is more likely to occur during tidal breathing (Mansell and Bryan 1972). Furthermore the function of the hemidiaphragms may also be different in childhood. As with all muscles, contractility is dependent on preload, in the case of the diaphragms this is the weight of the abdominal contents. In the decubitus posture, the child's smaller abdominal width will mean that the dependent hemidiaphragm will be under a smaller preload and therefore function less efficiently (Agostini et al 1964).

A recent report by Heaf et al (Heaf et al 1983) has provided support for this theory. Ten infants with unilateral lung disease (congenital diaphragmatic hernia, hypoplastic lung and unilateral atelectasis) were studied. Transcutaneous oxygen tension (TcpO2) improved in 9 of the 10 subjects when the good lung was positioned uppermost, the reverse pattern to that seen in adults (Figure 30). Four subjects had Kr81m ventilation lung scans which demonstrated that ventilation was preferentially distributed away from the dependent to the uppermost lung (Figure 31).

As with adults this pattern may have important therapeutic implications for the care of sick infants with unilateral lung disease. Arterial oxygenation can be maximised by careful positioning and a recent preliminary report suggests that infants with unilateral gas trapping due to interstitial emphysema can be successfully treated by placing the affected lung in the dependent position (Cohen et al 1984). Ventilation to this lung

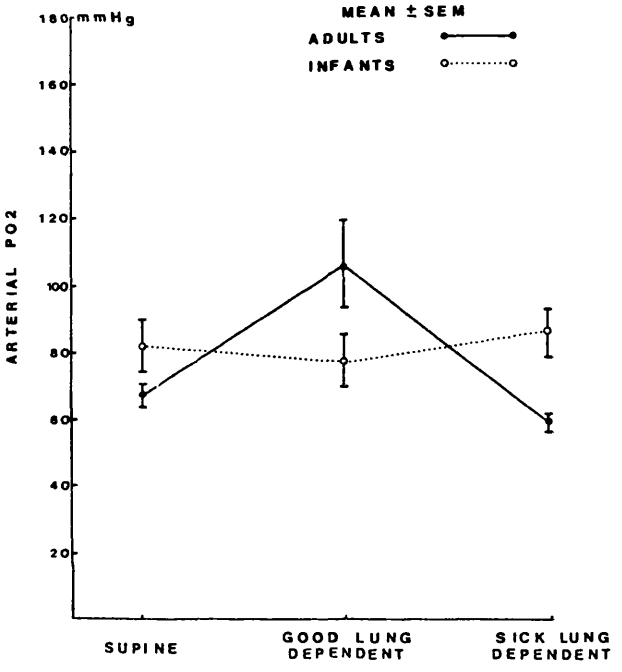


FIGURE 30

Effect of posture on arterial oxygenation in adults and children with unlateral lung disease.

Note the different patterns in the two age groups.

Data from Remolina et al and Heaf et al.

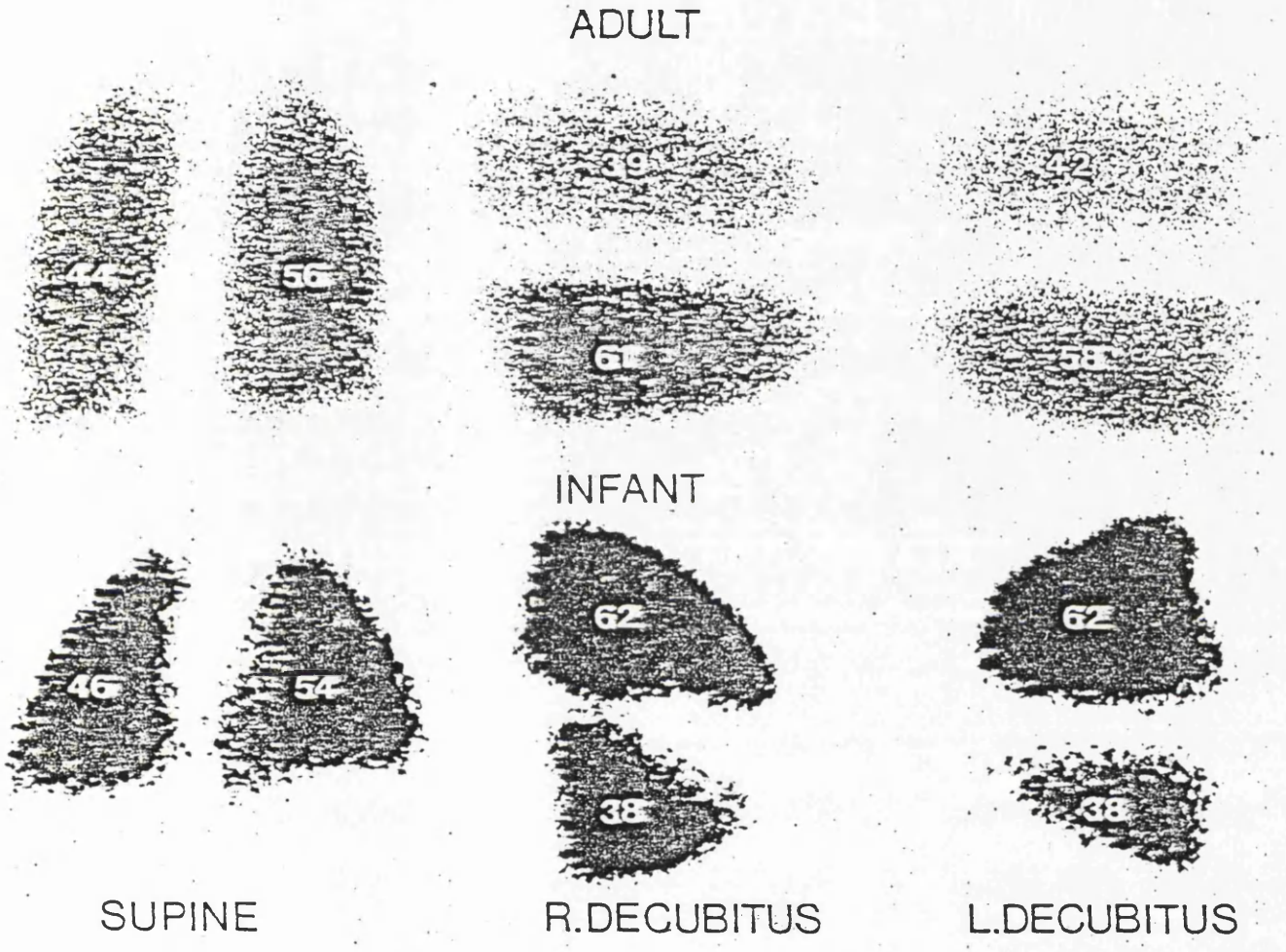


FIGURE 31

Posterior supine, right and left decubitus ventilation images in a healthy 31 year old adult (upper scans) and a 2 month old infant after repair of congenital diaphragmatic hernia.

Numbers superimposed over images represent fractional distribution of ventilation to each lung. Ventilation is preferentially distributed to the upper lung in the infant.

is reduced and hence the likelihood of accumulation of interstitial gas.

If regional ventilation is distributed differently in neonates, infants and very young children, the important question arises as to when the adult pattern is adopted. Anecdotal evidence suggests that this pattern of regional ventilation continues beyond early childhood but no studies attempting to answer this have been reported.

L.E. was a 5 year old child with Alagille's syndrome, (a syndrome characterised by multiple genetic defects including intra hepatic biliary hypoplasia and peripheral pulmonary stenosis, (Alagille et al 1975)), admitted to intensive care in respiratory failure. Diuretic therapy relieved pulmonary oedema but revealed widespread consolidation in the left upper lobe (Figure 32). Arterial oxygenation was critical and alteration of posture produced marked changes in gas exchange (Table 9) similar to that observed by Heaf et al in infants and would suggest that the "infant pattern" may persist beyond infancy.

To investigate these problems regional ventilation was investigated in a group of neonates, infants, children and adults.

TABLE 9

Arterial blood gases in L.E. with left upper lobe pneumonia.

Note improvement in oxygenation when good lung positioned uppermost.

| | Right side down (Good lung dependent) | Left side down (Good lung uppermost) |
|---|---|---|
| Ventilator Pressures | 20/3 | 20/3 |
| F(I)O2 | 0.4 | 0.4 |
| pH | 7.26 | 7.28 |
| P(A)CO2 | 43.4 | 43.3 |
| P(A)O2 | 71.6 | 90.4 |

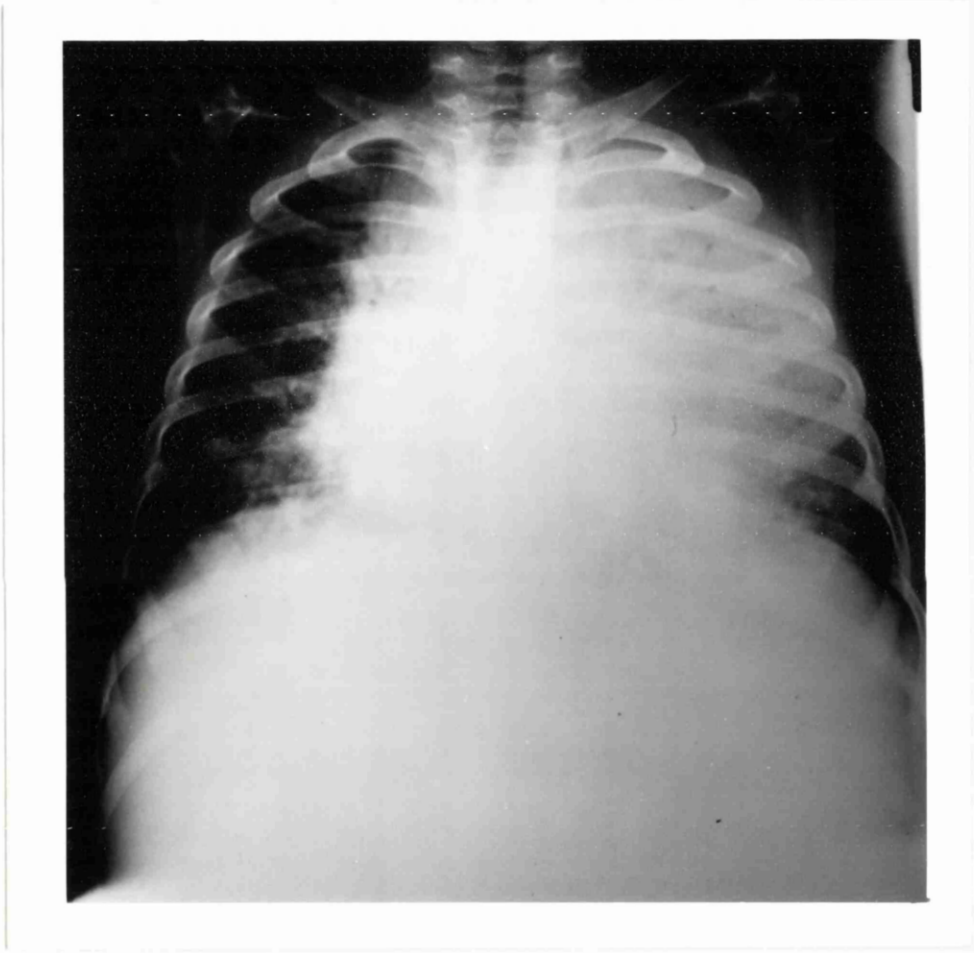

FIGURE 32

Chest radiograph of L.E. demonstrating predominantly unilateral lung disease.

## 1. INFANTS AND VERY YOUNG CHILDREN

The effect of posture on regional ventilation was assessed with steady state Kr81m ventilation images in 20 children, 12 boys and 8 girls, age range 7 days to 1.93 years. All were inpatients at the Hospital for Sick Children undergoing investigation for respiratory symptoms or requiring ventilatory support as part of their management. Supine, left and right lateral decubitus ventilation images were acquired and analysed to determine fractional ventilation to each lung in the three postures.

## 2. OLDER CHILDREN AND ADULTS

Fourty three children, 22 boys and 21 girls, mean age 10.5 years (2.0 to 16.9) were studied. All were attending for V/Q lung scan as part of their respiratory assessment. Supine, right and left decubitus Kr81m ventilation images were acquired as for infants.

Supine, right and left lateral ventilation lung scans were also performed on 16 adult volunteers, 7 men and 9 women, aged from 18.9 to 50.2 years (mean 30.7).

Children were divided into three subgroups on the basis of the interpretation of their chest radiograph by an independent radiologist:-

GROUP 1 Normal chest radiograph

GROUP 2 Unilateral radiographic abnormalities

GROUP 3 Bilateral radiographic abnormalities

**ANALYSIS**

Differences between fractional ventilation to the right lung (VfR) in the three postures were tested for significance with paired student 't' tests. Analysis was performed after the subjects had been divided into four groups:

A. Age 0 to 2 B. Age 2 to 10 C. Age 10 to 18 D. Age 18 and above.

These groups were further subdivided on the basis of the interpretation of the chest radiograph.

**RESULTS** (Appendix 7)

GROUP A: INFANTS AND VERY YOUNG CHILDREN (AGE 0 TO 2)

In the supine posture mean fractional ventilation to the right lung (VfR) was 57.7% (+/-10.4) (Figure 33). When the right lung was dependent VfR fell to 42.4% (+/-14.2) and when uppermost rose to 69.0%(+/-13.9). Both changes were significant ($p<0.001$) (Figure 33). In only two children (subjects 8,12) did VfR fall when the right lung was uppermost. These children conformed to the pattern seen in the rest of the group in the

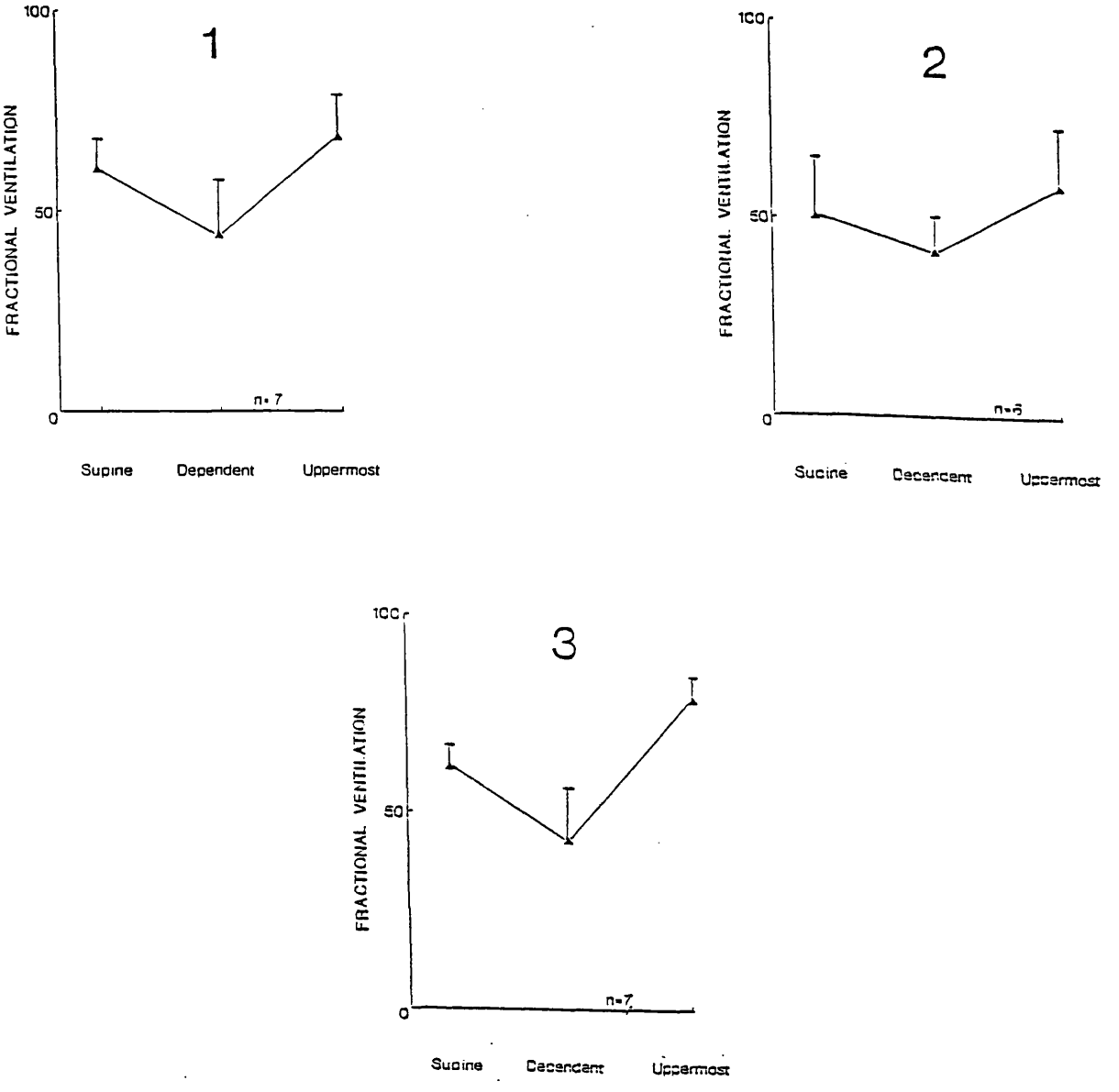


FIGURE 33

Fractional ventilation to right lung (%) when supine, dependent and uppermost. Vertical lines represent one standard deviation.

ALL CHILDREN UNDER 2 YEARS OF AGE

GROUP 1 Normal chest radiograph

GROUP 2 Unilateral radiographic abnormalities

GROUP 3 Bilateral radiographic abnormalities

left lateral decubitus posture i.e. a redistribution of ventilation to the uppermost lung.

Chest radiographic appearances made no difference to this pattern of regional ventilation.

GROUP B: CHILDREN AGED 2 to 10 YEARS (Appendix 7)

In the supine posture mean VfR was 46.1% (+/-12.6). When the right lung was dependent VfR fell to 36.0% (+/-12.8) and when uppermost rose to 56.1%(+/-9.9) (Fig 34). Both changes were significant ($p<0.0005$). The difference between VfR (dependent) and VfR (uppermost) was also highly significant ($p<0.0005$). Redistribution of ventilation away from the dependent toward the uppermost lung was seen in all children.

Again chest radiographic appearances made no difference to this pattern of regional ventilation.

GROUP C: CHILDREN AGED 10 to 18 years. (Appendix 7)

In the supine posture mean VfR was 57.2% (+/-7.3). When the right lung was dependent VfR fell to 48.0% (+/-8.2) and when uppermost rose to 62.9%(+/-7.9) (Fig 35). Both changes were significant ($p<0.0005$). The difference between VfR (supine) and VfR (uppermost) was also highly significant ($p<0.0005$). Four children showed the adult or mixed pattern of regional ventilation. One child demonstrated the adult pattern in both

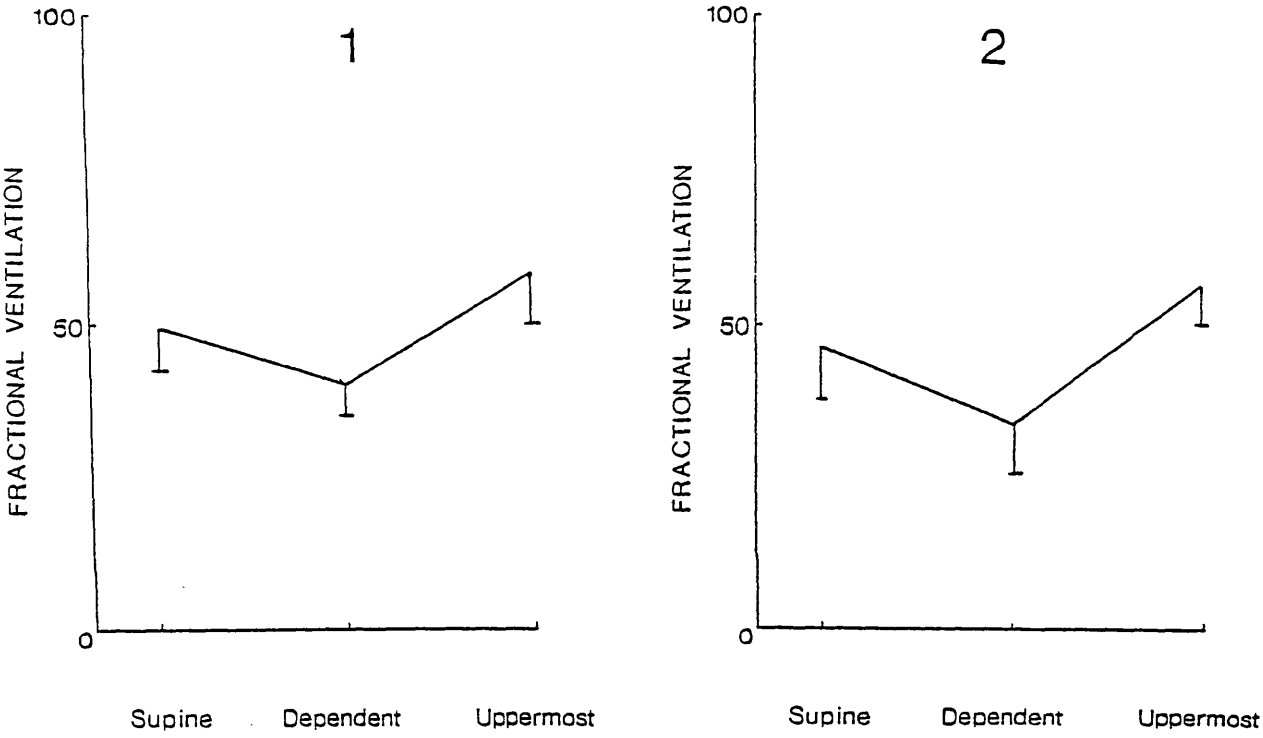


FIGURE 34

Fractional ventilation to right lung (%) when supine, dependent and uppermost. Vertical lines represent one standard deviation.

CHILDREN AGED 2 TO 10 YEARS

GROUP 1 Normal chest radiograph (n=9)

GROUP 2 Bilateral radiographic abnormalities (n=5)

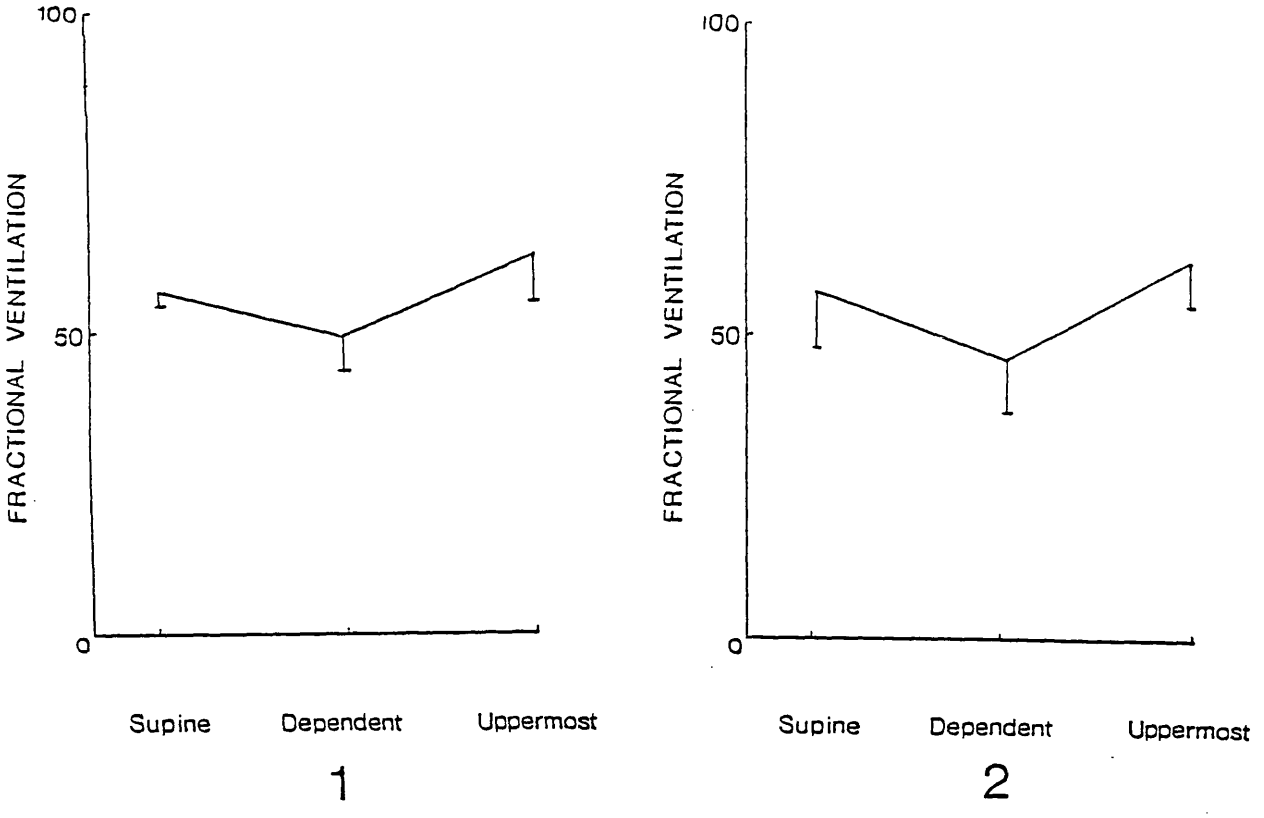


FIGURE 35

Fractional ventilation to right lung (%) when supine, dependent and uppermost. Vertical lines represent one standard deviation.

CHILDREN AGED 10 TO 18 YEARS

GROUP 1 Normal chest radiograph (n=7)

GROUP 2 Bilateral radiographic abnormalities (n=12)

right and left decubitus postures (JB) while 3 others (IH, WW, SD) demonstrated this pattern in the left decubitus posture.

GROUP D: 18 years and above.

A different pattern was observed in this group. In the supine posture mean VfR was 52.4% (+/-1.5). This rose when dependent to 53.4% (+/-4.9) and when uppermost fell to 48.9 (+/-7.7) (Fig 36). The change in ventilation from supine to uppermost and from dependent to uppermost reached significance although the change from supine to dependent did not. When the right lung was dependent VfR rose in 9 subjects and fell in 6. In 2 it remained unchanged. When uppermost VfR fell in 11 and rose in 6. In 8 VfR rose when dependent and fell when uppermost. The opposite was observed in three subjects while the remaining 6 showed a mixed pattern.

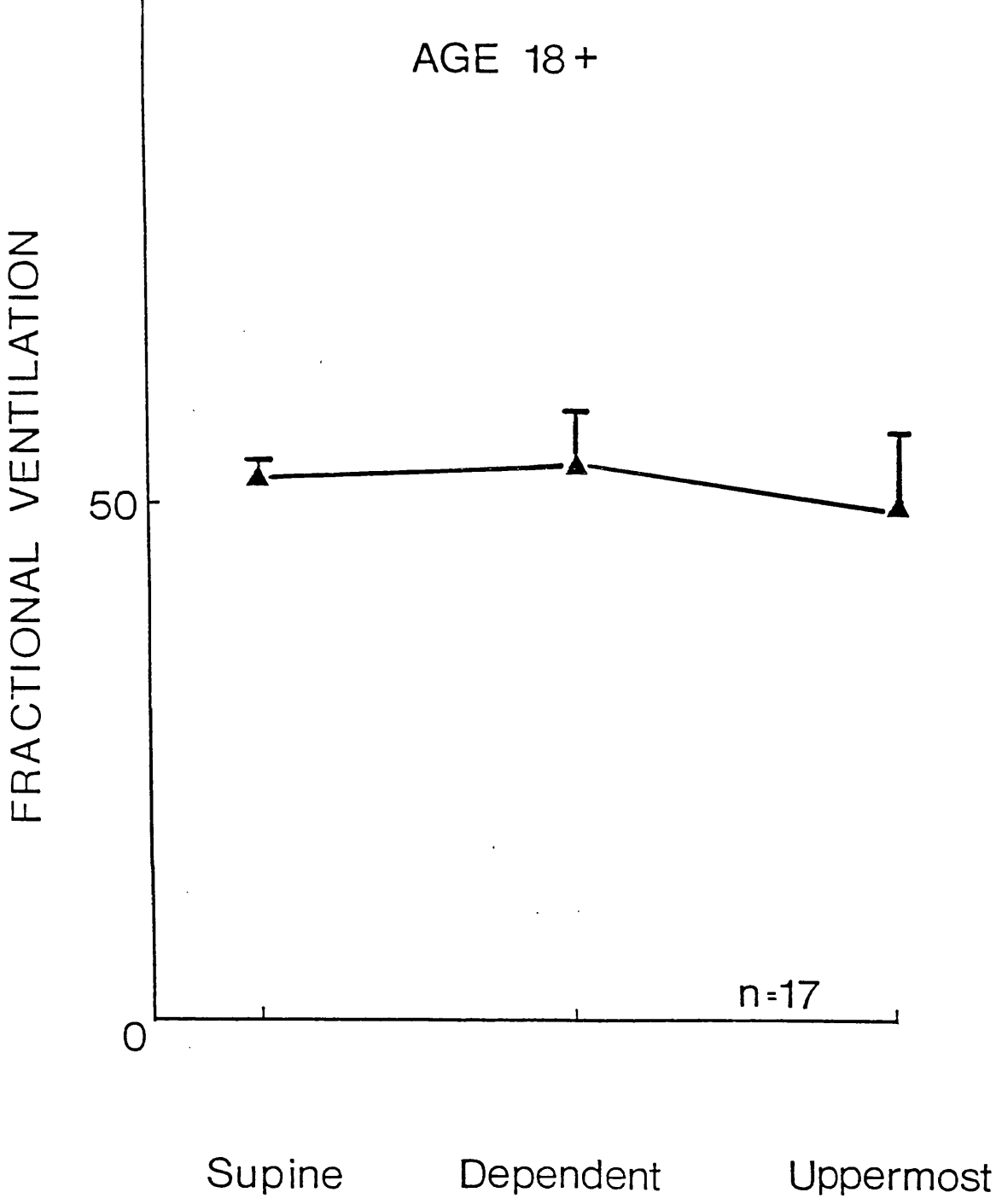


FIGURE 36

Fractional ventilation to right lung (%) when supine, dependent and uppermost. Vertical lines represent one standard deviation.

ADULT VOLUNTEERS (18 years and over)

Standard pulmonary function tests (PFTs) were performed on all subjects old enough to cooperate. Forced expiratory volume in one second (FEV1), forced vital capacity (FVC) and peak expiratory flow rate (PEFR) were recorded. Results of these tests were expressed as an FEV1:FVC ratio or in the case of PEFR as percent predicted estimated on height (Polgar and Promadhat). Subjects were divided into two groups according to the result:-

NORMAL PFTS:-

FEV1:FVC>80%, NORMAL FVC AND PEFR > 80% PREDICTED

ABNORMAL PFTS:-

FEV1:FVC < 80% OR PEFR < 80% PREDICTED

RESULTS

PFTs were recorded in 48 subjects. Three of these were not included in the analysis as left decubitus ventilation images were not performed. Their inclusion did not affect the analysis of redistribution of ventilation from the supine to right decubitus posture.

Distribution of ventilation in the children is depicted in Figure 37. Again a similar pattern was seen. Ventilation fell in the dependent lung and rose in the uppermost, demonstrating that the gravitational effects occurred independently of lung function.

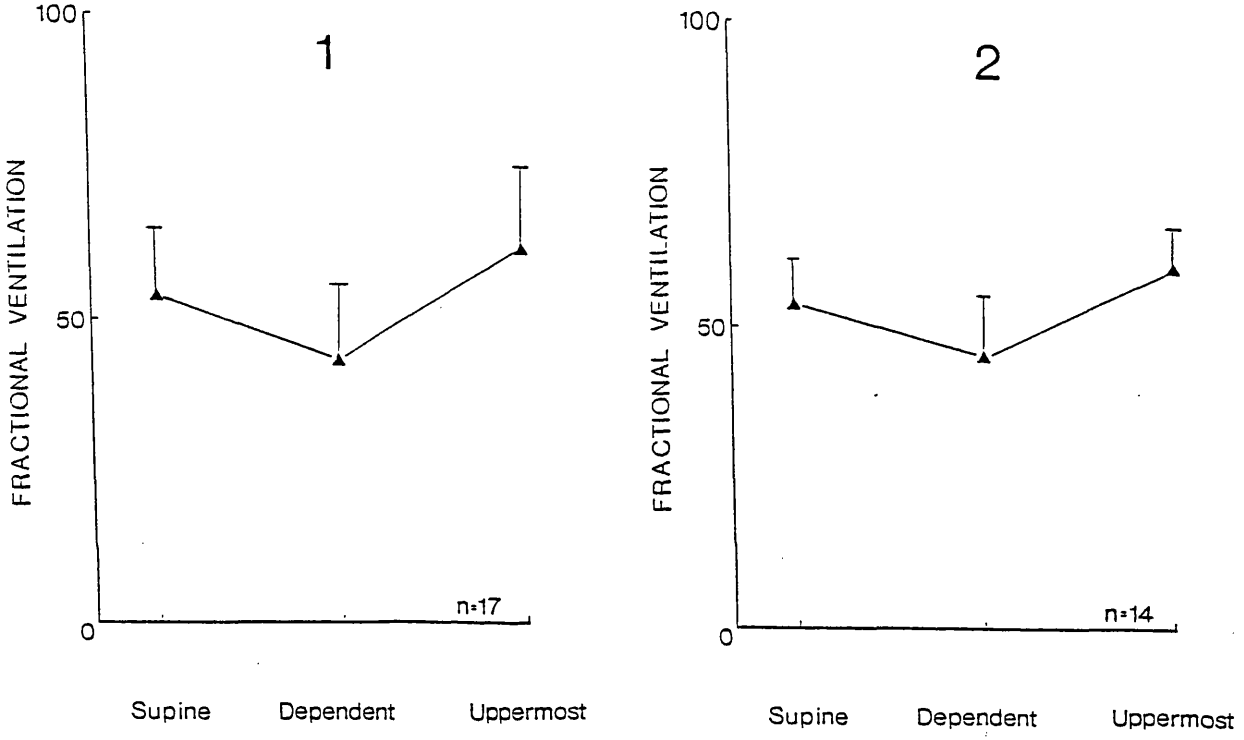


FIGURE 37

Fractional ventilation to right lung (%) when supine, dependent and uppermost. Vertical lines represent one standard deviation.

1 Normal pulmonary function tests

2 Abnormal pulmonary function tests

Data from the three age groups were amalgamated and using a standard linear regression program the relationship between age and postural changes in regional ventilation was studied. The data were also analysed to identify any difference between males and females.

Change in VfR from supine to dependent was expressed as:

$$\frac{\text{VfR (dependent)} - \text{VfR (supine)}}{\text{VfR (supine)}} * 100\ \%.$$

When positioned uppermost change in ventilation to the right lung was similarly expressed:

$$\frac{\text{VfR (uppermost)} - \text{VfR (supine)}}{\text{VfR (supine)}} * 100\ \%$$

RESULTS

Changes in VfR are plotted against age in Figures 38 and 39. Fractional ventilation to the right lung rose when moved from supine to uppermost in all but two children under 10 years of age, a mixed pattern was seen in the second decade but the majority (10 out of 14 subjects over 20 years) demonstrated the reverse pattern. The uppermost lung was preferentially ventilated up until the age of 20, when the distribution was reversed.

Figure 39 demonstrates that ventilation was redistributed in a similar fashion in the other decubitus position.

There was no demonstrable difference between males and females. The slopes for the regression line for the two sexes were very similar (0.94 cf 1.04) as were the Y intercepts (-30 cf -29).

## DISCUSSION

This study of infants and very young children confirms and extends the work of Heaf et al (Heaf et al 1983) demonstrating that in infants and very young children, ventilation is preferentially distributed to the uppermost lung, regardless of the radiographic appearances of the lungs. When nursing critically ill infants and very young children with unilateral lung disease these differences should be considered if optimal blood gases are to be achieved. It may also explain the observation that children with unilateral gas trapping can be effectively treated by placing the diseased lung dependent (Cohen et al 1984).

This reversal of the adult pattern can be explained by differences in the respiratory system of infants and adults. The resting negative pleural pressure, which is largely due to the opposing elastic recoil of the lungs and the chest wall helps to

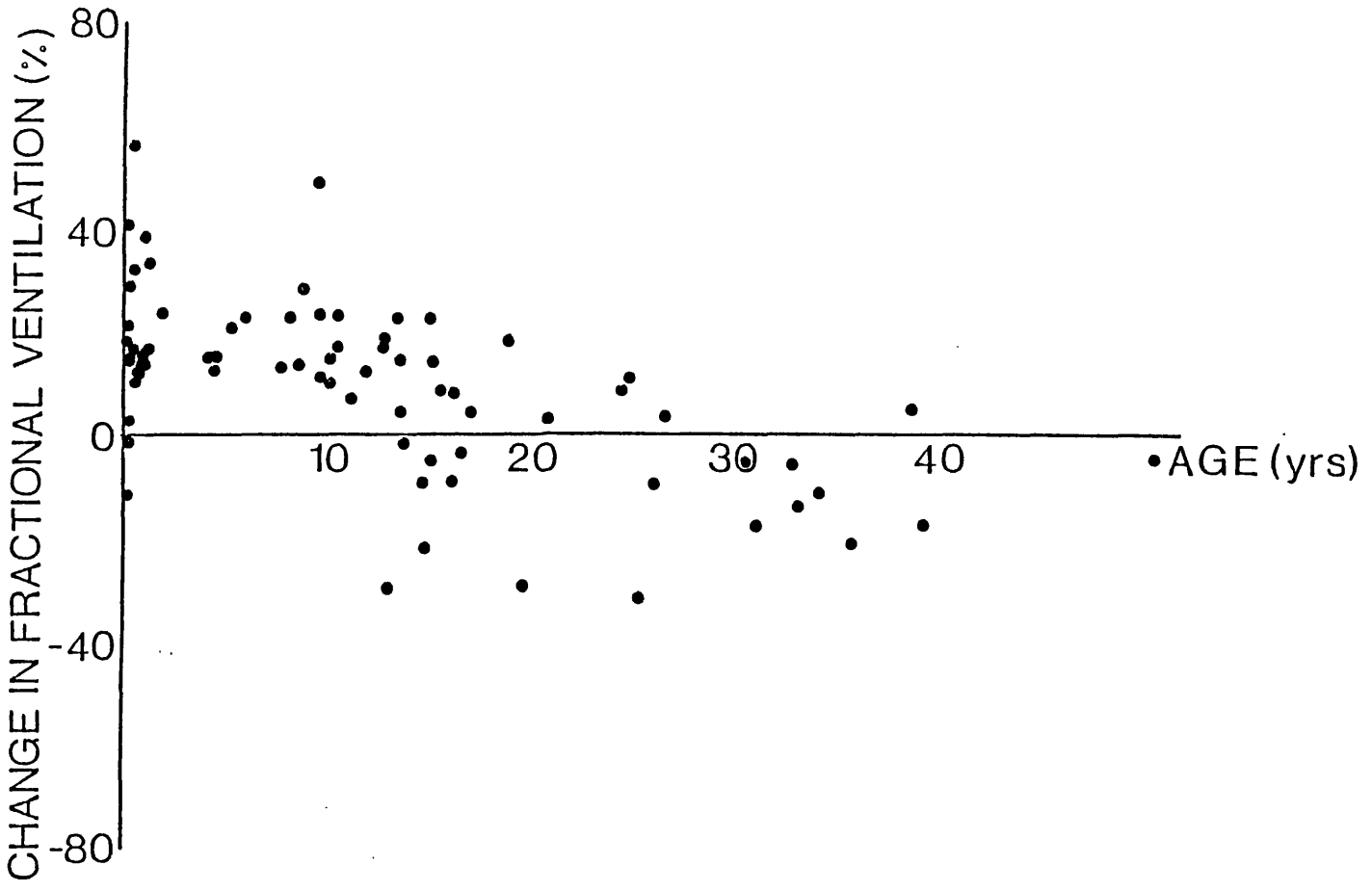


FIGURE 38

Change in fractional ventilation to the right lung when moved from supine to left decubitus (Right side up). Positive values for this fraction represent distribution of ventilation towards the upper lung.

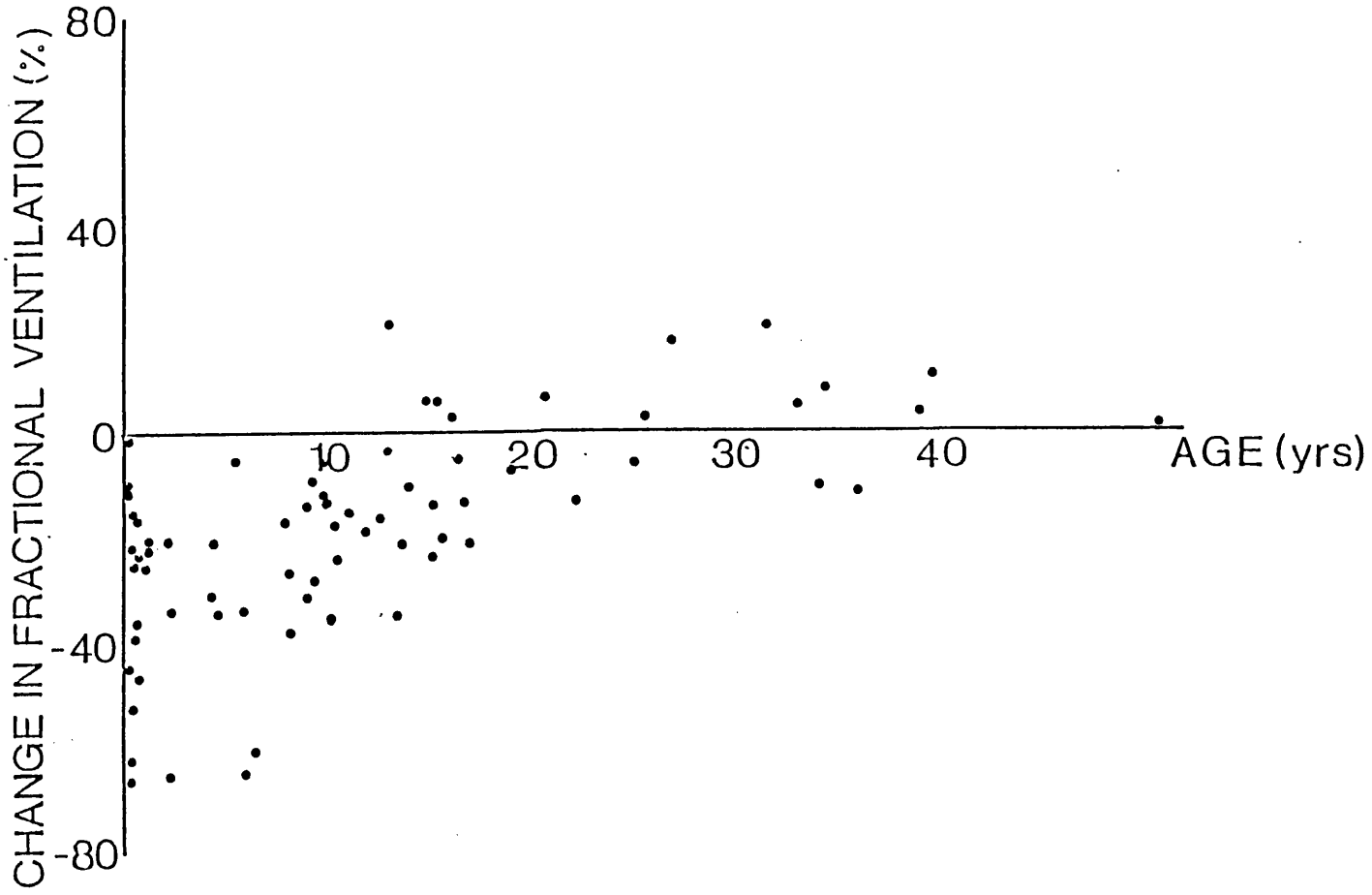


FIGURE 39

Change in fractional ventilation to the right lung when moved from supine to right decubitus (Right side down). Negative values for this fraction represent distribution of ventilation towards the upper lung.

maintain the patency of peripheral intrapulmonary airways. As this distending pressure approaches atmospheric pressure so the likelihood of airway closure increases (Mansell et al 1966). It is not, however, uniformly distributed throughout the thorax.

The weight of the lungs distends the uppermost more than the dependent regions, creating a vertical intrathoracic pressure gradient with the more negative values in the uppermost regions (Kaneko et al 1964).

The infant's chest is considerably smaller than that of the adult but a study of different sized animals suggests that the change in pleural pressure from top to bottom of the lung should be largely independent of body size (Agostini et al 1970). Thus the major influence on airway closure is likely to be the mean resting pleural pressure rather than the relative size of the subject.

The infant's chest wall is floppier than the adult's and the resting pleural pressure is closer to atmospheric pressure (Agostini 1959, Avery et al 1961, Helms et al 1981). It follows therefore that in dependent lung regions peripheral airway closure is more likely to occur. In this regard the infant behaves like the adult breathing at artificially low lung volumes. Under these circumstances pleural pressure in dependent regions approaches atmospheric pressure, airway closure occurs and in the lateral decubitus posture ventilation is distributed towards the uppermost lung (Milic Emili et al 1966).

Diaphragmatic function is also likely to differ in adults

and infants in lateral decubitus postures. The force of contraction or contractility of each hemidiaphragm is proportional to resting muscle fibre length and hence maximum force is generated at low lung volumes (Pengelly et al 1971). The greater the contractility of the hemidiaphragm, the greater the ventilation to that lung. Muscle fibre length itself is determined by the preload on the hemidiaphragm of which a major component in the lateral decubitus postures is the weight of the abdominal contents (Agostini et al 1964). Supine or prone, the preload is similar for both hemidiaphragms although overall preload may be symmetrically increased in the prone posture as the anterior abdominal wall is compressed (Fleming et al 1979). In lateral decubitus postures the weight of the abdominal contents will preferentially load the dependent hemidiaphragm thus improving its contractility. Hence the fractional ventilation to the dependent lung should be greater (Svanberg 1966).

In the adult there is a considerably greater preload on the dependent hemidiaphragm but in the infant the difference between preload on the uppermost and dependent hemidiaphragms must be smaller because the abdomen is narrower. Hence in infants and very young children there is likely to be less difference in contractility between dependent and uppermost hemidiaphragms and therefore less discrepency between the fractional ventilation to each lung. It is interesting to note that when the functional advantage of diaphragmatic loading is removed by muscle paralysis and intermittent positive pressure ventilation the anaesthetised adult subject shows a reversal of the usual increase in

ventilation to the dependent lung (Rehder et al 1972).

The data from the study of older children and adult volunteers demonstrate that preferential distribution of ventilation toward uppermost lung regions continues beyond infancy and early childhood. All children studied between the age of 2 and 10 demonstrated the "infant" pattern in both the left and right decubitus posture and no effect of age was observed. Beyond this age there was a gradual change until the adult pattern was adopted, at approximately 20 years.

The scatter plots (Figs 38 and 39) suggest that the relationship between age and the distribution of regional ventilation in different postures may not be a simple linear one. The adult pattern only emerges beyond the age of 10 and although there is a wide scatter of results in the group of adult volunteers the transition is virtually complete by the age of 20. The change is independent of sex, chest radiograph appearances and pulmonary function.

As detailed earlier in the discussion, the resting intrapleural pressure is nearer atmospheric in infants and therefore airway closure is more likely to occur in dependent lung regions. Ventilation will be redistributed toward uppermost regions and in the decubitus posture the uppermost lung will ventilate more effectively. If this hypothesis is correct the "infant" pattern should continue up to the age at which airway closure does not occur during tidal breathing. Work by Mansell

et al (Mansell et al 1972) has demonstrated that this can occur in children up to the age of 10, the age at which a trend toward the "adult" pattern of regional ventilation was seen.

Further support is provided by studies of capillary oxygen tension and its relationship with age. Mean oxygen tension rises to peak values in adolescence (Gaultier et al 1978) and this could be explained by the changing pattern of regional ventilation seen in childhood. While ventilation is preferentially distributed to uppermost lung regions in childhood, the dependent lung regions are better perfused (Chapter 7). This will result in ventilation/perfusion mismatch and hence lower arterial oxygen tension. When the adult pattern is adopted ventilation and perfusion will be distributed to the same (dependent lung regions) and arterial oxygen tension will thus be higher. The work of Gaultier et al suggests that this occurs from the age of 10, the age at which the transition to the "adult" pattern of regional ventilation becomes noticeable.

1. The pattern of regional ventilation in children is different from that seen in adults. Redistribution of ventilation away from the dependent lung and toward the uppermost was seen in all but 2 of 37 children under 10 years. A mixed pattern was seen in the second decade and by the age of 20 the adult pattern predominated.

2. Radiographic appearances and results of pulmonary function tests made no difference to this pattern. There was no demonstrable difference between the pattern seen in boys and girls.

3. These differences can be explained by the properties of the immature lung and chest wall.

4. When nursing critically ill infants and very young children with unilateral lung disease these differences should be considered if optimum blood gases are to be achieved.

# CHAPTER 7

## EFFECT OF POSTURE ON THE DISTRIBUTION OF PULMONARY PERFUSION IN CHILDREN

## INTRODUCTION

Two published reports have demonstrated that ventilation is preferentially distributed to uppermost lung regions in infants, the reverse of that seen in adults (Heaf et al 1983, Davies et al 1985). These studies have shown that gas exchange may be improved in infants with unilateral lung disease by positioning them "good lung uppermost". The opposite has been found in adults (Remolina et al 1981).

In neither paediatric study was pulmonary blood flow assessed although in the discussion it was proposed that its distribution is similar in children and adults. This has not been documented and a study was therefore conducted to examine the effect of posture on regional pulmonary blood flow in children.

## METHODS

Pulmonary perfusion was studied using Tc99m MAA injected into a peripheral vein. Regional ventilation was imaged with steady state Kr81m ventilation images. Details are given in Chapter 2.

## ANALYSIS

All images were stored on a dedicated computer. Regions of interest corresponding to right and left lung were identified

and activity within each was calculated.

CALCULATION OF FRACTIONAL PERFUSION AND VENTILATION WHEN SUPINE

The distribution of perfusion to the right lung (QfR) when supine was expressed as:

$$\frac{Rc}{Rc + Lc} * 100 \ \%$$

where Rc is Tc99m counts in right lung and Lc is Tc99m counts in left lung, both determined from the first perfusion image.

Fractional ventilation (VfR) to the right lung was calculated in a similar fashion.

CALCULATION OF DECUBITUS FRACTIONAL PERFUSION AND VENTILATION

As the macroaggregates lodge in the capillaries and the half life of Tc99m is 6 hours, the second perfusion image represents the sum of activity in the lung injected in both supine and lateral decubitus postures. To allow for this activity detected within each lung in the first perfusion image was subtracted from the activity in the same lung in the second perfusion image. Thus:

$$QfR\ (Decubitus) = \frac{R'c - Rc}{(R'c - Rc) + (L'c - Lc)} * 100\%$$

where R'c and L'c are activity in right and left lung respectively after both injections of Tc99m MAA.

This provided the distribution of the radionuclide injected in the lateral decubitus posture and QfR in the lateral decubitus posture was then calculated.

The radionuclide Kr81m decays rapidly (half life 13 seconds) and therefore no such manipulation was required for the ventilation images prior to calculating VfR in each position.

AP chest radiographs were taken in infants while PA films were taken in older children. All had lateral chest radiographs. These were classified independently by a consultant radiologist as normal (N = 6) or abnormal (N = 7) without knowledge of the V/Q scan results.

PATIENTS

Thirteen children aged 0.5 months to 11.3 years were studied (Table 10). All were patients attending the Hospital for Sick Children, London for the investigation of respiratory symptoms. Seven underwent ventilation imaging in the supine and lateral decubitus postures.

TABLE 10

Fractional perfusion to the right lung in 13 children aged 0.5 to 11.3 years when supine and in one decubitus position

UNILAT - Unilateral radiographic abnormalities

BILAT - Bilateral radiographic abnormalities

NORMAL - Normal chest Xray

| | | | SUPINE | RIGHT DECUBITUS | CHANGE |
|---|---|---|---|---|---|
| NAME | AGE | XRAY APPEARANCES | QfR | QfR | |
| AE | 0.5 | UNILAT | 65.5 | 66.8 | +1.3 |
| JM | 0.8 | UNILAT | 28.9 | 31.6 | +2.7 |
| PG | 1.0 | NORMAL | 53.0 | 59.4 | +6.4 |
| DM | 1.3 | UNILAT | 60.0 | 62.5 | +2.5 |
| TH | 2.6 | NORMAL | 56.7 | 63.1 | +6.4 |
| BK | 6.4 | BILAT | 53.0 | 35.0 | +2.0 |
| DJ | 6.4 | UNILAT | 29.0 | 33.0 | +4.0 |
| NC | 9.3 | UNILAT | 63.7 | 70.6 | +6.9 |
| JA | 9.9 | NORMAL | 55.9 | 62.8 | +6.9 |
| FK | 11.3 | NORMAL | 19.1 | 19.3 | +0.2 |
| | | | SUPINE | LEFT DECUBITUS | |
| | | | QfR | QfR | |
| RE | 0.7 | NORMAL | 57.0 | 50.0 | -7.0 |
| GC | 1.1 | NORMAL | 50.7 | 45.9 | -4.8 |
| LB | 1.8 | NORMAL | 46.6 | 46.5 | -0.1 |

TABLE 11

Fractional ventilation to the right lung in 7 children aged 0.8 to 11.3 years when supine and in one decubitus position

UNILAT - Unilateral radiographic abnormalities

BILAT - Bilateral radiographic abnormalities

NORMAL - Normal chest Xray

| | | | SUPINE | RIGHT DECUBITUS | CHANGE |
|---|---|---|---|---|---|
| NAME | AGE | XRAY | VfR | VfR | |
| JM | 0.8 | UNILAT | 36.0 | 17.0 | -19.0 |
| PG | 1.0 | NORMAL | 59.3 | 37.5 | -21.8 |
| BK | 6.4 | BILAT | 44.0 | 32.0 | -12.0 |
| DJ | 6.4 | UNILAT | 23.0 | 9.0 | -14.0 |
| NC | 9.3 | UNILAT | 61.5 | 52.2 | -9.3 |
| JA | 9.9 | NORMAL | 56.0 | 51.0 | -5.0 |
| FK | 11.3 | NORMAL | 26.1 | 23.3 | -1.8 |

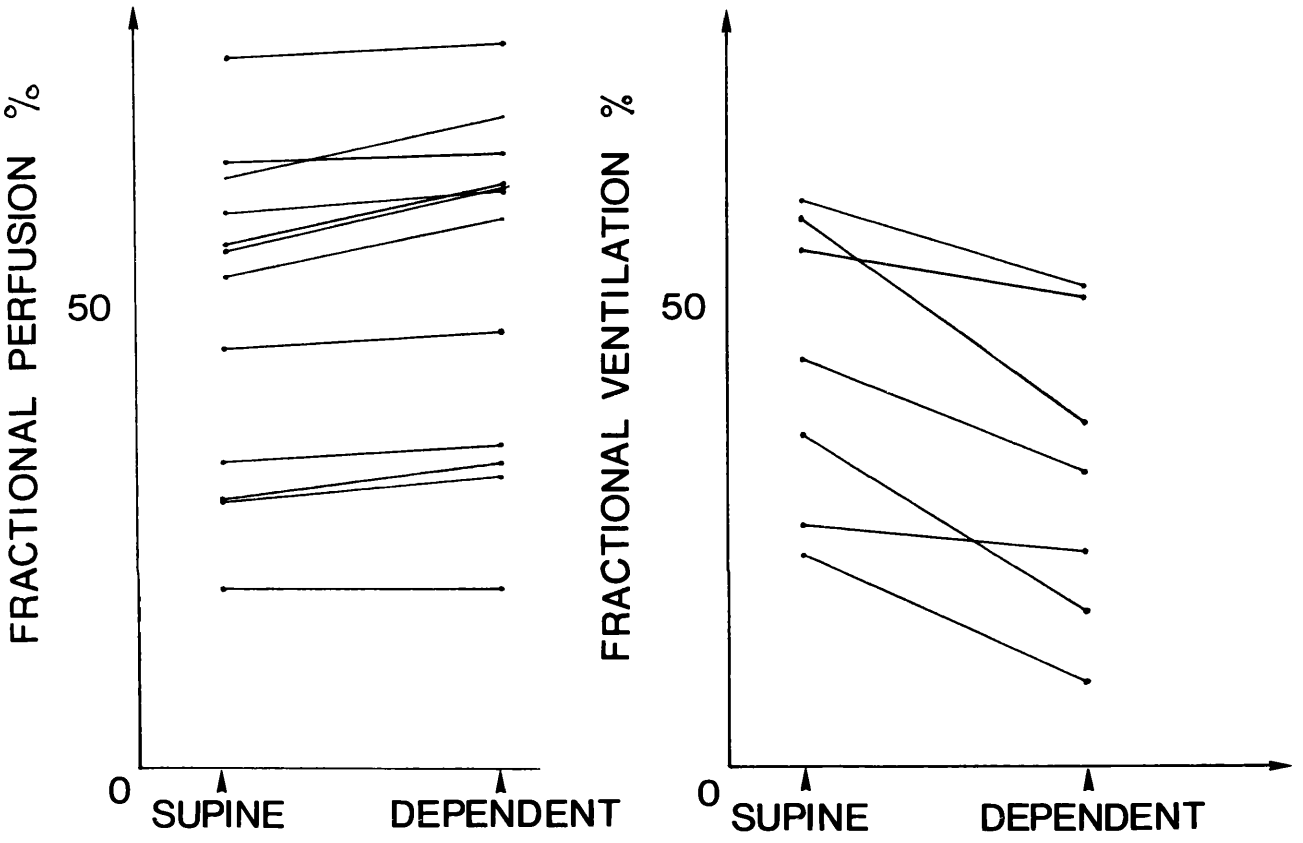


A B

FIGURE 40

Fractional perfusion (A) and fractional ventilation (B) to the right lung when supine and dependent.
Note that perfusion falls and ventilation rises in the dependent lung

RESULTS

10 children had supine and right decubitus scans while 3 had supine and left decubitus scans. Fractional perfusion to the dependent lung increased in all subjects studied (Table 10). In children having right decubitus scans mean QfR supine was 46.5% (19.1-65.5) rising to 50.4% (19.3-70.6) when dependent. Ventilation was distributed in the reverse direction (Table 11). Mean VfR supine was 43.7% (23.0-61.5) falling to 31.7% (9.0-52.2) when dependent.

DISCUSSION

The data from this study provide direct evidence that the effect of gravity on pulmonary blood flow is the same in children and adults.

Nevertheless despite the similar pattern of perfusion, there may be important differences between pulmonary blood flow in children and adults. Buyan has used a similar technique in adults (Bhuyan et al 1989). Seven patients were studied, one of whom had bilateral pleural effusions which might be expected to alter distribution of ventilation and perfusion and also affect external detection of the radionuclides. Excluding this single subject mean change in fractional perfusion in this group was 6.95% compared with 3.9% seen in children in this study.

These differences could be explained by examining the factors that influence the distribution of perfusion, the pulmonary arterial pressure, pulmonary venous pressure and to a

lesser extent alveolar pressure. West has proposed a theoretical model in which the lung may be divided into 4 zones according to the relative values of these factors (West 1972) (Figure 41).

In zone 1 (the uppermost lung region) alveolar pressure is greater than pulmonary arterial pressure and no flow occurs. In zones 2, 3, and 4 where pulmonary arterial pressure is greater than alveolar pressure or pulmonary venous pressure blood will flow through the capillary bed.

Pulmonary artery pressure remains relatively constant throughout childhood (Rudolph 1974) while lung height greatly increases. Zone 1 will therefore increase as the child grows. As this is the zone of absent perfusion, West's model would predict that the perfusion gradient between dependent and uppermost regions will be less in children reaching a maximum when growth is complete. Observations from this study bear out this theoretical model.

This observed difference may be another reason why pulmonary gas exchange is different in children and adults with unilateral lung disease. The smaller gradient in pulmonary perfusion in childhood will result in better perfusion of the uppermost lung regions and as these regions are preferentially ventilated in infants and young children V/Q matching may be better preserved.

## CONCLUSION

The pattern of regional perfusion is similar in children and adults, although the absolute difference between perfusion of uppermost and dependent lung regions is less in children. This may be one factor explaining the observation that arterial oxygenation can be improved in infants with unilateral lung disease when positioned good lung uppermost.

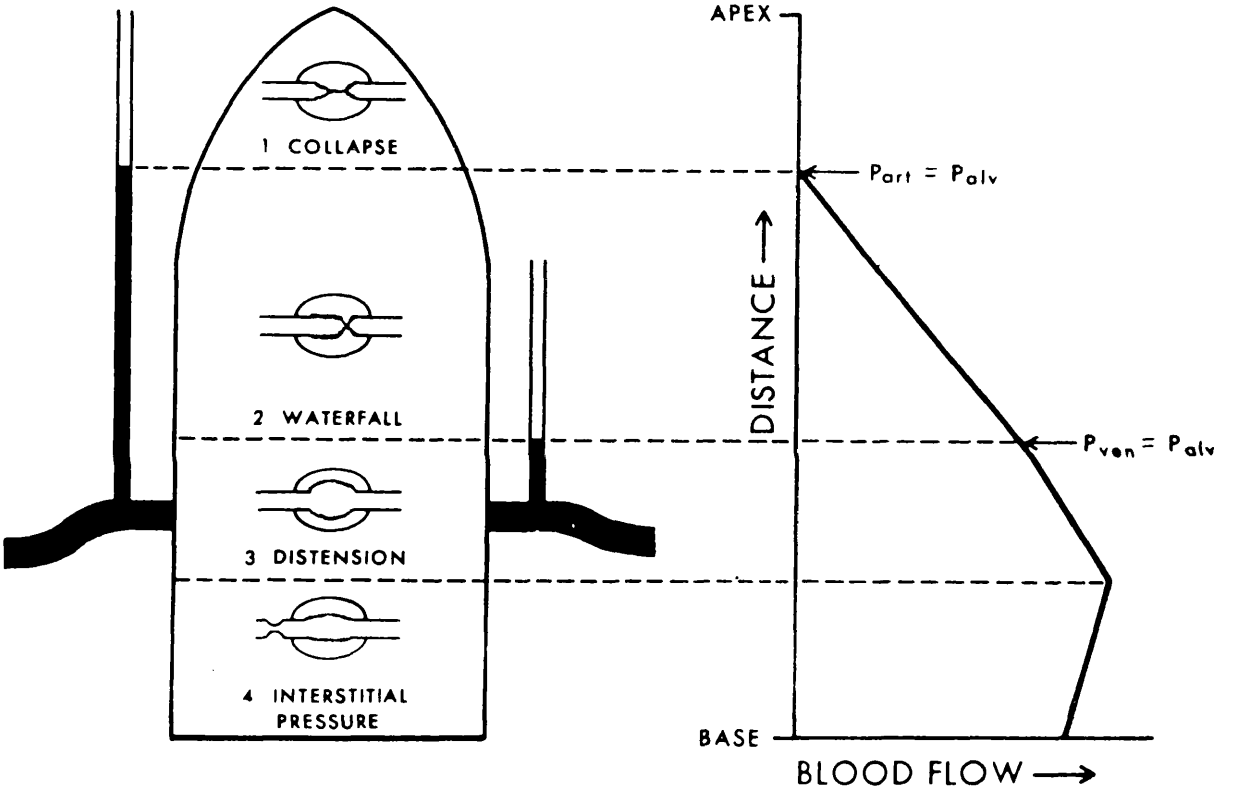


FIGURE 41

Theoretical representation of pulmonary perfusion (after West). See text for explanation

# CHAPTER 8

## APPLICATIONS OF DYNAMIC KR81M VENTILATION IMAGING

## INTRODUCTION

The studies reported in Chapter 4 demonstrated that dynamic steady state ventilation imaging can provide an accurate picture of regional ventilation, allowing separation of regional ventilation and volume of distribution of the radionuclide. Physiological and clinical applications of this technique are presented in this chapter.

Further investigations of regional ventilation in different postures have been conducted and it has also been used to study airflow from individual healthy and diseased lungs during a maximal expiratory manoeuvre. Its use in clinical practise is discussed with particular reference to asthma, scoliosis and obstruction of a main bronchus.

# 1. THE EFFECT OF POSTURE ON REGIONAL VENTILATION

## PHYSIOLOGICAL CONSIDERATIONS

It is difficult to provide a satisfactory physiological explanation for the finding that the adult pattern of regional ventilation is adopted at approximately 20 years of age (Chapter 6). If this is related to the higher intrathoracic pressure seen in children and greater airway closure in dependent lung regions during tidal breathing, the work of Mansell et al suggests that the adult pattern would be seen toward the end of the first decade of life (Mansell et al 1972).

The age at which the adult pattern of regional ventilation is established is as yet uncertain. Anecdotal evidence exists to suggest that this pattern continues beyond infancy and early childhood (Chapter 6) yet an eight year old child (T.B.) with right lower lobe collapse/consolidation ventilated for severe cerebral contusion demonstrated the "adult pattern", arterial blood gases improving when the good lung was dependent (Table 12).

TABLE 12

Arterial blood gases in patient T.B. (aged 8) in right and left decubitus positions.

T.B.

| | Right side down (Good lung uppermost) | Left side down (Good lung dependent) |
|---|---|---|
| Ventilator Pressures | 30/2 | 30/2 |
| F(I)O2 | 0.45 | 0.45 |
| pH | 7.53 | 7.53 |
| P(a)CO2 | 28.5 | 26.1 |
| P(a)O2 | 50.4 | 78.3 |

The findings in adults reported in Chapter 6 are not in full agreement with the studies of Amis et al (Amis et al 1984) which showed a clear gradient of ventilation from dependent to uppermost lung regions in a similar age range of healthy adults. Their methodology involved the use of the steady state Kr81m image as a marker of regional ventilation and the longer lived isotope Kr85m to measure regional lung volume.

This discrepancy might be explained if the adult volunteers in the studies reported in Chapter 6 breathed from different lung volumes. No instructions were given during imaging to maintain a constant end expiratory volume yet it can be demonstrated that alteration of FRC can radically affect the pattern of distribution of ventilation. Milic Emili (Milic Emili et al 1966) showed that distribution of inspired air is not constant, at low lung volume upper regions are preferentially ventilated while the reverse pattern is seen at FRC and above.

To confirm this three adult volunteers underwent ventilation scans while breathing close to total lung capacity (TLC) and then residual volume (RV). After positioning in the right lateral decubitus posture they were asked to take a full breath in and then breathe with their normal tidal volume from this point (TLC). Simultaneous tidal volume recordings were made using a differential pressure pneumotachograph to ensure end expiratory volume remained close to TLC and did not drift down. A 200

kilocount steady state Kr81m ventilation image was acquired and analysed as described in Chapter 2. A second Kr81m ventilation image was then acquired while the volunteer breathed tidally from RV.

TABLE 13

Effect of resting lung volume on regional distribution of ventilation in 3 healthy adult volunteers:

VfL - Fractional ventilation to left lung

VfR - Fractional ventilation to right lung

| SUBJECT | BREATHING AT | |
|---|---|---|
| | TLC | RV |
| H.V. | | |
| VfL (%) (UPPERMOST) | 34 | 54 |
| VfR (%) (DEPENDENT) | 66 | 46 |
| H.D. | | |
| VfL (%) (UPPERMOST) | 39 | 57 |
| VfR (%) (DEPENDENT) | 61 | 43 |
| I.G. | | |
| VfL (%) (UPPERMOST) | 37 | 50 |
| VfR (%) (DEPENDENT) | 63 | 50 |

Fractional ventilation to right and left lung determined from the two images is displayed in Table 13. While breathing close to TLC, all three demonstrated preferential distribution of ventilation to the dependent lung:- "the adult pattern", while at RV, the reverse "childhood pattern" was seen.

These results are in agreement with the work of Milic Emili et al (Milic Emili et al 1966) and demonstrate that steady state imaging is sufficiently sensitive to detect the different patterns of regional ventilation at varying resting lung volumes.

This sensitivity has recently been confirmed by work of Bhuyan (Bhuyan et al 1989). Steady state Kr81m imaging in a group of 7 adults demonstrated that ventilation was preferentially distributed to the dependent lung in 6 of these patients. The reverse pattern was seen in one subject who had large, bilateral pleural effusions which might be expected to affect regional ventilation. The presence of a considerable volume of fluid within the thorax will reduce lung volume. Functional residual capacity will therefore be nearer residual volume. Milic Emili et al have demonstrated that at this lung volume ventilation will be preferentially distributed to upper lung regions similar to the distribution seen in children. Such a pattern was observed in this case.

The discrepancy between the results reported in this chapter and those of Amis et al could also be attributed to postural changes in individual lung volumes. Previous radiological studies in adults have demonstrated that lung volume falls when dependent (Vacarezza et al 1946) and it has been clearly demonstrated that total Kr81m activity is affected by regional lung volume (Chapter 4). Total Kr81m activity within each lung may therefore change when the child or adult is repositioned independently of any change in regional ventilation. Thus in children total Kr81m

activity (the steady state image) may exaggerate the redistribution of ventilation to the uppermost lung. In adults this change in lung volume would have the opposite effect and reduce the difference between Kr81m activity in uppermost and dependent lung.

The possibility that children show similar changes in lung volume was therefore studied in a group undergoing V/Q scanning by examining changes in lung heights in the erect and supine AP CXR.

## PATIENTS AND METHODS

AP erect and right lateral decubitus chest radiographs were taken in 18 children. These two films were then used to measure changes in lung heights in the two positions and by inference changes in lung volume.

Right and left lung heights, defined as the distance from lung apex to hemidiaphragm in the mid clavicular line, were measured on each radiograph. Identical tube to film distances of 152 cms were used to eliminate magnification errors, and therefore no correction was made for magnification. Statistical significance of the changes was assessed using paired student 't' tests.

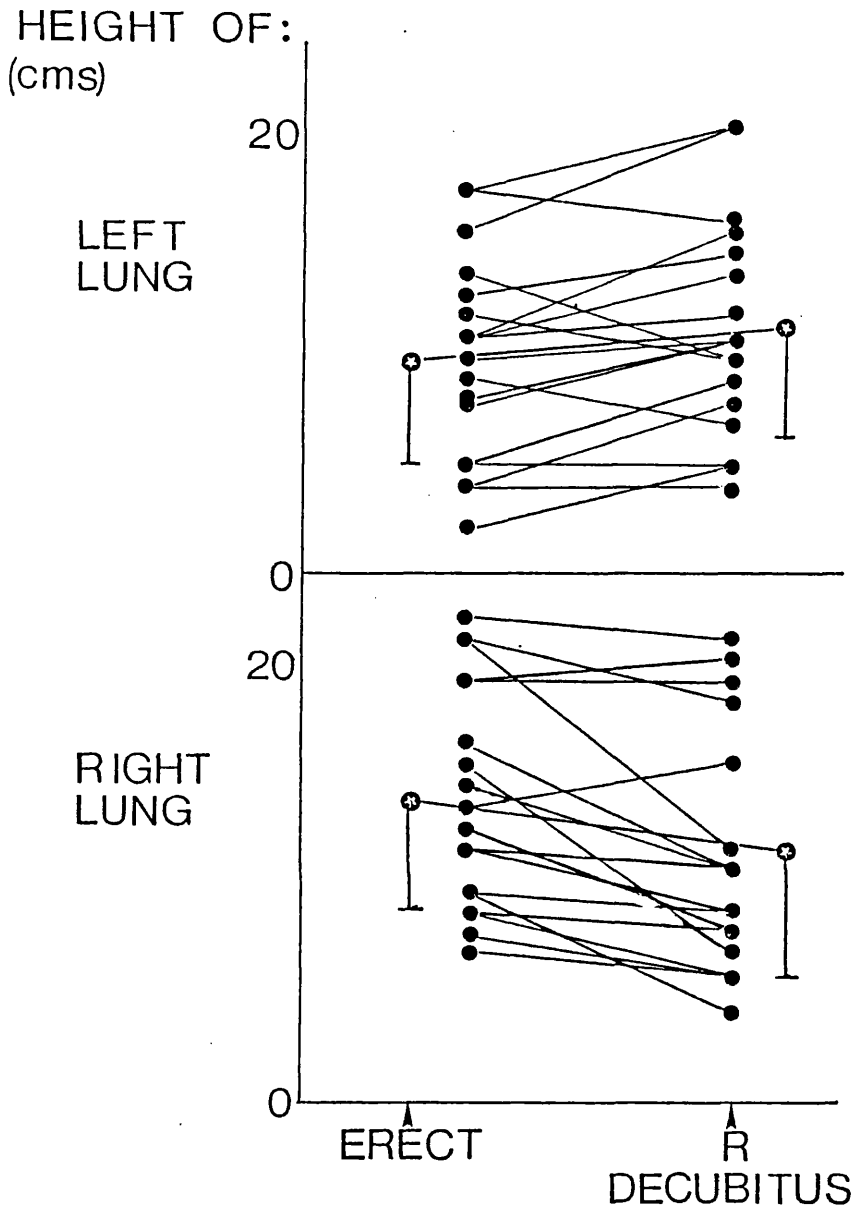


FIGURE 43

Measurement of lung heights in erect and right lateral decubitus positions.

RESULTS (Appendix 8 Figure 43)

Mean height of the left lung in the erect position was 17.5 (SD 2.4) cms rising to 18.3 (SD 2.6) cms when uppermost. Mean height of the right lung erect was 18.3 (SD 2.6) falling to 15.8 (SD 2.8) cms when dependent. Both changes were significant ($p<0.05$). The height of the left lung rose in 13, fell in 3 and remained unchanged in 2. Similarly the height of the right lung fell in 13, rose in 2 and remained unchanged in 2. Total Kr81m activity may therefore increase when the lung is uppermost independently of any change in ventilation giving a falsely elevated value for fractional ventilation to the uppermost lung.

## SEPARATION OF LUNG VOLUME AND VENTILATION USING DYNAMIC IMAGING

This problem could be overcome if it were possible to analyse lung volume and ventilation separately. Dynamic steady state ventilation imaging can separate tidal from resident Kr81m activity and therefore offers an alternative technique to study the effect of gravity on regional tidally exchanged Kr81m activity alone.

## PATIENTS AND METHODS

Dynamic steady state ventilation images were acquired in five subjects (4 children and 1 adult) in the supine and left decubitus posture. Scans were analysed as described in Chapter 4.

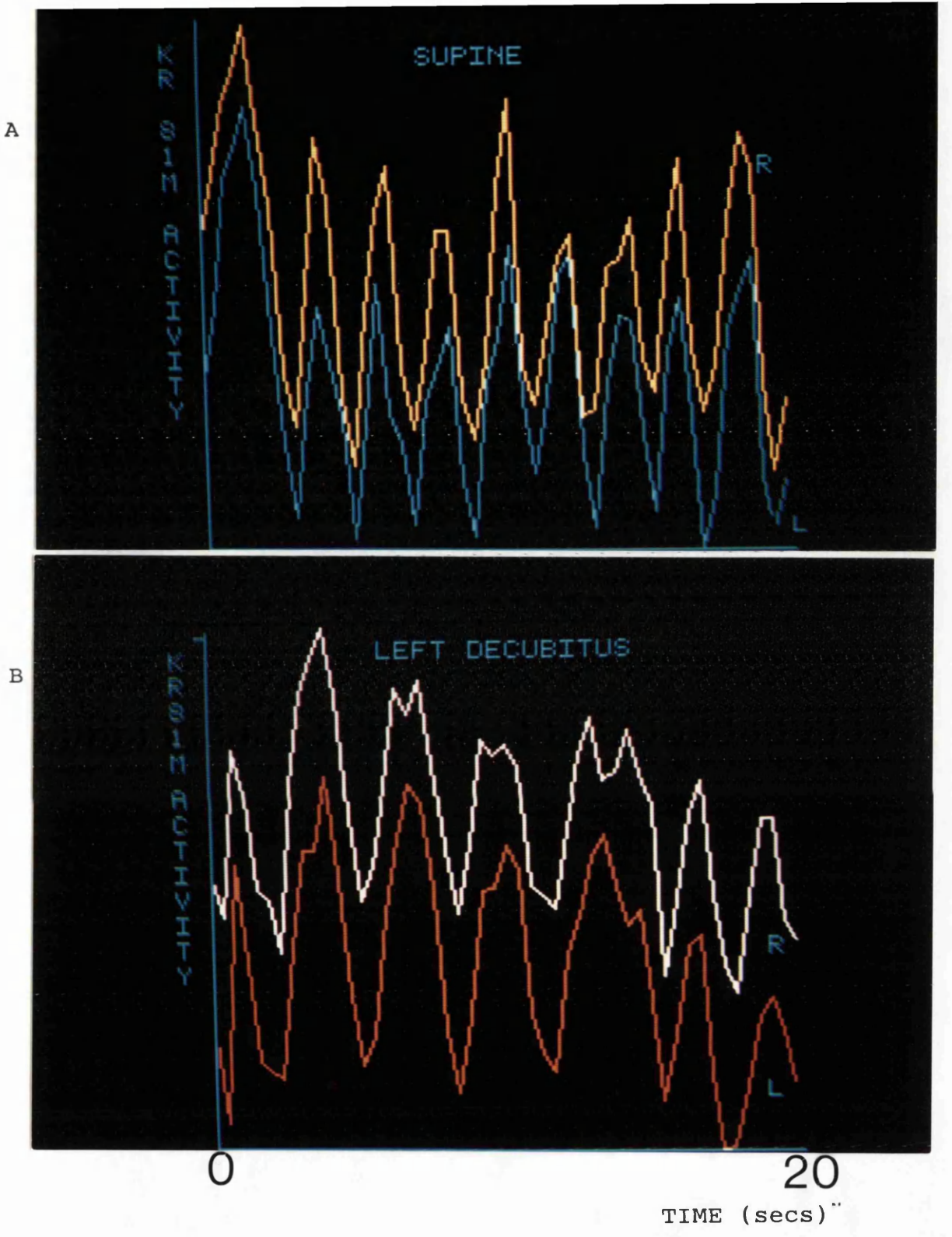


FIGURE 44

Dynamic steady state images supine (A) and left lateral decubitus (B). Patient SN. See text for explanation.

An example (SN) is illustrated in Figure 44. Regions of interest corresponding to right and left lung were drawn on the supine and left lateral decubitus image and activity/time profiles constructed for both lungs. Inspection of the supine dynamic scan (A) showed similar end expiratory activity levels and tidal fluctuations of Kr81m in right and left lung. However in the left lateral decubitus posture (B) although the end expiratory level fell in the dependent (left) lung the tidal fluctuations were greater suggesting that while the volume of the left lung had fallen, tidal ventilation to it had increased.

Using total Kr81m activity (the conventional steady state Kr81m image) fractional ventilation to this lung fell by 3.8%, while measurement of tidal Kr81m activity suggested that fractional ventilation rose by 2.1%.

Results from all 5 subjects are depicted in Table 14. They suggest that the adult pattern of regional ventilation may be adopted at a younger age than is estimated from studies assessing fractional ventilation with steady state Kr81m images. These results would be in line with physiological studies discussed in chapter 6 (Mansell et al 1972, Gaultier et al 1978). Further work in older children is obviously necesary to test these preliminary results and identify more precisely the age at which ventilation (independent of volume change) follows the adult pattern. It would then be possible to determine optimum management of critically ill children with unilateral lung disease.

TABLE 14

Change in fractional ventilation to left lung measured by total Kr81m activity (static image) and tidal Kr81m activity derived from dynamic image.

| | | F(V)L MEASURED BY | |
|---|---|---|---|
| | | 1 | 2 |
| AGE (years) | | Total Kr81m Activity | Tidal Kr81m |
| ID 5.8 | SUPINE | 49.8 | 59.2 |
| | DEPENDENT | 31.4 | 35.4 |
| | CHANGE | -17.4 | -24.5 |
| LJ 7.7 | SUPINE | 47.4 | 47.8 |
| | DEPENDENT | 39.8 | 44.3 |
| | CHANGE | -7.6 | -3.5 |
| SN 9.6 | SUPINE | 46.3 | 50.7 |
| | DEPENDENT | 42.5 | 52.8 |
| | CHANGE | -3.8 | +2.1 |
| RL 13.4 | SUPINE | 49.5 | 45.5 |
| | DEPENDENT | 37.8 | 50.8 |
| | CHANGE | -11.7 | +5.3 |
| RB 24.9 | SUPINE | 46.9 | 45.1 |
| | DEPENDENT | 43.9 | 48.1 |
| | CHANGE | -3.0 | +3.0 |

## 2. NONINVASIVE REGIONAL BRONCHOSPIROMETRY USING DYNAMIC VENTILATION IMAGING

The clinical manifestations of most respiratory illnesses are a consequence of narrowing of intrathoracic airways and subsequent airflow limitation. These effects can be seen at rest in severe disease but in mild or moderate cases they may only be elicited during a maximal respiratory effort. Spirometric measurements during such manoeuvres allow objective functional assessment and have become a cornerstone of respiratory investigations. They are now widely used in paediatric practise although the patient cooperation needed limits application to children old enough to understand and perform these respiratory manoeuvres. It is difficult to obtain reliable results below the age of 6 but in older children their value is now unquestioned.

These measurements are made at the mouth and can therefore only give a global assessment of airflow. Separate analysis of each lung is impossible yet most respiratory diseases will not have a uniform effect on pulmonary function. Dynamic ventilation imaging can record airflow from each lung or lung region, offering the possibility of noninvasive regional bronchospirometry (Chapter 4).

### PATIENTS AND METHODS

Dynamic ventilation images were acquired in 5 patients and 4 adult volunteers aged 7.1 to 32.7 years during a forced vital

capacity manoeuvre. The method of spirometry and dynamic ventilation imaging and analysis are described in Chapter 2. FEV1 and FVC were simultaneously measured at the mouth either by a dry wedge spirometer (volunteers) or differential pressure pneumotachograph (children).

Subjects were seated in front of the gamma camera breathing from an air/Krypton 81m mixture. Once activity was steady, the dynamic image was started and subjects were asked to inhale slowly to total lung capacity. They then exhaled as rapidly and completely as possible. Traces from the wedge spirometer were aligned with the dynamic image while the pneumotachograph and Kr81m signal were synchronised using an electronic digital timer. In all cases Kr81m activity was corrected for radioactive decay. Three studies are depicted in Figure 45.

To allow comparison between subjects and to test the accuracy of this technique the fractions of FVC and Kr81m activity exhaled at 0.5, 1.0 and 1.5 seconds were calculated for each subject. Agreement between these measurements was analysed using student 't' tests.

## RESULTS

Figure 45 shows three examples of regional dynamic ventilation imaging during a FVC manoeuvre and the simultaneous spirometric tracings. There is obvious close agreement between spirometry and dynamic imaging apparent even in one child who

interrupted the forced expiration and took a short breath before completing the manoeuvre (subject 2).

Results for the 9 subjects are tabulated in Table 15 and depicted graphically in Figure 46. Comparison of spirometry and dynamic imaging at 0.5, 1.0 and 1.5 seconds shows close agreement. Linear regression coefficients were 0.71, 0.97 and 0.99 respectively. The improving coefficients with longer scanning times are likely to be due to the relatively long frame times (5 frames per second - each frame lasting 0.2 seconds) allowed by the dedicated computer.

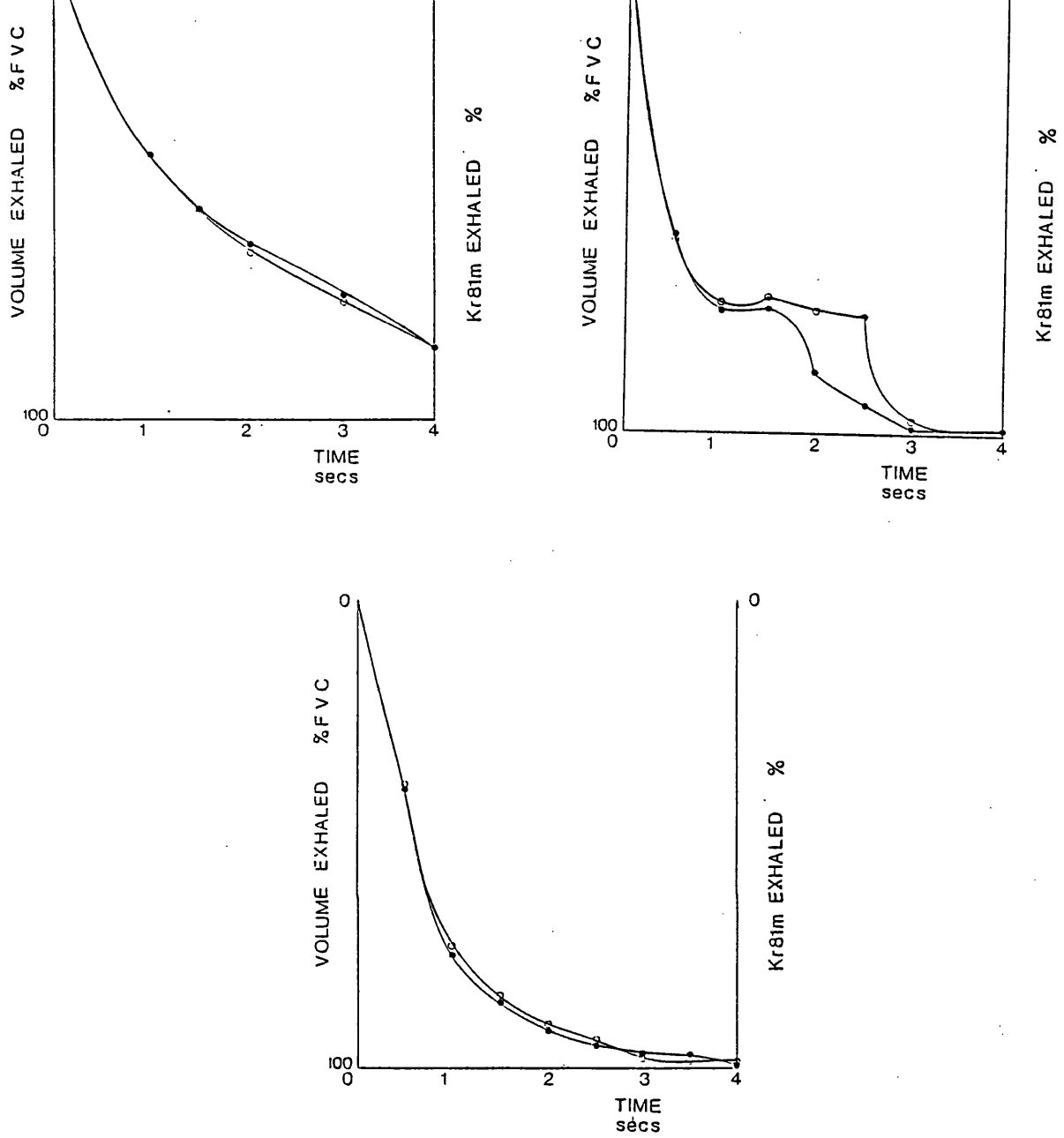





FIGURE 45

Time (in seconds) is on the abscissa while volume exhaled, expressed as a percentage of forced vital capacity is on one side of the ordinate.This starts at the top at 0% down to 100% at the bottom.

Kr81m activity is also on the ordinate and is expressed as a percentage of the total activity exhaled.

Filled circles :- spirometric trace
Open circles :- Kr81m activity

TABLE 15

Forced expired volume (FEV) and fraction of Kr81m activity (Kr81) exhaled in 0.5, 1.0 and 1.5 seconds in 9 subjects studied.

V= VOLUNTEER

| NAME | AGE | DIAGNOSIS | FEV1 0.5 secs | Kr81 0.5 secs | FEV1 1.0 secs | Kr81 1.0 secs | FEV1 1.5 secs | Kr81 1.5 secs |
|---|---|---|---|---|---|---|---|---|
| RE | 7.1 | Lung cyst | 0.67 | 0.68 | 0.74 | 0.73 | 0.74 | 0.72 |
| KR | 9.2 | Asthma | 0.39 | 0.40 | 0.61 | 0.62 | 0.76 | 0.79 |
| CT | 10.6 | Bronch-iectasis | 0.61 | 0.52 | 1.0 | 1.0 | - | - |
| LH | 12.8 | Haemo-ptysis | 0.5 | 0.38 | 0.77 | 0.74 | 0.87 | 0.87 |
| B | 17.4 | CF | 0.28 | 0.27 | 0.47 | 0.46 | 0.59 | 0.60 |
| GR | 20.9 | V | 0.45 | 0.54 | 0.84 | 0.79 | 0.96 | 0.93 |
| BL | 26.5 | V | 0.51 | 0.47 | 0.87 | 0.84 | 0.96 | 0.95 |
| CP | 28.0 | V | 0.54 | 0.54 | 0.82 | 0.86 | 0.91 | 0.92 |
| HD | 32.7 | V | 0.56 | 0.54 | 0.77 | 0.70 | 0.89 | 0.87 |
| | | | (r=0.71) | | (r=0.97) | | (r=0.99) | |

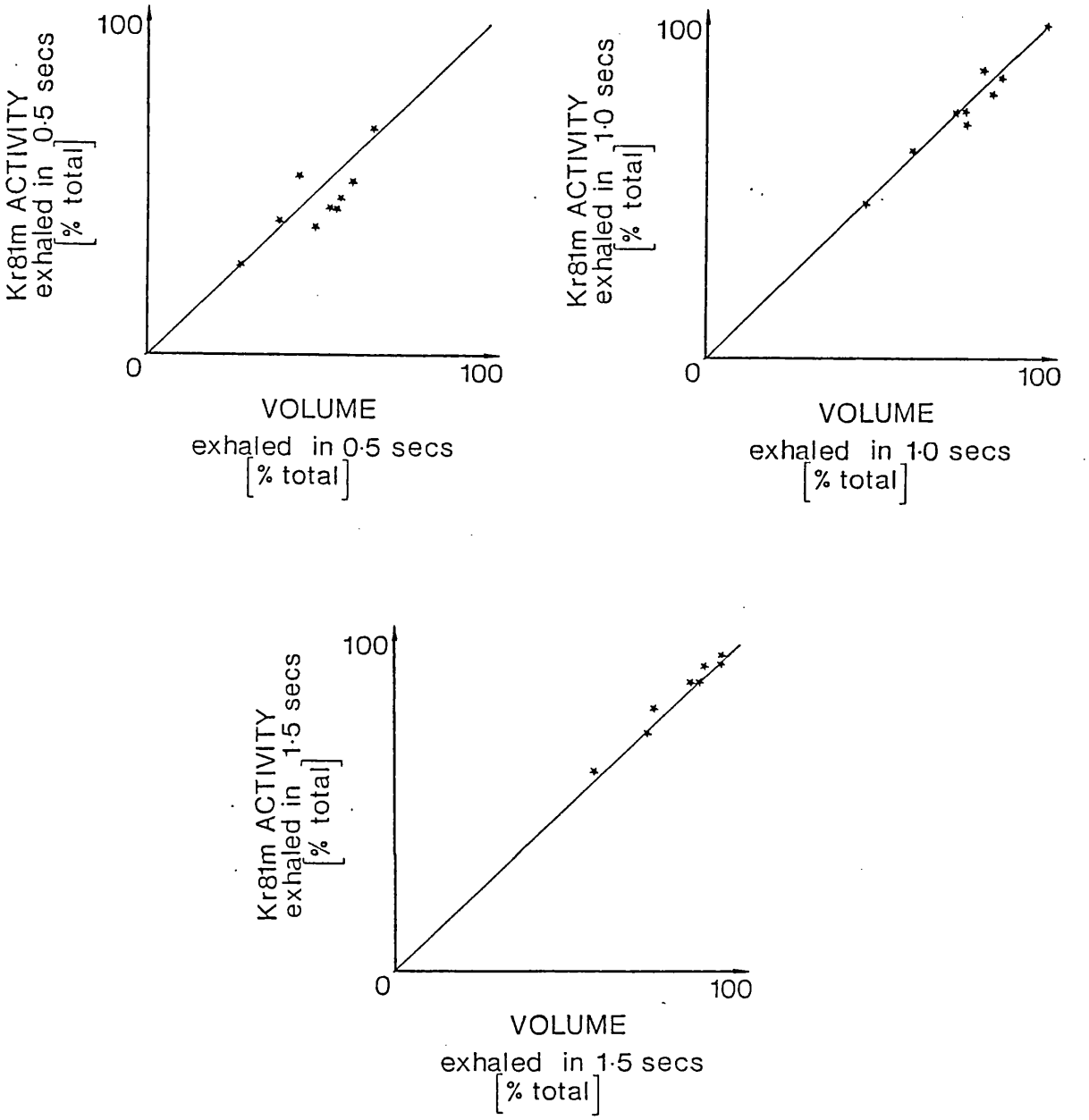


**FIGURE 46**

ABSCISSA:
% Fraction of FVC exhaled

ORDINATE:
% Fraction of Kr81m activity exhaled

A. At 0.5 seconds, B at 1.0 seconds, C at 1.5 seconds

Lines of identity are drawn. The 9 points represent data from the 9 patients.

## 3. CLINICAL APPLICATIONS OF DYNAMIC VENTILATION IMAGING DURING FORCED EXPIRATORY MANOEUVRE

### A. REGIONAL BRONCHOSPIROMETRY IN A CHILD WITH OBSTRUCTION OF THE LEFT MAIN BRONCHUS

GH was a 12 year old boy who presented with a 9 week history of wheeze initially diagnosed as asthma but unresponsive to standard bronchodilator therapy. Chest radiography (Figure 47) revealed hilar lymphadenopathy and a penetrated view of the carina showed severe narrowing of the left main bronchus. Pulmonary function tests showed global reduction of airflow at low lung volumes and gas trapping, compatible with the chest radiograph.

Steady state Kr81m imaging (Figure 47) showed grossly reduced ventilation to the left lung, fractional ventilation being only 19%. Thoracotomy was performed, a histological diagnosis of Hodgkins disease was made on biopsy material and chemotherapy started. V/Q scan repeated 8 weeks later demonstrated that ventilation to the left lung had returned almost to within normal limits (VfL = 44%).

In this case pre and post treatment dynamic ventilation images were acquired during a vital capacity manoeuvre. Pre treatment dynamic image is depicted in Figure 48.

A

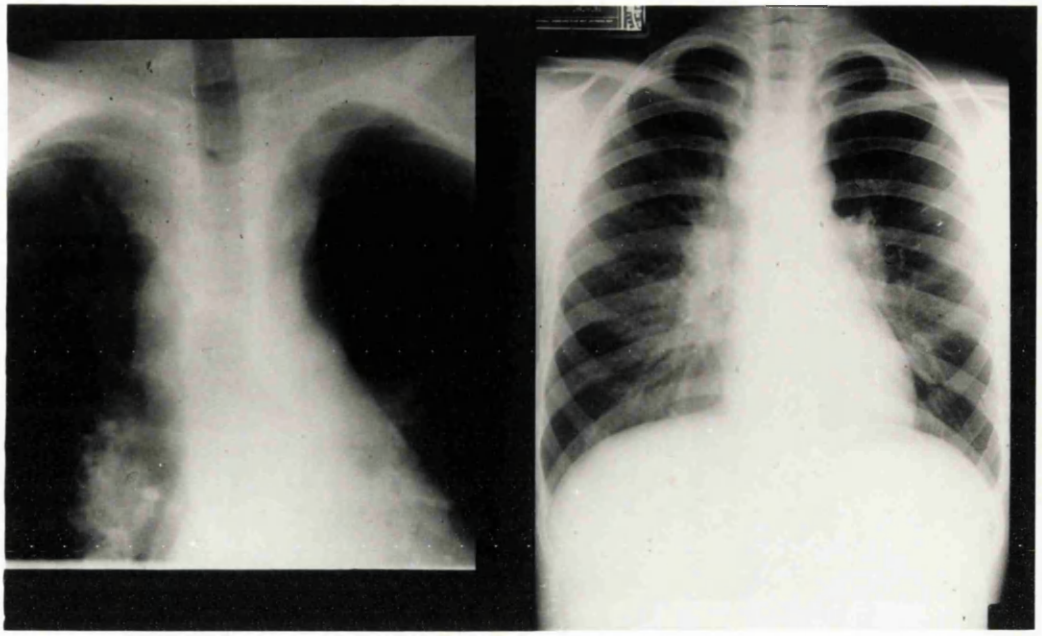

B

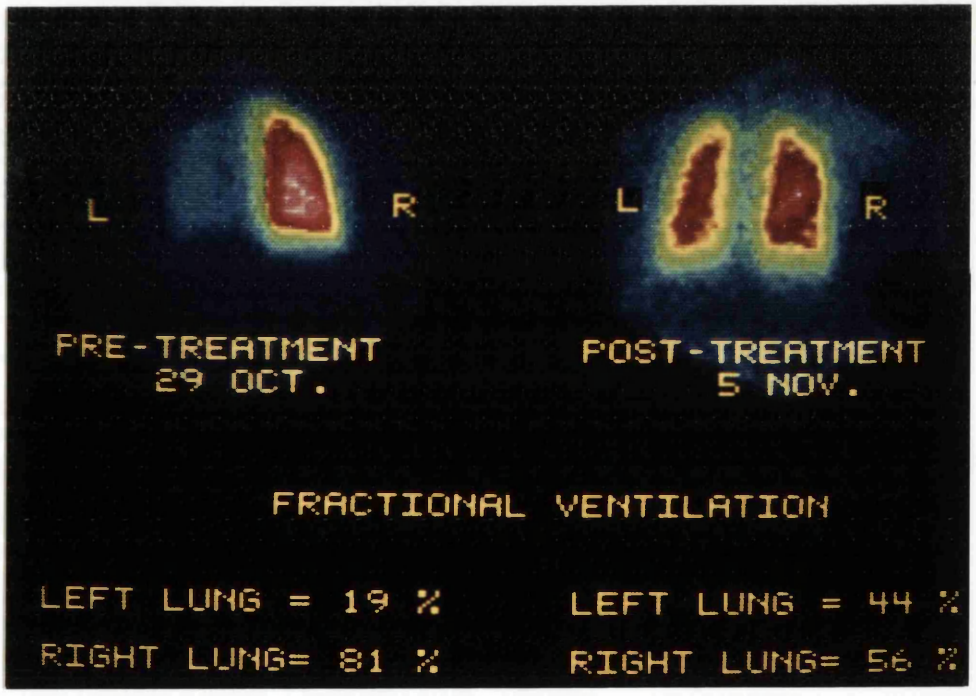


FIGURE 47

A. Pretreatment chest radiograph and penetrated view of carina (GH). Note hilar lymphadenopathy.

B. Pre- and post-treatment steady state ventilation image (GH)

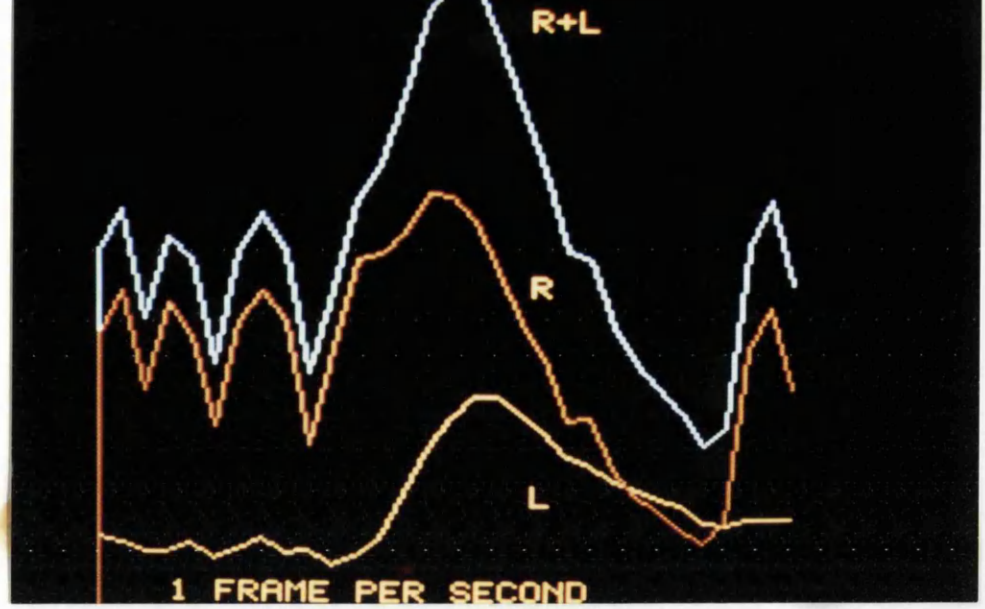


B

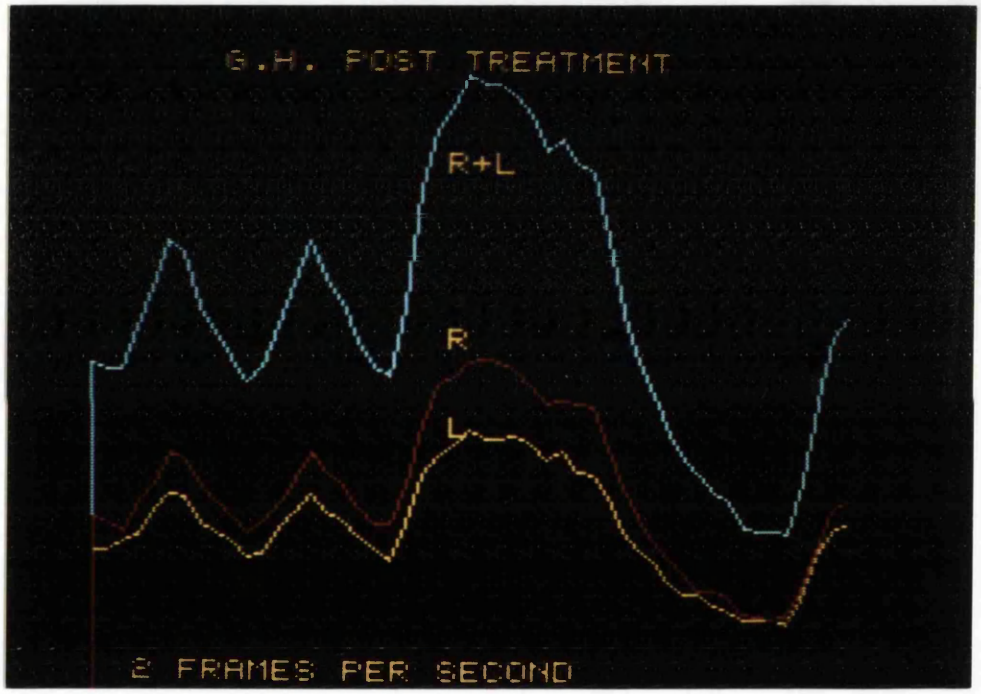


TIME (secs)

FIGURE 48

A. Pre treatment dynamic ventilation image (GH).

B. Post treatment dynamic ventilation image (GH).

Blue trace represents activity from both lungs combined, the red trace the right lung and the yellow trace the left lung.
Note the marked phase shift and reduction in amplitude of the left lung in the pre treatment scan. Both disappear on the post treatment image.

During tidal breathing obvious fluctuation was seen in the right lung, with little if any in the left. Activity in the right lung rose rapidly when the child was asked to take a full breath in while activity in the left lung rose only slowly, lagging behind the right. It was interesting to note that activity over the left lung was continuing to rise while that in the right was static or falling, suggesting airflow from right to left lung.

The child then performed a forced expiration. Activity within the right lung fell very rapidly while that in the left lung fell much more slowly. Activity levels in the two lungs crossed and the amount of Kr81m in the left lung did not fall to its previous level, indicative of gas trapping. Fluoroscopy during this procedure would presumably have shown mediastinal shift toward the right lung. Activity within the right lung, as would be expected, fell well below the end expiratory plateau observed prior to this manoeuvre.

In the post treatment dynamic image (Figure 48) the pattern of activity in the two lungs was similar with no evident time difference between the two. Activity was more evenly distributed and the activity profiles recorded over left and right lung during the forced vital capacity manoeuvre were parallel.

## B. REGIONAL BRONCHOSPIROMETRY IN AN ASTHMATIC CHILD BEFORE AND AFTER BRONCHODILATOR THERAPY.

The second example is that of a 10 year old boy with persistent wheezing from the age of three. A clinical diagnosis of asthma was made and the child was started on intermittent beta sympathomimetic bronchodilators. He was referred for further investigations when persistent radiographic changes in the lingula were noted and the possibility of foreign body inhalation was raised.

The child was asked to perform a forced vital capacity manoeuvre before and after a single dose of a metered dose aerosol (Salbutamol 100 micrograms). Simultaneous dynamic ventilation images were acquired (Figure 49).

Activity in the right lung prior to bronchodilator therapy was higher than that in the left but gradually equalised during expiration, suggesting there was incomplete emptying of the left lung compatible with obstruction of one of the bronchi within the left lung.

Airflow was more symmetrical post bronchodilator, with marked improvement of airflow from the left lung suggesting that the obstruction was reversible by bronchodilator therapy and more likely to be due to bronchospasm than a fixed obstruction such as a foreign body.

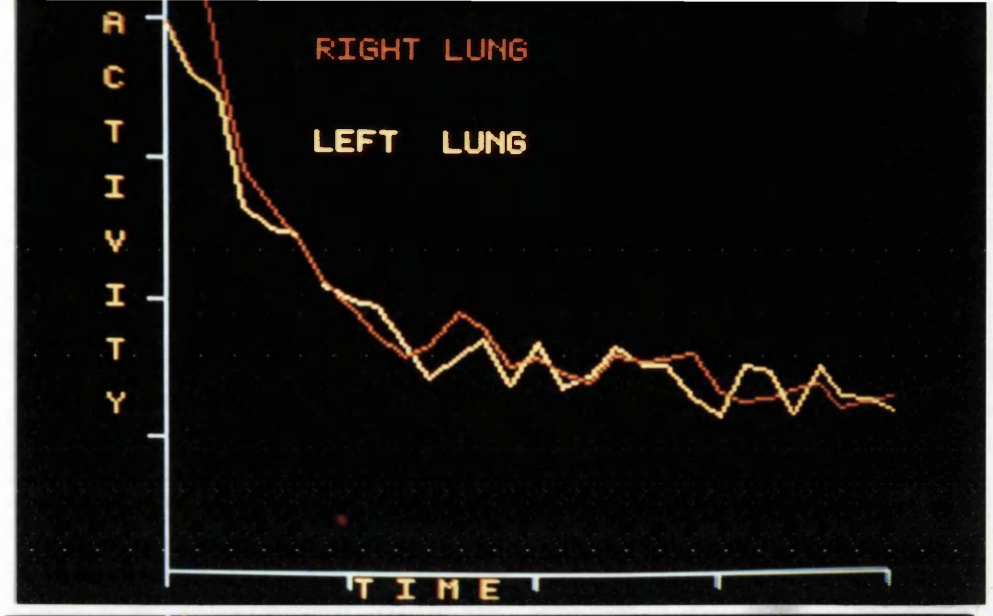


B

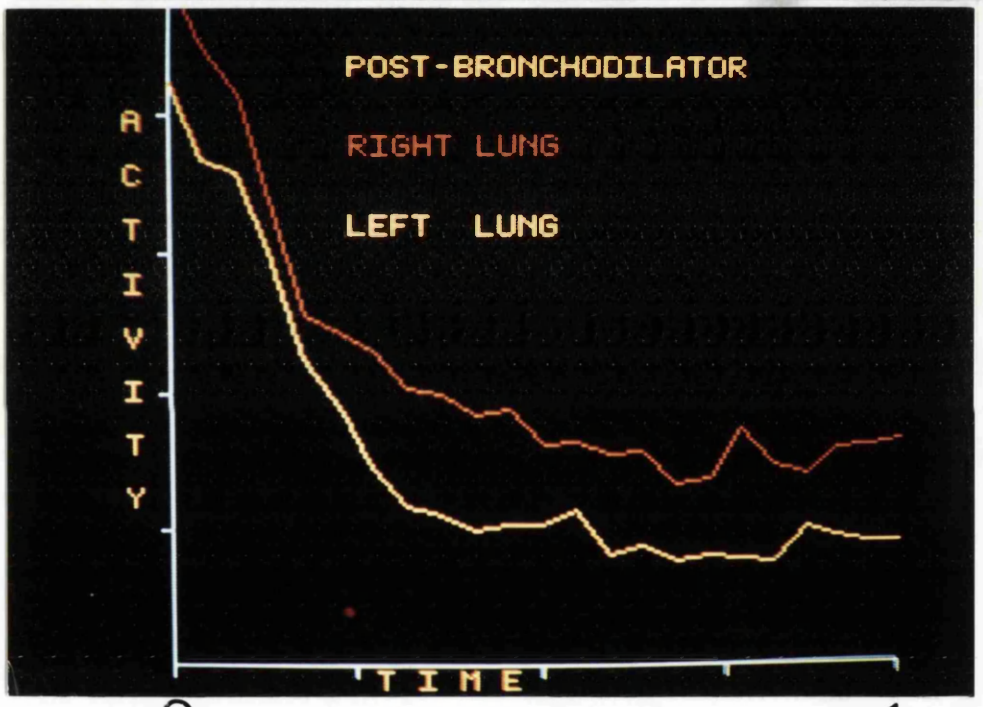


0 4 Seconds

FIGURE 49

A. Pre bronchodilator dynamic ventilation image.

B. Post bronchodilator dynamic ventilation image.

C. DYNAMIC IMAGING IN A CHILD WITH SCOLIOSIS

The third example was from a 12 year old child with kyphoscoliosis attending for respiratory assessment. As well as standard 4 view V/Q scan a dynamic ventilation image was acquired during a forced vital capacity manoeuvre (Figure 50).

This figure is a composite of steady state and dynamic image with the steady state image in the top right corner. The dynamic scan demonstrates that airflow during exhalation was more rapid from the left lung and enabled clear separation of the lungs to study regional lung function in this condition.

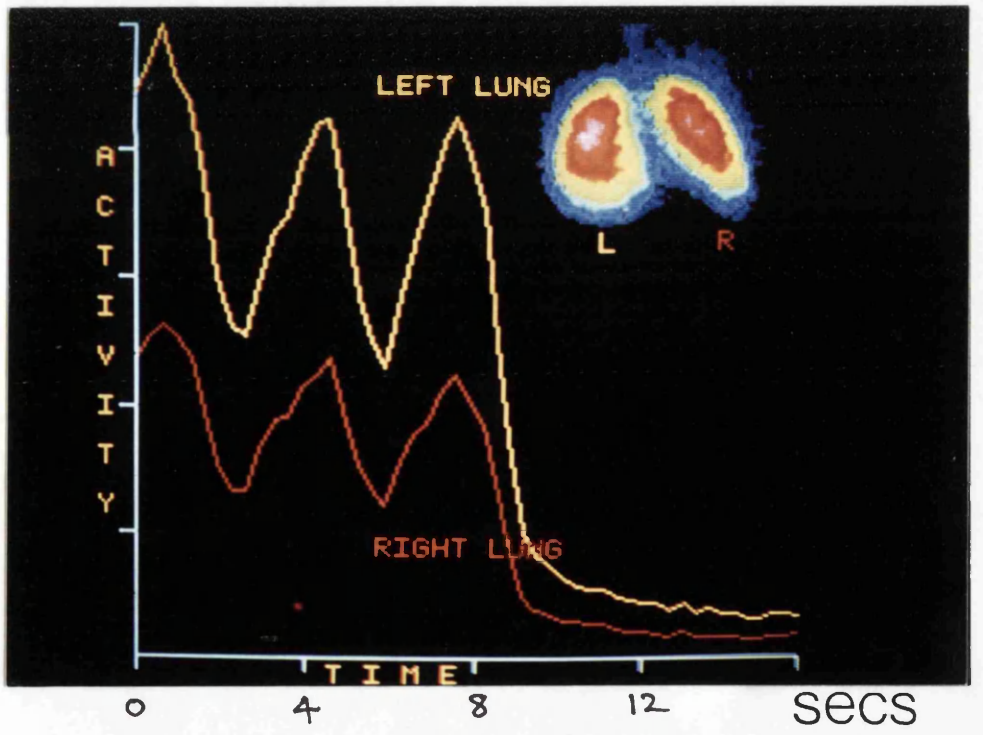


FIGURE 50

Composite static and dynamic ventilation image during forced expiration in a child with kyphoscoliosis.

1 Dynamic Kr81m ventilation imaging can separate the confounding effects of changing lung volume on regional ventilation assessed by the steady state Kr81m image.

2. Dynamic Kr81m images closely follow spirometric signals during a forced vital capacity manoeuvre and can be used for regional bronchospirometry.

3. Possible clinical applications of the technique have been demonstrated in 3 children, one with fixed obstruction of the left main bronchus, one with reversible airway disease and one with scoliosis.

# CONCLUSIONS

1.

Kr81m ventilation/Tc99m MAA perfusion imaging is well established in the investigation of paediatric pulmonary disease. The combined dosages from Kr81m and Tc99m are within acceptable limits for secondary investigations.

2.

Theoretical analysis, using the model of Fazio and Jones demonstrates that Kr81m activity reflects regional ventilation up to specific ventilation values of 10.0 $min.^{-1}$ Clinical experience and animal work suggest that at higher values of 14 $min^{-1}$ activity still provides an image of regional ventilation.

3.

Dynamic steady state ventilation imaging enables total Kr81m activity to be divided into "resident" and "tidally exchanged" Kr81m. "Total" and "tidally exchanged" Kr81m activity provide a very similar picture of distribution of ventilation in a lung model. "Tidally exchanged" Kr81m is more closely related to regional ventilation and demonstrates that when there is a gross discrepancy between regional lung volume and ventilation total Kr81m may misrepresent the distribution of ventilation.

4.

There is close agreement in regional ventilation calculated from total and tidally exchanged Kr81m in vivo.

5.

The relative contribution of tidally exchanged Kr81m to the total is similar in children and adults in line with the theoretical analysis that the steady state Kr81m image reflects regional ventilation throughout childhood.

6.

Tc99m MAA "spillover" into the Kr81m image is small, contributing between 0.1% and 4.7% of recorded activity.

7.

Insertion of a Kr81m reservoir into the administration system made no difference to resultant images. Differences in regional activity in the two images varied between 0 and 5.3%.

8.

Values for fractional ventilation and perfusion were derived for children with normal chest radiographs and homogenous distribution of radionuclide. In posterior images mean relative distribution of ventilation to right and left lung was 1.16 (1 to 1.5) and 1.29 (1.04 to 1.55) in anterior images. This difference is probably due to a proportion of activity within the left lung being absorbed by the heart when ventilation is imaged from the front. Relative perfusion of right and left lungs in posterior images was 1.13 (0.82 to 1.36).

The relative distribution of ventilation to the right and left lung fell from high values in infancy in line with published post mortem lung weights.

9.

Long term sequelae of foreign body inhalation were studied using V/Q scans in 21 children. Adverse prognostic factors identified were delayed removal, impaction in the left lung and collapse/consolidation on the initial radiograph.

10.

The effects of gravity on regional ventilation were studied in children and adults. In 20 children under the age of 2 fractional ventilation to the right lung was 57.7% supine, 42.4% dependent and 69% uppermost. In the 2-10 year age group these figures were 46.1%, 36% and 56.1%, in the 10-18 year age group 57.2%, 48% and 62.9% but in adults the reverse pattern was seen 52.4% rising to 55.4% when dependent, falling to 48.9% when uppermost. Xray appearances and pulmonary function tests made no difference to this pattern.

These differences should be taken into consideration when nursing critically ill infants with unilateral lung disease.

11.

The dependent lung is preferentially perfused in both children and adults, although the difference in perfusion of the right lung in the supine and right decubitus postures was less (3.9%) in children than in adults (7.0%).

12.

Dynamic ventilation imaging confirmed that the uppermost lung is preferentially ventilated although preliminary results

indicated that the adult pattern might be adopted at a slightly younger age than suggested by the steady state image .

13.

Non invasive regional bronchospirometry was validated in 9 subjects. Close agreement was seen between spirometric traces and Kr81m activity.

14.

Clinical applications of dynamic Kr81m scanning during forced expiration were demonstrated in 3 children, one with obstruction of the left main bronchus, one with reversible airway obstruction and one with scoliosis.

# REFERENCES

Abdulmaid DA, Ebeid AM, Motaweh MM, Kleibo IS. Aspirated foreign bodies in the tracheobronchial tree: report of 250 cases. Thorax 1976;31:635-640.

Agostini E. Volume pressure relationships of the thorax and lung in the newborn. J Appl Physiol 1959;14:909-13.

Agostini E, Mead J. Handbook of Physiology, American Physiological Society 1964 Vol 1; Section 3:393-394.

Alagille D, Odievre M, Gautier M, Dommerques JP. Ductular hypoplasia associated with characteristic facies, vertebral malformations, retarded physical, mental and sexual development and cardiac murmur. J Pediatr 1975;86:63-71.

Alderson PO, Secker-Walker RH, Strominger DB, McAlister WH, Hill RL, Markham J. Quantitative assessment of regional ventilation and perfusion in children with cystic fibrosis. Radiology 1974;111:151-155.

Amis TC, Jones HA, Hughes JMB. Effect of posture on inter-regional distribution of pulmonary perfusion and Va/Q ratios in man. Respiration Physiology 1984;56:169-182.

Amis TC, Jones HA, Hughes JMB. Effect of posture on inter-regional distribution of pulmonary ventilation in man. Respiration Physiology 1984;56:145-167.

Amis TC, Jones T. Krypton 81m as a flow tracer in the lung: Theory and Quantitation. Bull Europ Physiopath Resp 1980;16:245-259.

Anger HO. Scintillation camera. The Review of Scientific Instruments 1958;29:159-165.

Angus GE, Thurlbeck WM. Number of alveoli in the growing lung. J Appl Physiol 1972;27:265-74.

Anthonisen NR, Milic-Emili J. Distribution of pulmonary perfusion in erect man. J Appl Physiol 1966;21:760-766.

Avery ME, Cook CD. Volume pressure relationships of lung and thorax in fetal, newborn and adult goats. J Appl Physiol 1961;16:1034-1038.

Aytac A, Yurdakul Y, Ikizler C, Olga R, Saylem A. Inhalation of foreign bodies in children. J Thoracic and Cardiovascular Surgery 1977;74:145-151.

Bake B, Wood L, Murphy B, Macklem PT, Milic-Emili J. Effect of inspiratory flow rate on regional distribution of inspired gas. J Appl Physiol 1974;37:8-17.

Ball WC, Stewart PB, Newsham LGS, Bates DV. Regional pulmonary

function studies with Xenon 133. J Clin Inv 1962;41 no 3:519-531.

Banks W, Potsic WP. Elusive unsuspected foreign bodies in the tracheobronchial tree. Clinical Paediatrics 1977:31-35.

Bergan F. The relative function of lung in supine, left and right lateral positions. J Oslo City Hosp 1952;2:185-204.

Bergan F. The investigation of the relative function of the right and left lung by bronchospirometry technique, physiology and application. Oslo University Press 1957 (Grune and Stratton, London and New York).

Bhuyan U, Peters AM, Gordon I, Davies H, Helms P. Effects of Posture on the Distribution of Pulmonary Ventilation and Perfusion in Children and Adults. Thorax 1989;44:480-484.

Bjure J, Erstoem Jodal B, Elgerfors B. Pulmonary gas exchange after radioisotope scanning of the lungs. Scand J Resp Dis 1970;51:242-248.

Blazer S, Naveh Y, Friedman A. Foreign body in the airway. Am J Dis Child 1980;13:468-471.

Bryan AC, Bentivoglio LG, Beerel F, MacLeish H, Zidulka A, Bates DV. Factors affecting regional ventilation and perfusion in the lung. J Appl Physiol 1964;19:395-402.

Carlens E, Dahlstrom G. The clinical evaluation of bronchospirometry. Am Rev Resp Diseases 1961;83:202-207.

Chandra R, Shamoun J, Braunstein P, Duhov OL. Clinical evaluation of an instant kit for preparation of Tc99m MAA for lung scanning. J Nucl Med 1973;14:702-705.

Chandra R. Introductory Physics of Nuclear Medicine. Lea and Febiger 1982;51-56.

Ciofetta G, Silverman M, Hughes J. Quantitative approach to the study of regional lung function in children using Kr81m. Br J Rad 1980;53:950-959.

Cohen RS, Smith DW, Stevenson DK, Moskowitz PS, Benjamin Graham C. Lateral decubitus posture as therapy for persistent focal pulmonary interstitial emphysema in neonates: A preliminary report. J Pediatr 1984;104:441-443.

Comroe JH, Fowler WS. Lung Function Studies 6. Detection of uneven alveolar ventilation during a single breath of oxygen. American Journal of Medicine 1951;10:408-413.

Cooney TP, Thurlbeck TM. The radial alveolar count method of Emery and Mithal: a reappraisal 1- Postnatal lung growth. Thorax 1982;37:572-579.

Daily WJ, Bondurant S. Direct measurement of respiratory pleural pressure changes in man. J Appl Physiol 1963;18:513-518.

Davies G, Reid L. Growth of alveoli and pulmonary arteries in childhood. Thorax 1970;25:669-81.

Davies H, Kitchman R, Helms P, Gordon I. Regional ventilation in infants and very young children: reversal of adult pattern. N Engl J Med 1985;1626-1628

Davis C. Inhaled foreign bodies in children. Arch Dis Childh 1966;41:402-406.

Dock W. Apical localisation of Thisis: Its significance in treatment by prolonged rest in bed. Amer Rev Tuberc 1946;53:297-305.

Dollery CT, Dyson NA, Sinclair JD. Regional variations in uptake of radioactive CO in the normal lung. J Appl Physiol 1960;15:411-417.

Dollfuss RE, Milic-Emili J, Bates DV. Regional ventilation of the lung studied with boluses of Xenon133. Resp Physiol 1967;2:234-246.

Dunnill MS. Postnatal growth of the Lung. Thorax 1962;17:329-33.

Dyson NA, Hugh-Jones P, Newbery GR, Sinclair JD, West JB. Studies of regional lung function using radioactive Oxygen. BMJ 1960;1:231-238.

Fazio F, Jones T. Assessment of regional ventilation by continuous inhalation of Krypton 81m. BMJ 1975;3:673-676.

Fazio F, Lavender JP, Steiner RE. Kr81m ventilation and Tc99m perfusion scans in chest disease: comparison with standard radiographs. Am J Roentgenol 1978;130:421-428.

Fazio F, Palla A, Santolicandro A, Solfanelli S, Fornai E, Giumtini C. Studies of regional ventilation in asthma using Kr81m. Lung 1979;156:184-194.

Fisher JT, Mortola JP. Statics of the Respiratory System in Newborn Mammals. Respir Physiol 1980;41:155-172.

Fleming PJ, Muller NL, Bryan H, Bryan AC. The effects of abdominal loading on rib cage distortion in premature infants. Pediatr 1979;64:425-428.

Fowler WS. Intrapulmonary distribution of inspired gas. Phys Review 1952;32:1-20.

Fowler WS, Cornish ER, Kety SS. Lung function studies 8. Analysis of alveolar ventilation by pulmonary N2 clearance curves. J Clin Inv 1952;31:40-50.

Freyschuss U, Lannergren, Frenckner B. Lung function after repair of congenital diaphragmatic hernia. Acta Paediatr Scand 1984;73:589-593.

Garnett ES, Goddard BA, Machell ES, Macleod WM. Quantitated scintillation scanning for the measurement of lung perfusion. Thorax 1969;24:372-373.

Gaultier C, Boule M, Allaire Y, Clement A, Buvry A, Girard F. Determination of capillary oxygen tension in infants and children. Assessment of methodology and normal values during growth. Bull Europeen de Physiopathologie Resp 1978;14:287-297.

Godfrey S, Hambleton G, Winlove P, Freedman N. Unilateral lung disease detected by radioisotopic lung scanning in children thought to have asthma. Br J Dis Chest 1977;71:7-18.

Godfrey S, McKenzie S. Place of radioisotopic lung function studies in paediatrics. Arch Dis Childh 1977;52:859-864.

Godfrey S, Ronchetti R, Stocks J, Hallidie-Smith K. Generalised pulmonary hyperinflation and Fallot's tetralogy in a neonate investigated by pulmonary physiological and radioisotope methods. Thorax 1975;30:452-459.

Gordon I, Helms P. Imaging the small lung. Arch Dis Childh 1982;57:696-701.

Gordon I, Helms P, Fazio F. Clinical applications of radionuclide scanning in infants and young children. Br J Rad 1981;54:576-585.

Grant BJB, Jones HA, Hughes JMB. Sequence of regional filling during a tidal breath in man. J Appl Physiol 1974;37:158-165.

Guisan M, Tisi G, Ashburn WL, Moser KM. Washout of Xe133 gas from the lungs: comparison with Nitrogen washout. Chest 1972;62:146-151.

Harboyan G, Nassif R. Tracheobronchial foreign bodies a review of 14 years experience. J Laryngol Otol 1970;403:403-412.

Harf A, Pratt T, Hughes JMB. Regional distribution of V(a)/Q in man at rest and with exercise measured with Kr81m. J Appl Physiol 1978;44:115-123.

Heaf D, Helms P, Gordon I, Turner H. Postural effects of gas exchange in infants. N Engl J Med 1983;308:1505-1508.

Helms P, Beardsmore CS, Stocks J. Absolute intraoesophageal pressure at functional residual capacity in infancy. J Appl Physiol 1981;51:270-275.

Iikura Y, Inui H, Nishikuza K, Umesato Y, Obata T, Masaki T, Nakakura T. Recent findings in exercised-induced late asthmatic response (EIA). Acta Paediatr Jpn 1983;25:379-384.

In Guk Kim, Brummitt WM, Humphry A, Siomra SW, Wallace WB. Foreign body in the airway: a review of 202 cases. Laryngoscope 1973;83:347-354.

Jones T. Theoretical aspects of the use of Krypton 81m. Br J Rad 1978; Special Report 15:33-37.

Kaneko K, Milic-Emili J, Dolovich MB, Dawson A, Bates DV. Regional distribution of ventilation and perfusion as a function of body position. J Appl Physiol 1966;21:767-777.

Kjellman B. Regional lung function studied with Xe133 in children with pneumonia. Acta Paediatr Scand 1967;56:467-476.

Knipping HW, Bolt W, Venrath H, Valentin H, Ludes H, Endler P. Eine neue Methode zur Prufung der Herz- und Lungenfunktion. Deutsche Medizinische Wochenschrift 1955;80:1146-1147.

Kosloske A. Bronchoscopic extraction of aspirated foreign bodies in children. Am J Dis Child 1982;136:924-927.

Krogh A, Lindhard J. The volume of the dead space in breathing and the mixing of gases in the lungs of man. J Physiol 1917;51:59-60.

Laennec RTH. "Of Emphysema and the Lungs" A Treatise on the Disease of the Chest and on Mediate Auscultation, New York, Samuel Wood and Sons 1830 p161, from "Classic Descriptions of Disease", Major RH, 1932 Published by Charles C Thomas.

Laennec RTH. "Of the Signs and Symptoms of Acute Pleurisy" A Treatise on the Diseases of the Chest and on Mediate Auscultation, New York, Samuel Wood and Sons 1830 p443, from "Classic Descriptions of Disease" Major RH, 1932 Published by Charles C Thomas.

Li DK, Treves S, Heyman S, Kirkpatrick JA, Lambrecht RM, Ruth TJ, Wolf AP. Krypton-81m: A better radiopharmaceutical for assessment of regional lung function in children. Radiology 1979;130:741-747.

Lillington GA, Fowler WS, Miller RD, Helmholz Jnr HF. Nitrogen clearance rates of right and left lung in different positions. J Clin Invest 1953;38:2026-2034.

Linton JSA. Longstanding intrabronchial foreign bodies. Thorax 1957;12:164-170.

Lowe D, Ross Russell RI. Tracheobronchial foreign bodies The position of the carina. J Laryngol Otol 1984;98:499-501.

Mansell A, Bryan C, Levison H. Airway closure in children. J Appl Physiol 1972;33:711-714.

Mattson SB, Carlens E. Lobar ventilation and oxygen uptake in man. J Thoracic Surg 1955;30:676-682.

McNeil B, Adelstein S. Pulmonary studies in Nuclear Medicine in clinical practise. Publishers Amsterdam Elsevier, North Holland 1978; 39-60.

Matthew DJ, Warner JO, Chrispin AR, Norman AP. The relationship between chest radiographic scores and respiratory function tests in children with cystic fibrosis. Pediatr Radiol 1977;5:198-200.

Martin C, Young AC. Ventilation perfusion variation within the lung. J Appl Physiol 1957;11:371-376.

Milic-Emili J, Henderson JAM, Dolovich MB, Trop D, Kanako K. Regional distribution of inspired gas in the lung. J Appl Physiol 1966;21:749-759.

Miller GA, Gianturco C, Neucks HC. The asymptomatic period in retained foreign bodies of the bronchus. Am J Dis Child 1957;95:282-284.

Modell H, Graham M. Limitations of Krypton-81m for quantification of lung scans. J Nucl Med 1982;23:301-305.

Moser KM, Guisan M, Cuomo A, Ashburn WL. Differentiation of pulmonary vascular from parenchymal diseases by ventilation perfusion scintiphotography. Annals of Internal Medicine 1971;75:597-605.

Mostafa AB, Childs PO, Williams NR, Causer DA. Regional pulmonary distribution of Krypton 81m gas delivered by different breathing systems. J Nucl Med 1985;26:191-193.

Muir AL, Hannan WJ, Bell D, Adie CJ, Wraith PK, Brash HM. Gated Ventilation Scanning: a new approach to regional pulmonary function. Thorax 1984;39:221.

Myers M. The Practical Estimation of Internal Radiation Doses from Kr81m and Similar Ultrashort lived Radionuclides. Nuclear Medicine Communications 1981;2:358-364.

Naimark A, Cherniak RM. Compliance of the Respiratory System in Health and Obesity. J Appl Physiol 1960;15:377-382.

Norris CM. Foreign Bodies in the air and food passages; a series of 250 cases. Ann Otol Rhinol Laryngol 1948;57:1049-1071.

Papanicolou N, Treves S. Pulmonary Scintigraphy in Paediatrics. Seminars in Nuclear Medicine 1980;10:259-285.

Pengelly CD, Alderson AM, Milic Emili J. Mechanics of the Diaphragm. J Appl Physiol 1971;30:797-805.

Piepsz A. Late Sequelae of Foreign Body Inhalation. A Multicentre Scintigraphic Study. Eur J Nucl Med 1988;13:578-581.

Polgar G, Promadhat V. Pulmonary function testing in children: Techniques and Standards 1971; published by W.B. Saunders Co.

Powell V. Inhaled foreign bodies: some complications and errors. Thorax 1965;20:48-52.

Puterman M, Gorodischer R, Leiberman A. Tracheobronchial foreign bodies; The impact of a postgraduate educational program on diagnosis, morbidity and treatment. Pediatr 1982;70:96-98.

Pyman C. Inhaled foreign bodies in childhood: A review of 230 cases. Med J Austral 1971:62-68.

Rehder K, Hatch DJ, Sessler AD, Marsh HM, Fowler WS. Effects of general anaesthesia, muscle paralysis and mechanical ventilation on pulmonary Nitrogen clearance. Anesthesiology 1971;35:591-601.

Remolina C, Khan AU, Santiago TV, Edelman NH. Positional hypoxaemia in unilateral lung disease. New England Journal of Medicine 1981;304:523-525.

Ronchetti R, Stocks J, Freedman N, Glass H, Godfrey S. Clinical application of regional lung function studies in infants and small children using N13. Arch Dis Childh 1975;50:595-603.

Rudolph AM. Congenital Diseases of the Heart. Year Book Medical Publishers, Chicago 1974.

Schwarz E. Retained foreign bodies in the tracheobronchial tree of children. JAMA 1961;175:242-243.

Secker-Walker RH, Hill RI, Markham J, Baker J, Wilhelm J, Alderson PO, Potchen EJ. The measurement of regional ventilation in man: a new method of quantification. J Nucl Med 1973;14:725-732.

Shirazy Majd N, Mofensen HC, Greensher J. Lower airway foreign body aspiration in children. Clinical Pediatrics 1977;16:13.16.

Slim MS, Yacoubian HD. Complications of foreign bodies in the tracheobronchial tree. Arch Surg 1966;92:388-393.

Stowens D. In Pediatric Pathology, The Williams and Wilkins Co, 1966. Page 3.

Svanberg L. Influence of posture on the lung volumes ventilation and circulation in the normals: a spirometric, bronchospirometric investigation. Scand J Clin Inv (Suppl) 1957;25:1-195.

Svanberg L. Bronchospirometry in the study of regional lung function. Scand J Respir Dis Suppl 62 1966:91-102.

Swingle HM, Eggert LD, Bucciarelli RL. New approach to management of unilateral tension emphysema in premature infants. Pediatrics 1984;74:354-357.

Tow DE, Wagner Jr HN, Lopez Majano V et al. Validity of measuring regional pulmonary arterial blood flow with macroaggregates of human albumin. Am J Roentgenol 1966;96:664-676.

Treves S, Ahnberg S, Laguarda R, Strieder DJ. Radionuclide evaluation of regional lung function in children. J Nucl Med 1974;5:582-587.

Udea H, Iio M, Kalihara S. Determination of regional pulmonary blood flow in various cardiopulmonary disorders. Jap Heart J 1964;5:431-444.

Vacarezza RF, Benge A, Lameri A, Labourt F, Gonzalez-Segura. The study of the two lungs separately in practical and research work. Diseases Chest 1943;9:95-114.

Wagner HN, Sabiston DC, Mcafee JG, Tow D, Stern HS. Diagnosis of massive pulmonary embolus in man by radioisotope scanning. New Engl J Med 1964;271:377-384.

West JB, Dollery CT, Naimark A. Distribution of blood flow in isolated lung. J Appl Physiol 1964;19:713-724.

West JB. Regional differences in gas exchange in the lung of erect man. J Appl Physiol 1962;17:893-898.

West JB, Dollery CT. Distribution of blood flow and ventilation-perfusion ratio in the lung, measured with radioactive CO2. J Appl Physiol 1960;15:405-410.

West JB, Dollery CT, Hugh Jones P. The use of radioactive CO2 to measure regional blood flow in the lungs of patients with pulmonary disease. Journal of Clinical Investigation 1961;40:1-12.

Williams HE, Phelan PD. The "missed" foreign body in children. Med J Austral 1969;625-628.

Wong Y-C, Silverman M. Dynamic ventilation lung scan in infancy using Kr81m. Progr Resp Res 1981;17:123-130.

Wong Y-C, Silverman M. Krypton 81m ventilation lung scans in the assessment of lung function during infancy. Mod Probl Paediat 1982;21:230-236.

Yasuhiko Kobayashi, Toshihiro Abe, Akitoshi Sato, Kanji Nagai, Yoshikazu Nagai, Chiharu Ibukiyama. Radionuclide angiography in

pulmonary sequestration. J Nucl Med 1985;26:1035-1038.

Zapletal A, Paul T, Samanek M. Pulmonary elasticity in children and adolescents. J Appl Physiol 1976;40:953.

# APPENDICES

Derived Kr81m activity for

A 3.5 kg neonate

B. 20 kg child

C. 50 kg child

using equation derived from the model of Fazio and Jones

$$\text{Kr81m activity} = K * \frac{V * Ci(81)}{V/Vol + Lambda}$$

V - Minute Ventilation
Ci(81) - inhaled concentration of Kr81m
V/Vol - Specific ventilation (L/L/min)
lambda - decay constant of Kr81m.

## A

### 3.5 kg neonate - mean respiratory rate 40/min

| Respiratory Rate | 30 | 40 | 50 | 60 |
|---|---|---|---|---|
| D.Sp | 7.7 | 7.7 | 7.7 | 7.7 |
| D.Sp x RR | 231 | 308 | 385 | 462 |
| V(min) | 735 | 980 | 1225 | 1470 |
| V(min) - D.Sp x RR | 504 | 672 | 840 | 1008 |
| Vol - D.Sp | 97.3 | 97.3 | 97.3 | 97.3 |
| V/Vol | 5.2 | 6.9 | 8.6 | 10.4 |
| (%) | 75 | 100 | 125 | 150 |
| Kr81m Activity | 60 | 67 | 71.2 | 74 |
| (%) | 90 | 100 | 106 | 110 |

D.Sp - Dead Space (mls)
RR - Respiratory rate per minute
V(min) - minute ventilation (mls)
Vol - Functional Residual Capacity (mls)

B

20 kg child - mean respiratory rate 15/min

| Respiratory Rate | 10 | 13 | 15 | 20 | 25 |
|---|---|---|---|---|---|
| D.Sp | 44 | 44 | 44 | 44 | 44 |
| D.Sp x RR | 440 | 572 | 660 | 880 | 1100 |
| V(min) | 1400 | 1820 | 2100 | 2800 | 3500 |
| V(min) - D.Sp x RR | 960 | 1248 | 1440 | 1920 | 2400 |
| Vol - D.Sp | 556 | 556 | 556 | 556 | 556 |
| V/VOL | 1.7 | 2.2 | 2.6 | 3.5 | 4.3 |
| (%) | 65 | 85 | 100 | 135 | 165 |
| Kr81m activity | 196 | 231 | 248 | 287 | 320 |
| (%) | 79 | 93 | 100 | 115 | 129 |

C

50 kg child - mean respiratory rate 13/min

| Respiratory Rate | 9 | 11 | 13 | 15 | 17 |
|---|---|---|---|---|---|
| D.Sp | 110 | 110 | 110 | 110 | 110 |
| D.Sp x RR | 990 | 1210 | 1430 | 1650 | 1870 |
| V(min) | 3150 | 3850 | 4550 | 5250 | 5950 |
| V(min) - D.Sp | 2160 | 2640 | 3120 | 3600 | 4080 |
| Vol - D.Sp | 1390 | 1390 | 1390 | 1390 | 1390 |
| V/Vol | 1.6 | 1.9 | 2.2 | 2.6 | 2.9 |
| (%) | 73 | 86 | 100 | 118 | 132 |
| Kr81m | 450 | 518 | 578 | 621 | 669 |
| (%) | 78 | 90 | 100 | 107 | 116 |

Decay correction for varying frame rates, end expiratory levels and respiratory rates.

A. 5 Frames per second

| | Respiratory Rate | | | |
|---|---|---|---|---|
| End expiratory count level | 10 | 20 | 30 | 40 |
| 1000 | 4108 | 1109 | 506 | 288 |
| 750 | 3081 | 832 | 379 | 216 |
| 500 | 2053 | 554 | 259 | 144 |
| 250 | 1027 | 277 | 126 | 72 |
| 100 | 411 | 111 | 51 | 29 |

B. 2.5 Frames per second

| | Respiratory Rate | | | |
|---|---|---|---|---|
| End expiratory count level | 10 | 20 | 30 | 40 |
| 1000 | 2054 | 554 | 253 | 144 |
| 750 | 1540 | 416 | 189 | 108 |
| 500 | 1026 | 277 | 126 | 72 |
| 250 | 513 | 138 | 63 | 36 |
| 100 | 205 | 55 | 25 | 14 |

Minute Ventilation to compartments 1 and 2, ratio of TOTAL and TIDAL Kr81m activity in compartments 1 and 2.

| RUN | 1 | 2 | 3 | 4 | 5 | 6 | 7 | 8 |
|---|---|---|---|---|---|---|---|---|
| Ventilation (mls/minute) | | | | | | | | |
| To 1: | 1008 | 3564 | 1026 | 5874 | 3510 | 2730 | 3625 | 6552 |
| To 2: | 1536 | 3906 | 1728 | 7627 | 5160 | 17329 | 7525 | 15561 |
| 1/2: | 0.65 | 0.91 | 0.59 | 0.77 | 0.68 | 0.16 | 0.48 | 0.42 |
| Total Kr81m activity | | | | | | | | |
| 1/2: | 0.37 | 0.65 | 0.60 | 0.93 | 0.96 | 0.36 | 0.74 | 0.57 |
| Tidal Kr81m activity | | | | | | | | |
| 1/2: | 0.56 | 0.98 | 0.64 | 0.95 | 0.66 | 0.21 | 0.43 | 0.30 |

Minute Ventilation to compartments 1 and 2, ratio of TOTAL and TIDAL Kr81m activity in compartments 1 and 2.

| RUN 9 | 10 | 11 | 12 | 13 | 14 | 15 | 16 |
|---|---|---|---|---|---|---|---|
| Ventilation (mls/minute) | | | | | | | |
| To 1:4400 | 6898 | 10061 | 7780 | 4334 | 3653 | 4404 | 3684 |
| To 2:4757 | 2260 | 9957 | 8599 | 4495 | 4219 | 4154 | 4504 |
| 1/2: 0.92 | 3.05 | 1.01 | 0.90 | 0.96 | 0.87 | 1.06 | 0.82 |
| Total Kr81m activity | | | | | | | |
| 1/2: 0.57 | 0.87 | 1.35 | 0.92 | 0.81 | 1.12 | 1.88 | 0.99 |
| Tidal Kr81m activity | | | | | | | |
| 1/2: 0.89 | 2.96 | 0.99 | 1.00 | 1.09 | 0.88 | 1.17 | 0.87 |

FRACTIONAL VENTILATION TO RIGHT LUNG

| Patient | Age (years) | Calculated from TOTAL Kr81m | Calculated from TIDAL Kr81m |
|---|---|---|---|
| TD (1) | 0.03 | 42.1 | 54.2 |
| DM | 0.26 | 66.9 | 69.5 |
| TD(2) | 0.28 | 44.2 | 53.2 |
| DR | 0.41 | 61.6 | 64.9 |
| AR | 0.46 | 53.4 | 61.7 |
| RP | 0.72 | 49.6 | 50.8 |
| RE | 0.79 | 54.3 | 55.8 |
| MA (1) | 1.51 | 34.2 | 35.0 |
| MA (2) | 1.51 | 32.5 | 39.0 |
| MS | 1.79 | 53.1 | 51.7 |
| JR | 2.18 | 63.4 | 60.0 |
| DH | 2.38 | 50.4 | 49.1 |
| AE | 3.05 | 62.7 | 56.4 |
| DG | 6.91 | 51.2 | 50.8 |
| VJ | 8.12 | 52.0 | 57.9 |
| BS | 8.42 | 62.5 | 66.1 |
| NC | 12.5 | 59.9 | 64.2 |
| DJ (1) | 12.6 | 50.6 | 50.6 |
| DJ (2) | 12.6 | 45.6 | 46.0 |
| DH | 15.1 | 51.3 | 53.7 |
| GB | 19.7 | 50.2 | 50.4 |
| RB | 24.9 | 47.1 | 46.0 |
| HD (1) | 33.5 | 55.6 | 55.6 |
| HD (2) | 33.5 | 49.5 | 51.0 |
| HD (3) | 33.5 | 52.5 | 54.4 |
| UB | 35.0 | 53.3 | 53.9 |
| UN | 38.6 | 53.3 | 57.5 |

RATIO OF TIDALLY EXCHANGED:TOTAL KR81M ACTIVITY IN SUBJECTS STUDIED

| Subject | Age (years) | Tidal/Total Kr81m |
|---|---|---|
| TD (1) | 0.03 | 0.12 |
| DM | 0.26 | 0.23 |
| TD (2) | 0.28 | 0.14 |
| DR | 0.41 | 0.56 |
| AR | 0.46 | 0.24 |
| RP | 0.72 | 0.36 |
| RE | 0.79 | 0.34 |
| MA (1) | 1.51 | 0.24 |
| MA (2) | 1.51 | 0.21 |
| MS | 1.79 | 0.21 |
| JR | 2.18 | 0.22 |
| DH | 2.38 | 0.24 |
| AE | 3.05 | 0.24 |
| DG | 6.91 | 0.44 |
| VJ | 8.12 | 0.22 |
| BS | 8.42 | 0.25 |
| NC | 12.5 | 0.11 |
| DJ (1) | 12.6 | 0.21 |
| DJ (2) | 12.6 | 0.22 |
| DH | 15.1 | 0.23 |
| GB | 19.7 | 0.16 |
| RB | 24.9 | 0.25 |
| HD (1) | 33.5 | 0.32 |
| HD (2) | 33.5 | 0.18 |
| HD (3) | 33.5 | 0.16 |
| UB | 35.0 | 0.20 |
| UN | 38.6 | 0.17 |

Relative distribution of ventilation and perfusion determined from posterior Kr81m ventilation and Tc99m MAA perfusion images in a group of children with normal chest radiographs and homogeneous distribution of radionuclide

| | AGE (years) | Ventilation (R:L) | Perfusion (R:L) |
|---|---|---|---|
| 1. | 0.01 | 1.18 | 1.22 |
| 2. | 0.02 | 1.50 | N/A |
| 3. | 0.21 | 1.01 | 1.27 |
| 4. | 0.38 | 1.06 | 1.16 |
| 5. | 0.50 | 1.50 | N/A |
| 6. | 0.62 | 1.04 | 1.22 |
| 7 | 0.92 | 1.50 | N/A |
| 8 | 1.71 | 1.17 | 0.98 |
| 9 | 1.83 | 1.16 | 1.20 |
| 10 | 2.00 | 1.08 | 1.08 |
| 11 | 2.25 | 1.15 | 0.98 |
| 12 | 2.50 | 1.26 | 1.36 |
| 13 | 2.58 | 1.26 | 1.26 |
| 14 | 2.66 | 1.00 | 1.01 |
| 15 | 3.25 | 1.24 | 1.11 |
| 16 | 3.33 | 1.08 | N/A |
| 17 | 3.50 | 1.08 | 0.82 |
| 18 | 3.83 | 1.30 | 1.05 |
| 19 | 4.33 | 1.05 | 1.19 |
| 20 | 4.38 | 1.12 | N/A |
| 21 | 5.04 | 1.19 | 1.14 |
| 22 | 5.04 | 1.23 | 1.08 |
| 23 | 5.50 | 1.08 | 1.13 |
| 24 | 5.92 | 1.32 | 1.21 |
| 25 | 6.92 | 1.32 | 1.13 |
| 26 | 7.50 | 1.13 | 1.23 |
| 27 | 7.75 | 1.12 | 1.09 |
| 28 | 10.66 | 1.20 | 1.20 |

N/A Not applicable: perfusion scan not performed.

## APPENDIX 6(continued)

Relative distribution of ventilation determined from posterior Kr81m ventilation in a group of adult volunteers.

(N.B. Perfusion scans not performed in adult volunteers)

| | AGE (years) | Ventilation (R lung:L lung) |
|---|---|---|
| 29 | 18.92 | 1.08 |
| 30 | 19.60 | 1.04 |
| 31 | 20.58 | 1.04 |
| 32 | 21.42 | 1.09 |
| 33 | 23.50 | 1.09 |
| 34 | 24.50 | 1.22 |
| 35 | 25.08 | 1.08 |
| 36 | 25.17 | 1.16 |
| 37 | 26.00 | 1.17 |
| 38 | 26.58 | 1.00 |
| 39 | 27.00 | 1.04 |
| 40 | 30.10 | 1.13 |
| 41 | 31.00 | 1.13 |
| 42 | 31.25 | 1.08 |
| 43 | 32.80 | 1.08 |
| 44 | 33.83 | 1.02 |
| 45 | 34.08 | 1.13 |
| 46 | 35.03 | 1.13 |
| 47 | 36.91 | 1.05 |
| 48 | 38.58 | 1.16 |
| 49 | 38.67 | 1.08 |
| 50 | 50.17 | 1.08 |

Relative distribution of ventilation and perfusion to right and left lung determined from anterior Kr81m ventilation and Tc99m MAA perfusion images in a group of children with normal chest radiographs and homogeneous distribution of radionuclide

| PATIENT | AGE (years) | Perfusion R:L | Ventilation R:L |
|---|---|---|---|
| 6. | 0.38 | 1.30 | 1.31 |
| 10 | 2.00 | 1.04 | 1.13 |
| 12 | 2.50 | 1.55 | 1.48 |
| 15 | 3.25 | 1.28 | 1.23 |
| 17 | 3.50 | 1.32 | 1.02 |
| 18 | 3.83 | 1.40 | 1.28 |
| 19 | 4.33 | 1.41 | 1.45 |
| 21 | 5.04 | 1.27 | 1.34 |
| 22 | 5.04 | 1.36 | 1.46 |
| 23 | 5.50 | 1.08 | 1.27 |
| 24 | 5.92 | 1.20 | 1.50 |
| 25 | 6.92 | 1.27 | 1.21 |
| 27 | 7.75 | 1.09 | 1.11 |
| 28 | 10.66 | 1.49 | 1.33 |

Children studied, radiographic category and fractional ventilation to the right lung (VfR).

CHILDREN UNDER 2 YEARS

1 = Normal chest radiograph : 2 = Unilateral changes : 3 = Bilateral changes

| SUBJECT | AGE (years) | RADIOGRAPH | FRACTIONAL VENTILATION TO R LUNG | | |
|---|---|---|---|---|---|
| | | | Supine | Dependent | Uppermost |
| TW | 0.02 | 1. | 59.0 | 53.0 | 52.0 |
| EM | 0.03 | 2 | 46.0 | 47.0 | 65.0 |
| JC | 0.03 | 3 | 64.0 | 35.0 | 78.0 |
| SP | 0.09 | 1 | 73.0 | 63.0 | 75.0 |
| JA | 0.10 | 2 | 67.0 | 62.0 | 66.0 |
| CV | 0.17 | 2 | 39.0 | 30.0 | 46.0 |
| MG | 0.18 | 1 | 65.0 | 22.0 | 84.0 |
| MB | 0.26 | 2 | 62.0 | 52.0 | 73.0 |
| SH | 0.30 | 3 | 55.0 | 26.0 | 86.0 |
| BP | 0.42 | 1 | 55.0 | 46.0 | 73.0 |
| CO | 0.46 | 3 | 63.0 | 38.0 | 73.0 |
| DF | 0.48 | 2 | 29.0 | 11.0 | 32.0 |
| AT | 0.54 | 1 | 59.0 | 44.0 | 66.0 |
| GM | 0.78 | 3 | 70.0 | 70.0 | 81.0 |
| CS | 1.00 | 3 | 56.0 | 43.0 | 78.0 |
| LM | 1.03 | 1 | 60.0 | 32.0 | 69.0 |
| PG | 1.04 | 3 | 59.3 | 37.5 | - |
| RD | 1.10 | 3 | 64.0 | 47.0 | 86.0 |
| GH | 1.24 | 2 | 59.0 | 46.0 | 69.0 |
| CF | 1.93 | 1 | 49.0 | 43.0 | 61.0 |

Fractional ventilation to the right lung

CHILDREN 2 - 10

| NAME | AGE | XRAY | SUPINE | DEPENDENT | UPPERMOST |
|---|---|---|---|---|---|
| AK | 4.3 | 3 | 52.0 | 33.0 | 60.0 |
| PC | 4.4 | 1 | 53.0 | 47.0 | 60.0 |
| EH | 4.6 | 1 | 52.0 | 34.0 | 60.0 |
| JM | 5.4 | 1 | 37.0 | 35.0 | 45.0 |
| ID | 5.8 | 1 | 56.0 | 37.0 | 69.0 |
| JG | 6.0 | 2 | 14.0 | 5.0 | 31.0 |
| DJ | 6.5 | 2 | 23.0 | 9.0 | - |
| LJ | 7.7 | 1 | 51.0 | 42.0 | 58.0 |
| PS | 8.1 | 3 | 52.0 | 32.0 | 67.0 |
| TJ | 8.1 | 1 | 55.0 | 40.0 | 68.0 |
| NC | 8.4 | * | 61.5 | 52.2 | 0.0 |
| BS | 8.4 | 1 | 50.0 | 43.0 | 59.0 |
| JA | 9.1 | * | 56.0 | 51.0 | 0.0 |
| JB | 9.2 | 3 | 32.0 | 23.0 | 51.0 |
| KT | 9.5 | 1 | 38.0 | 36.0 | 47.0 |
| SN | 9.6 | 3 | 51.0 | 45.0 | 57.0 |
| KD | 9.8 | 1 | 53.0 | 46.0 | 59.0 |
| AK | 9.9 | 3 | 44.0 | 37.0 | 51.0 |

* - Not performed

Fractional ventilation to the right lung

CHILDREN 10 - 18

| NAME | AGE | XRAY | SUPINE | DEPENDENT | UPPERMOST |
|---|---|---|---|---|---|
| JA | 10.3 | 3 | 58.0 | 44.0 | 72.0 |
| EW | 10.3 | 1 | 56.0 | 46.0 | 66.0 |
| RG | 11.1 | 3 | 53.0 | 45.0 | 57.0 |
| AH | 11.9 | 1 | 56.0 | 48.0 | 69.0 |
| JC | 12.6 | 3 | 50.0 | 42.0 | 59.0 |
| CB | 12.8 | 1 | 53.0 | 51.0 | 63.0 |
| TW | 12.9 | 1 | 58.0 | 41.0 | 70.0 |
| RL | 13.4 | 3 | 48.0 | 31.0 | 59.0 |
| SM | 13.5 | 3 | 68.0 | 49.0 | 72.0 |
| DH | 13.5 | 3 | 53.0 | 42.0 | 61.0 |
| SD | 13.7 | 3 | 78.0 | 70.0 | 77.0 |
| TF | 14.7 | 2 | 55.0 | 43.0 | 59.0 |
| IH | 14.7 | 1 | 55.0 | 55.0 | 50.0 |
| JM | 15.0 | 1 | 60.0 | 46.0 | 68.0 |
| DH | 15.1 | 3 | 47.0 | 45.0 | 50.0 |
| AH | 15.1 | 3 | 54.0 | 44.0 | 61.0 |
| SE | 15.6 | 3 | 54.0 | 42.0 | 59.0 |
| PC | 16.1 | 2 | 65.0 | 62.0 | 71.0 |
| JB | 16.1 | 1 | 55.0 | 56.0 | 50.0 |
| WW | 16.5 | 3 | 59.0 | 51.2 | 57.0 |
| AP | 16.9 | 3 | 66.0 | 53.0 | 70.0 |

Fractional ventilation to right lung

ADULTS

| NAME | AGE | SUPINE | DEPENDENT | UPPERMOST |
|---|---|---|---|---|
| PW | 18.9 | 52.0 | 48.0 | 62.0 |
| GB | 19.7 | 51.0 | 51.0 | 36.0 |
| GR | 20.6 | 51.0 | 55.0 | 53.0 |
| LS | 24.4 | 55.0 | 48.0 | 60.0 |
| RB | 24.9 | 52.0 | 49.0 | 58.0 |
| JB | 25.1 | 54.0 | 56.0 | 37.0 |
| RR | 26.0 | 55.0 | 55.0 | 50.0 |
| AD | 26.6 | 50.0 | 59.0 | 52.0 |
| AG | 30.2 | 53.0 | 51.0 | 50.0 |
| RK | 31.1 | 52.0 | 63.0 | 43.0 |
| HD | 32.9 | 52.0 | 55.0 | 49.0 |
| JF | 33.8 | 50.0 | 45.0 | 43.0 |
| MD | 34.1 | 58.0 | 58.0 | 47.0 |
| JS | 35.8 | 53.0 | 47.0 | 42.0 |
| UN | 38.6 | 54.0 | 56.0 | 57.0 |
| MP | 39.1 | 52.0 | 58.0 | 43.0 |
| KE | 50.2 | 52.0 | 53.0 | 49.0 |

Right and left lung heights, erect and decubitus, in 18 children.

| | | LEFT LUNG | | | RIGHT LUNG | | |
|---|---|---|---|---|---|---|---|
| | | 1 | 2 | | 1 | 2 | |
| NAME | AGE | Erect | Uppermost | (2-1) | Erect | Dependent | (2-1) |
| AK | 4.3 | 15.0 | 15.0 | 0 | 14.0 | 13.0 | -1.0 |
| PC | 4.4 | 13.5 | 15.0 | 1.5 | 13.5 | 13.0 | -0.5 |
| JM | 5.4 | 18.5 | 17.5 | 1.0 | 18.0 | 13.5 | -4.5 |
| JG | 6.0 | 17.0 | 16.0 | -1.0 | 15.0 | 12.0 | -3.0 |
| LJ | 7.7 | 15.0 | 17.0 | 2.0 | 15.0 | 14.5 | -0.5 |
| TJ | 8.1 | 17.5 | 18.0 | 0.5 | 16.5 | 14.0 | -1.5 |
| KT | 9.5 | 16.5 | 18.0 | 1.5 | 16.0 | 16.0 | 0.0 |
| KD | 9.8 | 16.5 | 18.0 | 1.5 | 18.5 | 15.5 | -3.0 |
| AK | 9.9 | 14.5 | 16.5 | 2.0 | 14.5 | 14.5 | 0.0 |
| EW | 10.3 | 18.0 | 20.5 | 2.5 | 17.0 | 18.0 | 1.0 |
| AH | 11.8 | 18.0 | 19.5 | 1.5 | 16.0 | 14.5 | -1.5 |
| JC | 12.6 | 19.5 | 17.5 | -2.0 | 20.0 | 20.5 | 0.5 |
| DH | 13.5 | 19.0 | 21.0 | 2.0 | 20.0 | 20.0 | 0.0 |
| IH | 14.6 | 21.5 | 21.0 | -0.5 | 21.0 | 16.0 | -5.0 |
| TF | 14.7 | 20.5 | 23.0 | 2.5 | 21.0 | 19.5 | -1.5 |
| SE | 15.6 | 18.0 | 18.5 | 0.5 | 17.5 | 15.5 | -2.0 |
| PO | 16.1 | 21.5 | 23.0 | 1.5 | 21.5 | 21.0 | -0.5 |
| AP | 16.9 | 14.5 | 14.5 | 0.0 | 14.5 | 13.0 | -1.5 |